UNIVERSITAT POLITÈCNICA DE CATALUNYA

REMOVAL OF BORON FROM AQUEOUS SOLUTIONS USING BIOPOLYMERS AND COMPOSITES

A thesis
submitted to the Department of Chemical Engineering
of the Universitat Politècnica de Catalunya
in fulfilment of the requirements
to obtain the degree of Doctor of Chemical Process Engineering

By

Hary Demey Cedeño

Supervised by

Dr. Ana Maria Sastre Requena
Dr. Montserrat Ruiz Planas

Barcelona, September 2014

UNIVERSITAT POLITÈCNICA DE CATALUNYA

REMOVAL OF BORON FROM AQUEOUS SOLUTIONS USING BIOPOLYMERS AND COMPOSITES

A thesis
submitted to the Department of Chemical Engineering
of the Universitat Politècnica de Catalunya
in fulfilment of the requirements
to obtain the degree of Doctor of Chemical Process Engineering

By

Hary Demey Cedeño

Supervised by
Dr. Ana Maria Sastre Requena
Dr. Montserrat Ruiz Planas

Vistiplau

Hary Demey Cedeño	Dr. Ana M. Sastre Requena	Dr. Montserrat Ruiz Planas

Barcelona, September 2014

AGRADECIMIENTOS

A Dios por brindarme la fortaleza necesaria para seguir adelante en los momentos más difíciles de mi etapa de formación.

A mi madre que a pesar de la distancia (>8000 km) ha estado presente en cada momento, y éstas cortas líneas son insuficientes para expresar el profundo amor que siento.

A mi hermano (Alejandro) y a mi padre por su apoyo incondicional en cada fase de mi vida.

A Eliezer por enseñarme a realizar las cosas con puntualidad, con eficiencia y sin estrés.

A mi abuela, quien día a día me guía con sus palabras de sabiduría, le agradezco por su apoyo maternal y por la sensación de tranquilidad que me brindan siempre sus consejos.

A mi abuelo, hombre sabio y lleno de juventud, quien con sus consejos me permiten formarme como persona. Gracias por enseñarme los valores de responsabilidad, honestidad, tenacidad y por formarme como un hombre trabajador.

A mis tías (Nancy, Yasmil, Naileth, Luisa) y tíos (Tovar, Javier, Robin) por estar ahí cuando más lo necesitaba, sin su apoyo definitivamente no hubiese sido posible llevar a cabo esta meta personal. Infinitamente gracias por darme valor para seguir adelante.

A mis primos (Jorge, Javier, Franchesca, Andrés, Victor) por hacerme reír y permitirme soñar con Venezuela y con todos los colores de mi mar Caribe, a través de las anécdotas cotidianas.

Gracias familia, por ser mi vista, mi olfato, mi gusto y mi tacto; gracias porque a través de vuestros mensajes he soñado y he estado presente con vosotros a pesar de estar ausente durante más de 3 años: muchos buenos momentos me he perdido, pero ha sido por una buena causa.

Un especial agradecimiento al grupo de investigación en el área de separación con biopolímeros de la Universidad Politécnica de Cataluña de Vilanova i la Geltrú, dirigido por Dra. Ana María Sastre y conformado por Montserrat Ruiz y Jesús Barrón, quienes dedicaron su tiempo y me orientaron de una manera excepcional en la realización de este trabajo. Muchas gracias por su apoyo y su calidad humana.

A mis compañeros de laboratorio quienes estuvieron presente y me ofrecieron su apoyo en la realización de este trabajo: Albert, Tobalina, Clement, Sergio, Jordi, Agnieska, Victoria.

A mis amigos y amigas (Rodrigo, Rafa, Cesar, Josep, Vero, Jaime, Leslie, Roger, Angel, Verena y Nerea) por acompañarme a lo largo de toda mi carrera, por brindarme su ayuda en esos momentos difíciles.

Un emotivo agradecimiento a Celia Llopis Mas por su ayuda, por ser mi ángel guardián en estas tierras catalanas, por los buenos consejos y por motivarme cuando lo necesité. A Iolanda Fernández por su buen humor, por su paciencia, y por su incondicional dedicación y entrega para la culminación de este trabajo

A Irene, Francina, Conchi, Elena; a los profesores Joaquim Casal, Nati Salvadó, Salvador Butí, Agustí Fortuny, Maria Teresa Coll, Emi Papiol, Miquel Bernadó, Lurdes Roset y Juan Jesus Perez quienes me ofrecieron su ayuda durante mi estancia en el departamento. A todos vosotros: Infinitas gracias.

AGRAÏMENTS

A Déu per brindar-me la fortalesa necessària per a seguir endavant en els moments més difícils de la meva etapa de formació.

A la meva mare que malgrat la distància ha estat present en cada moment, i aquestes curtes línies són insuficients per expressar-li la profunda estimació que sento per ella.

Al meu germà (Alejandro) i al meu pare pel seu suport incondicional en cada fase de la meva vida.

A Eliezer per ensenyar-me a realitzar les coses amb puntualitat, eficiència i sense estrès.

A la meva àvia, qui dia a dia em guia amb les seves paraules de saviesa, li agraeixo el seu suport maternal i la sensació de tranquil·litat que em brinden sempre els seus consells.

Al meu avi, home savi i ple de joventut, qui amb els seus consells em permet formar-me com a persona. Gràcies per ensenyar-me els valors de responsabilitat, honestedat, tenacitat i per formar-me com un home treballador.

A les meves tietes (Nancy, Yasmil, Naileth, Luisa) i tiets (Tovar, Javier i Robin) per estar al meu costat en els moments més importants, sense el seu suport definitivament no hagués estat possible portar a terme aquesta fita personal. Infinitament agraït per donar-me valor per seguir endavant.

Als meus cosins (Jorge, Javier, Franchesca, Andres i Victor) per fer-me riure i permetrem somiar amb Veneçuela i amb tots els colors del meu mar Carib, a través de les anècdotes quotidianes.

Gràcies família, per ser els meus ulls, olfacte, gust i el meu tacte; gràcies perquè a través dels vostres missatges he somiat i he estat present amb vosaltres a pesar d'estar absent durant més de tres anys: molts bons moments m'he perdut, però ha estat per una bona causa.

Un especial agraïment al grup d'investigació en l'àrea de separació amb biopolimers de la Universitat Politècnica de Catalunya de Vilanova i la Geltrú, dirigit per Dra. Ana Maria Sastre i conformat per Montserrat Ruiz i Jesús Barrón, que han dedicat el seu temps i em van orientar d'una forma excepcional en la realització d'aquest treball. Moltes gràcies pel seu suport i la seva qualitat humana.

Als meus companys de laboratori, els quals van estar presents i em van oferir el seu suport en la realització d'aquest treball: Albert, Tobalina, Clement, Sergio, Jordi, Agnieska i Victoria.

Als meus amics i amigues (Rodrigo, Rafa, Cèsar, Josep, Vero, Jaime, Leslie, Roger, Angel, Verena i Nerea) per acompanyar-me al llarg de tota la meva carrera, per brindar-me la seva ajuda en aquests moments difícils.

Un emotiu agraïment a Celia Llopis Mas pel seu suport, per ser el meu àngel protector en aquestes terres catalanes, pels bons consells i per motivar-me quan ho vaig necessitar. A Iolanda Fernández pel seu sentit de l'humor, per la seva paciència i per la seva incondicional dedicació i entrega per la culminació d'aquest treball.

A Irene, Francina, Conchi, Elena; als professors Joaquim Casal, Nati Salvadó, Salvador Butí, Agustí Fortuny, Maria Teresa Coll, Emi Papiol, Miquel Bernadó, Lurdes Roset i Juan Jesús Pérez als quals em van oferir el seu suport durant la meva estància al departament d'Enginyeria Química. A tots vosaltres: Infinites gràcies.

REMERCIMENTS

À mes amis de l'École des mines d'Alès:

Pour toute la période où j'ai été à l'école des mines d'Alès; je dois, avant tout, vous remercier pour votre manière de faire les choses pour qu'un petit étranger comme moi se sente comme chez lui.

Merci beaucoup, parce que malgré toutes les difficultés vous étiez toujours là pour me soutenir, pour me faire rire et pour me motiver dans les moments le plus difficiles.

Je dois vous dire que, depuis le Venezuela où j'ai entrepris un grand voyage de 8.000 km vers l'Europe, j'ai découvert de nombreuses cultures et coutumes que je ne connaissais pas avant. J'ai rencontré des gens de nombreux pays et j'ai partagé des idées qui ont été d'une grande valeur pour ma formation.

Ce grand voyage qui a commencé, il y a 3 ans, dans une ville qui s'appelle Valencia au Venezuela, a été le départ d'une belle aventure dans ma courte vie. Merci à vous, j'ai connu des gens d'une grande valeur humaine et extrêmement chaleureux.

Dans mon spirit resteront tous ces bons souvenirs de la cafète et du laboratoire; je n'oublierai jamais les conseils d'André Brun: ''Comment planter des tomates''. Je n'oublierai pas les conseils de ma marraine (Sylvie Spinelli) pour la préparation des confitures, et de pizzas-maison.

Je me souviendrai toujours des idéaux de révolution de Thierry Vincent et d'Eric Guibal. Les idéaux de révolte resteront vivants dans mon cœur; et comme mon parrain Rosario, je m'achèterai un Bazooka…

À Jose, Diego, Gustavo, Aziza, Nibal, Margarita, Dana, Cris, merci pour les bons moments qu'on a partagé ensemble. Je n'oublierai pas les blagues de Dedée et de la bonne humeur en général de tous (Jean-Claud, Mumu, Ingrid, Lionel). Mais surtout je n'oublierai jamais une personne très précieuse qui m'a énormément aidé pendant mon stage, une amie inconditionnelle: Cathy.

Quand je prendrai le chemin de retour, je me souviendrai vivement que "La France" est beaucoup plus qu'un grand pays. La France est beaucoup plus que le cœur de l'Europe et je sais que je continuerai toujours à cultiver mon Français (grâce à ma prof. de Français Sandra).

À tous vous: Merci beaucoup!

To my family: My reason to fight.

‘’Un camino de mil millas comienza con un solo paso’’.

INDEX

REMOVAL OF BORON FROM AQUEOUS SOLUTIONS USING BIOPOLYMERS AND COMPOSITES

Hary Demey Cedeño

Departament d'Enginyeria Química

Universitat Politècnica de Catalunya

This thesis summarizes the work published in the following papers:

[1] SORPTION OF BORON ON ALGINATE GEL BEADS
M. Ruiz, C. Tobalina, H. Demey-Cedeño, J. A. Barron-Zambrano, A. M. Sastre.
Reactive and Functional Polymers, **73** (2013) 653-657.

[2] BORON REMOVAL FROM AQUEOUS SOLUTIONS BY CALCIUM ALGINATE BEADS
M. Ruiz, J.A. Barron-Zambrano, H. Demey, A. M. Sastre.
EMChIE 2010 Conference Proceedings, **Vol. 2**, pp.783-791.
In: Dewil, R., Appels, L., Hulsmans, A. (Eds).
Leuven (2010) ISBN: 9789081548601.

[3] BORON REMOVAL FROM AQUEOUS SOLUTIONS USING ALGINATE GEL BEADS IN FIXED-BED SYSTEMS.
H. Demey, M. Ruiz, A. Barron-Zambrano, A.M. Sastre.
Journal of Chemical Technology and Biotechnology, **89** (2014) 934-940.

[4] EQUILIBRIUM AND DYNAMIC STUDIES FOR ADSORPTION OF BORON ON CALCIUM ALGINATE GEL BEADS USING PRINCIPAL COMPONENT ANALYSIS (PCA) AND PARTIAL LEAST SQUARES (PLS).
M. Ruiz, L. Roset, H. Demey, S. Castro, A. M. Sastre, J. J. Pérez.
Materialwissenschaft und Werkstofftechnik, **44** (2013) 410-415.

[5] DEVELOPMENT OF A NEW CHITOSAN/$Ni(OH)_2$-BASED SORBENT FOR BORON REMOVAL
H. Demey, T. Vincent, M. Ruiz, A. M. Sastre, E. Guibal.
Chemical Engineering Journal, **244** (2014) 576-586.

[6] BORON RECOVERY FROM SEAWATER WITH A NEW LOW-COST ADSORBENT MATERIAL
H. Demey, T. Vincent, M. Ruiz, A. M. Sastre, E. Guibal.
Chemical Engineering Journal, **254** (2014) 463-471.

[7] REMOVAL OF BORON FROM AQUEOUS SOLUTIONS BY A NEW ADSORBENT: COMPOSITE OF ALGINATE-ALUMINA.
H. Demey, A. Canadell, M. Ruiz, J.A. Barron Zambrano, A. M. Sastre.
Arabian Journal of Chemistry, (2014) submitted to publication.

[8] EFFECT OF SODIUM SALTS ON BORON REMOVAL USING ALGINATE GEL BEADS
H. Demey, M. Ruiz, J. A. Barron-Zambrano, M.T. Coll, A. Fortuny, A. M. Sastre.
Water Research, (2014) submitted to publication.

SUMMARY

The growing concern over environmental pollution in recent decades has placed increasing focus on research into the development of sustainable processes associated with the removal of contaminants in waters. Water is scarcer than three decades ago, and there is still no satisfactory solution for the removal of pollutants.

One element that has gained worldwide prominence is boron. Although it is a nutrient needed in small amounts for human and plant metabolism, higher levels are toxic to most plants and are associated with reproductive problems in humans. The World Health Organization (WHO) suggests a maximum concentration in drinking water of 2.4 mg L^{-1}, but many countries have not yet adopted this recommendation in their water treatment controls.

At present, there is no general method for boron removal; several techniques can be used, such as electrodialysis, precipitation, chemical coagulation and electrocoagulation, complexation/nanofiltration, phytoremediation, ion exchange, reverse osmosis and adsorption with different materials. The selection of a particular treatment technology should be made not only on the basis of its efficiency but also with consideration of the associated environmental and financial costs.

Biopolymers are a potential solution that has received little attention in the literature. Biopolymers and their derivatives are diverse and abundant in nature; they exhibit fascinating properties and are increasingly important in many applications thanks to their environmentally-friendly characteristics. A small number of publications report the possibility of using tannin gel (Morisada et al., 2011), cellulose cotton (Liu et al., 2007) or chitosan modified with N-methy-D-glucamine (Sabarudin et al., 2005), sugars (Matsumoto et al., 1999; Morisada et al., 2011) and diols (Gazi and Shahmohammadi, 2012; Oishi and Maehata, 2013; Fortuny et al., 2013). Biosorption is an effective, simple and cost-beneficial method for the removal of contaminants from waters.

This thesis focuses on the development of a sorption-based separation process, using biopolymers and composites for boron removal. The work has been carried out at the Department of Chemical Engineering of the Universitat Politècnica de Catalunya (UPC) in the framework of two research projects: *Desarrollo de procesos de separación/recuperación de boro mediante la utilización de membranas en configuración de fibra hueca con re-extracción por dispersión así como sorción sobre biopolimeros (Ref.: CTQ2008PPQ-00417/PPQ)* and *Técnicas avanzadas de separación utilizando líquidos iónicos como extractantes-disolventes en tecnología de membrana con renovación de membrana líquidas (HFRILM) y en procesos de adsorción (Ref.: CTQ2011PPQ-22412/PPQ)* financed by the Spanish Ministry of Science and Innovation (MICINN) and the FPI fellowship (BES 2009-026847) awarded by the MICINN. The doctoral training has been completed by three short stays at the Ècole des Mines d'Alès-France, also financed by the MICINN (REF.: EEBB-2011 44393; EEBB-2012 05455; EEBB-2013 07447).

This work is a continuation of research that has been underway at the Department of Chemical Engineering (UPC) for many years, on the development of advanced separation processes for the removal of valuable compounds or contaminants from aqueous solutions. It focuses on the elimination of boron from aqueous solutions, contributing to the state of the art on separation technologies (examples of which include the development of new composites based on the encapsulation of metal hydroxides in biopolymers).

Alginate and chitosan were effectively used as sorbents for boron recovery in the current research. Immobilization techniques were implemented using the technology described by Guibal et al., 2010; active materials are trapped in situ and distributed throughout the polymer support, creating a more stable adsorbent than those obtained by the traditional impregnation method, in which the active material is released partially from the pores of the polymer support while successive adsorption-desorption cycles are performed.

Three composite materials have been synthesized in order to improve the sorption capacity, the selectivity towards boron species, and the mechanical properties of the raw sorbents: calcium alginate/alumina (CAAl), which improves the sorption capacity of alginate in neutral medium; chitosan/nickel(II) hydroxide [chiNi(III)] and chitosan/Iron(III) hydroxide [chiFer(III)], which increase the sorption uptake of chitosan and improve the handling of hydroxides in the adsorption process, and are stable enough to be used in aggressive environments such as seawater without affecting sorption uptake.

CHAPTER I

INTRODUCTION

1.1 BORON: GENERAL ASPECTS

Improved knowledge of boron science in recent years has been of great importance to commerce and the environment, the research over the last decades has determined its scope as an essential element in chemical processes. Boron is located in Group 13 of the periodic table, followed by Al, Ga, In and Tl, is situated on the borderline between metals and non-metals, which makes it a metalloid with atomic number 5, atomic mass 10.81 amu and a +3 oxidation state (its behavior is similar for some aspects to that of its neighbors, aluminum, carbon and silicon). Its isotopes include ^{10}B and ^{11}B. Boron is a poor conductor of electricity at room temperature and highly refractory at higher temperatures, with a melting point of 2300 ºC that makes it difficult to prepare in a state of high purity. It has many applications, in the manufacturing of Pyrex and other heat resistant glass, in the production of detergents, soaps, stain removers, glass wool, fiberglass, porcelain enamel, herbicides, fertilizers, in metallurgy, etc. (Malavé, 2005).

Boron is widely distributed in nature and usually appears as borates. Studies of borate compounds have shown that boron atoms generally coordinate with three or four atoms of oxygen to form $[BO_3]$ or $[BO_4]^-$ groups. The simplest structure is the α-rhombohedral boron network, whose unit cell contains 12 equivalent atoms in the form of an icosahedron, which can be described as two pentagonal pyramids separated by bases related by a rotation of 36° (Figure 1.1).

Two Nobel awards (to Lipscomb in 1976 and to Brown and Wittig in 1979) have underlined the importance of B compounds to bonding theory and organic chemistry. The chemistry of boron, with the possible exception of carbon, is the most interesting and diverse case, as a result of the electron deficiency of many of its compounds: boron has only three valence electrons, which, when incorporated in three bond pairs, leave a p-orbital unfilled in the valence shell.

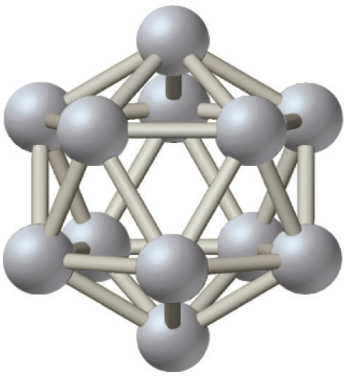

Figure 1.1. Boron icosahedral structure.

The electronic configuration of boron [He]$2s^2 2p^1$ suggests that it might form univalent compounds. Boron utilizes three valence electrons to combine with other elements to form trigonal planar compounds of type BR_3 with covalent bonds (where R is hydroxyl, alkoxy, aryloxy, alkyl, halogen, etc.) (Schubert, 2003).

An important feature of boron is the very small size of the B^{3+} cation (three-coordinate boron, 0.01 Å; four-coordinate boron, 0.11 Å), which leads high ionic potential and a particular affinity for electronegative elements. Schubert, 2003 also explains that since boron has one more valence orbital (*s, p_x, p_y, p_z*) than valence electrons, trivalent boron compounds tend to form complexes with electron donors, including reversible reactions with anionic Lewis bases to form tetrahedral anions in which boron has a formal negative charge.

According to Power and Woods, 1997, and Malavé, 2005, boron is not found free in nature and is usually bound to oxygen. It exists mostly as borates, less frequently as boric acid, and is rarely linked to fluorine ion to form BF_4^-. The main sources of boron are formed by deposits of various minerals such as borax (tincal) $Na_2[B_4O_5(OH)_4].8H_2O$, colemanite $Ca[B_3O_4(OH)_3].2H_2O$, kernite $Na_2[B_4O_5(OH)_4].2H_2O$ and ulexite $NaCa[B_5O_6(OH)_6].5H_2O$.

The electrophilicity of boron, coupled with a related tendency to readily and reversibly form esters and anhydrides through condensation-bearing hydroxyl groups (including B-OH compounds), justifies its extensive use in industry as well as its essential biological roles.

1.2 BORON DISTRIBUTION IN THE ENVIRONMENT

According to Hilal et al., 2011 boron concentration in the Earth's crust varies from 1 to 500 mg kg^{-1} depending on the nature of the soil. Krauskopf, 1972 estimated an average concentration in the Earth's crust of 10 mg kg^{-1} (boron accounts for 0.001% of the Earth's elemental composition). The total amount of boron stored in lithosphere was presented by Argust, 1998. Boron distribution in the environment can be summarized as follows:

- Continental and oceanic crusts (10^{18} kg B).
- Commercial borate deposits (10^{10} kg B).
- Coal deposits (10^{10} kg B).
- Biomass (10^{10} kg B).

The distribution of boron in the hydrosphere was also identified by Argust, 1998:

- Oceans (10^{15} kg B)
- Groundwater (10^{11} kg B)
- Surface waters (10^{8} kg B)
- Ice (10^{11} kg B)

1.2.1 Boron in seawater

Boron is the tenth most abundant element in oceanic salts (Mellor, 1980), varying in concentration in seawater from 0.52 mg L^{-1} in the Baltic Sea to as much as 9.57 mg L^{-1} in the Mediterranean Sea. The global average, however, is between 4.6-4.8 mg L^{-1} (Argust, 1998).

Boron can be transmitted from seawater to the atmosphere through a process whereby boron salts are injected into the atmosphere directly at the water-air interface, and through the volatilization of boron as boric acid, H_3BO_3. Anderson et al., 1994 have determined that between 1.3 and 1.4 million tons of boron are transmitted to the atmosphere from marine sources each year via these mechanisms (Argust, 1998; Romheld and Marschner, 1991).

It has also been suggested that boron may be present in other reservoirs in the hydrologic cycle, such as groundwater, surface water and ice (Argust, 1998). In most groundwater, boron concentration varies greatly, from 0.017 mg L^{-1} to 1.9 mg L^{-1}, as a result of several parameters (proximity to sea, geothermal activity, presence of boron-rich minerals, etc.).

1.2.2 Boron mining and processing

Boron in rocks is usually found in mines in arid regions of Turkey, Argentina, Chile, Russia, China, Peru, and the United States; Turkey and the United States are the largest producers of boron in the world. Global commercial borate deposits are estimated at 10 million metric tons, and Turkey has almost 72% of the world's boron reserves.

Although the largest boron deposits on Earth are found in central and western Turkey, many are still untapped. The United States (Mojave Desert, California) is home to the largest open-pit and the largest borax mine in the world, producing nearly half of the world's borates.

The main steps in the mining and processing of borates at the borax mine in California are as follows (Argust, 1998): i) the overburden (the clay material that covers the ore) and the borate ore itself are loosened by explosive blasting; ii) the overburden is removed and the borate ore is then extracted with mechanical shovels, transported to a primary crusher and stockpiled for processing; iii) the borate ore is dissolved and screened,

thickened in settling tanks, and the solution cooled in vacuum crystallizers to form the crystallized product, then dried and cooled before being sent to silos to await shipping; iv) borate not recovered from the mining and processing stages emerges in mixtures of insoluble material and impurities separated during the processing stages, called gangues, which are moved to stockpiles or solar ponds, where they are concentrated by solar action for subsequent reprocessing. Dust houses recover the dust created during the crushing stages to be reused in processing.

The general procedure for obtaining boric acid consists in adding finely ground borate into hot sulfuric acid solution, stirring continuously. After the reaction, the precipitated sulfates are separated and the remaining solution is filtered and allowed to crystallize. Borax is obtained by refining sodium borates by dissolution and subsequent recrystallization, and also by reaction between boric acid and sodium carbonate.

Figure 1.2 (adapted from U.S. Geological Survey data 2006-2013) shows the increase of boron production in Turkey over the last decade; in the last three years alone it has increased by 20% (from $2.0x10^6$ to $2.5x10^6$ metric tons). The main four borates (colemanite, kernite, tincal, and ulexite) make up 90% of the borates used by industry worldwide. Although borates can be used for more than 300 applications, over three-quarters of the world's supply is sold for four end uses: ceramics, detergents, fertilizers and glass.

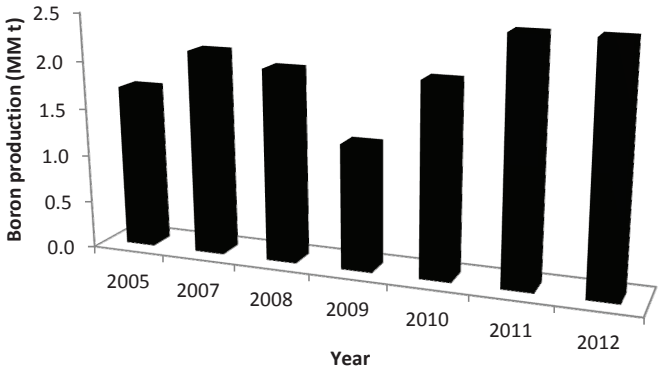

Figure 1.2. Boron production in Turkey.

Data provided by U.S. Geological Survey (2006-2013).

Figure 1.3 shows the main global uses of borates; the production of glass, ceramics, detergents and fertilizers are the primary markets for boron compounds (glass and ceramics account for more than half of worldwide production). Table 1.1 summarizes the boron production of major global producer countries; as can be seen, production has increased to meet the anticipated rise in borate consumption in 2014 and the coming years, driven by strong demand in South American and Asian ceramics, glass and agricultural markets. Boron consumption was projected to increase 7% annually through 2013, spurred by a projected 19% increased in Chinese consumption. Demand for borates was expected to shift slightly away from detergents and soaps toward glass and ceramics.

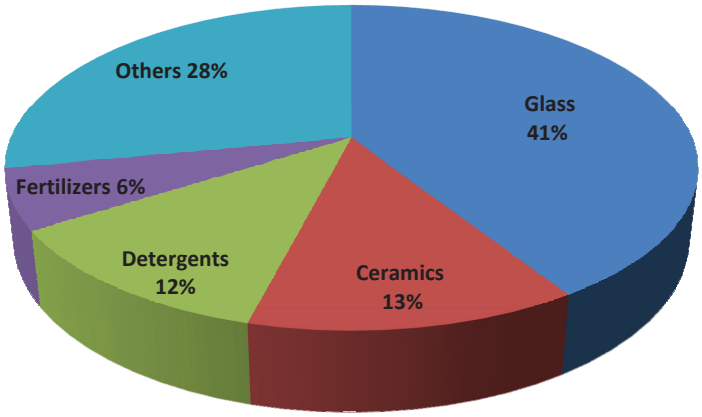

Figure 1.3. Main uses of boron compounds.

Table 1.1. World boron production and reserves

Production expressed in thousand metric tons of boric oxide (B_2O_3)								
Major producers	**2005**	**2007**	**2008**	**2009**	**2010**	**2011**	**2012**	**Reserves**
Turkey	1700	2130	2000	1300	2000	2500	2500	60000
United States	1150	**W**	**W**	**W**	**W**	**W**	**W**	40000
Argentina	820	550	785	750	600	600	600	2000
Bolivia	68	50	56	83	97	135	140	**NA**
Chile	590	528	583	608	504	489	500	35000
China	140	145	140	145	150	100	100	32000
Iran	3	2	2	2	2	1	1	1000
Kazakhstan	30	30	30	30	30	30	30	**NA**
Peru	9	10	350	187	293	293	300	4000
Russia	400	400	400	400	400	400	400	40000
World total (rounded)	4910	3845*	4346*	3505*	4076*	4548*	4571*	214000

W = Withheld to avoid disclosing company proprietary data, NA = Not available, *excluding US production.

Data provided by U.S. Geological Survey (2006-2013).

China has low-grade boron reserves and anticipates substantial demand for boron in the near future; Chinese imports from Turkey, United States, Chile and Russia are expected to increase during the next few years. European and emerging markets have introduced more stringent heat conservation requirements in their building standards, so increased borate consumption for fiberglass insulation is expected. On-going investment in new technologies and the continued rise in demand are expected to fuel growth in global production in the coming years. In Table 1.1 Production data for the United States was not provided by the

U.S. Geological Survey to avoid disclosing proprietary data (since two companies produce borates in southern California).

Borate deposits around the world (Table 1.1) are associated with volcanic activity and arid climates. Approximately 70% of Turkish deposits consist basically of colemanite, while U.S. deposits consist primarily of tincal, kernite and, to a lesser extent, ulexite and colemanite (U.S. Geological Survey, 2013).

1.3 BORON TOXICITY

1.3.1 Toxicity in humans

Boron is an element found in nature with an estimated average concentration in the Earth's crust of 10 ppm (Woods, W., 1994). However, industrial activities have raised boron concentration in the rivers of several borax-producing countries in recent years.

The greatest exposure to boron for most populations comes from food; food groups rich in boron include fruit, mushrooms, leafy vegetables, nuts and legumes. Meacham and Hunt, 1998 found that meat and fish are low in boron. Consequently, vegetarians are the most exposed population. Rainey et al., 1999 reported a typical daily boron intake in the US population of 1.14 mg day^{-1} for men, 0.96 mg day^{-1} for women and a mean intake of 1.47 mg day^{-1} for vegetarian men and 1.29 mg day^{-1} for vegetarian women. Water could be an important source of boron; water deposits located close to large-scale borax mines have been found to contain high boron concentrations.

There is clear evidence that boron compounds are metabolized in the human body. Orally, boron is readily absorbed by animals and humans through the gastrointestinal tract. Over 90% of an orally administered boron dose is excreted in the urine in a short period of time by both humans and animals (Jansen et al., 1984; Schou et al., 1984; Vanderpool et al., 1994; Usuda et al., 1998). Studies in rats and of boron miners indicated that boron can be absorbed by inhalation (Culver et al., 1994; Wilding et al., 1959) but it is not known how much can be absorbed directly through the mucous membranes of the respiratory tract. Research carried out by Draize and Kelley, 1959, indicates that boron is not absorbed dermally by humans or animals but can be absorbed through damaged skin tissue.

Boron in the body exists primarily as undissociated boric acid and is distributed through the soft tissues (Ku et al., 1991; Naghii and Samman, 1996). Although it does not accumulate in soft tissues, boron has a tendency to accumulate in bone, reaching higher accumulated levels after 1−4 weeks than those observed in plasma (Ku et al., 1991; Chapin et al., 1997). Boric acid is not degraded in the body but can form complexes with biomolecules through concentration-dependent mechanisms (Institute for Evaluating Health Risks, 1997; WHO, 1998).

Studies in laboratory animals revealed the effects produced by a continuous dose of boron in the reproductive organs; the results showed reduction in testis mass, atrophy, degeneration of the spermatogenic epithelium, reduced fertility and sterility (Weir and Fisher, 1972; Seel and Weeth, 1980; US National Toxicology Program, 2010; Fail et al., 1991; Dixon et al., 1979; Linder et al., 1990; Treinen and Chapin, 1991; Ku et al., 1993). Other adverse health effects have also been reported, such as high prenatal mortality, decreased fetal body

mass, and malformations of the eyes, cardiovascular system and axial skeleton (Price et al., 1996a; Price et al., 1996b; Field et al., 1989).

The symptoms of acute boron poisoning are nausea, vomiting, diarrhea, skin rashes and peeling of the epidermis. In severe cases death occurs after 5 days by cardiovascular collapse and shock (Harvey et al., 1975). The estimated lethal doses of boric acid are 15−20 grams for adults and 5−6 g for children (Siegel and Wason, 1986; Dixon et al., 1976; Santé Canada, 1990).

It should be noted that there is insufficient data linking boron exposure to cancer. Studies conducted in laboratory animals were deemed inadequate (US EPA, 2004) and it was concluded that there is insufficient data to determine the carcinogenic potential of boron in humans.

1.3.2 Effect on mammalian sperm motility

Different authors have reported the influence of boron exposure on the mammalian organism, but the most important effect is probably boron's ability to disrupt the reproductive system (Cox, 2004). Although boron is not classified as a carcinogenic substance (no evidence was found by US EPA, 2004 in laboratory tests), it can seriously affect the reproductive system in mammals.

Studies performed by the National Institute of Environmental Health Science under its national toxicology program have shown that sperm from rats and mice fed regularly with boric acid exhibits lower motility. As shown in Figure 1.4 (adapted from Ku and Chapin, 1994), increasing the boron dose decreases sperm motility further (even at the lowest doses tested, motility was affected). It was also found that at higher exposure levels, boric acid inhibits the release of sperm from the testes and can cause atrophy of the reproductive organs in both rats and mice; further research showed that boric acid inhibits the formation of DNA in sperm cells (Cox, 2004).

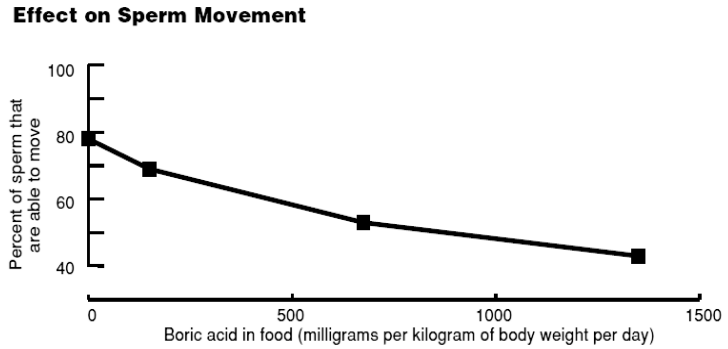

Figure 1.4. Effect of boric acid on sperm motility.

Figure adapted from the literature (Ku and Chapin, 1994).

Several studies performed with mice and female rabbits during pregnancy showed higher mortality rates in animals fed with boron: a reduction in litter size of around 50% was observed at a dose of 4500 mg L^{-1}, while no litters were produced in animals that received a higher dose of 9000 mg L^{-1}. Examination of three generations of rats confirmed a significant reduction in the number of litters when the mother consumed boron (Cox, 2004).

1.3.3 Toxicity in plants

Tolerance in different plant species is related to the rate of boron accumulation rather than the resistance of tissues to the resulting toxicity. As such, some plants are more tolerant than others; tolerant plants accumulate boron at a very low rate whereas sensitive plants accumulate it very quickly. Boron is an essential element in plant nutrition and growth, but there is an important micronutrient-toxic boron duality: a minimum concentration is required for the plant's survival but an excessive concentration produces negative effects and may lead to poor performance in plant crops.

The adverse effects of boron on plants have been extensively reviewed (Hilal et al., 2011). In most crops, the symptoms of boron toxicity present as burned edges on older leaves, yellowing of the leaf tips, accelerated decay, and ultimately death; the adverse physiological effects may also include reduced root cell division, retarded shoot and root growth, inhibition of photosynthesis, deposition of lignin and suberin, and reduced leaf chlorophyll (Hilal et al., 2011). The appearance and severity of these effects depend on the amount excess of boron and the tolerance level of the plant (Nadav, 1999).

In general, boron toxicity in plants is due to the quality of the irrigation water used and the soil boron content. The main types of soils affected by excess boron content are usually those derived from marine sediments and soils in arid or semi-arid regions where low rainfall results in very little leaching (Rodriguez-Guerrero et al., 2009). Table 1.2 shows the tolerance levels of certain crops and the maximum permissible boron concentrations to ensure satisfactory yields (Hilal et al., 2011); an optimal concentration for a given crop may be harmful or insufficient to other plants. In general, an irrigation water boron content greater than 4 mg L^{-1} is unsuitable for most crops.

Table 1.2. Boron tolerance limits for agricultural crops

Tolerance	Concentration of boron in soil water (mg L^{-1})	Agricultural crop
Extremely sensitive	< 0.5	Lemon*, blackberry*
Very sensitive	0.5−0.75	Orange*, apricot*, grapefruit*, avocado*, peach*, cherry*, plum*, persimmon*, grape* walnut*, pecan*, onion
Sensitive	0.75−1.0	Garlic, sweet potato, wheat, sunflower, mung bean*, sesame*, lupine*, strawberry* Jerusalem artichoke*, kidney bean*, snap bean, lima bean*, peanut
Moderately sensitive	1.0−2.0	Broccoli, red pepper, pea*, carrot, radish, potato, cucumber, lettuce*
Moderately tolerant	2.0−4.0	Cabbage*, turnip, barley, cowpea, oats, corn, artichoke*, tobacco*, mustard*, sweet clover*, squash, muskmelon*, cauliflower, Kentucky bluegrass*
Tolerant	4.0−6.0	Tomato, sugar beet, red beet, parsley*, purple vetch*, alfalfa*
Very tolerant	6.0−10.0	Sorghum, cotton, celery*
Extremely tolerant	10.0−10.5	Asparagus*

*Tolerance based on reduction in vegetative growth. Table adapted from the literature (Hilal et al., 2011).

1.3.4 Dose response and permissible boron levels in Spain

All substances have toxic effects when consumed in high doses. European Union directive 67/548/EEC on the classification, packaging and labeling of dangerous substances classifies boron and boron derivatives as category 2 *toxic materials with adverse effects on reproduction*. This classification is based on animal experiments, in which very high doses that are not commonly encountered in daily human life were used.

Such effects have only been observed in boron mine workers, who are subject to excessive exposure through respiration. Investigations conducted in rats by Price et al., 1996a, Price et al., 1994, Price et al., 1990 and Heindel et al., 1992 were identified as critical studies by the US EPA, 2004 because their results provided the data points for the No Observed Adverse Effects Level (NOAEL) and Low Observed Adverse Effects Level (LOAEL). Adverse effects on reproductive organs were found in dogs, rats, mice and other animals by Weir and Fisher,1972, Seal and Weeth, 1980, the US National Toxicology Program, 2010, Fail et al., 1991, Dixon et al., 1979, Linder et al., 1990, Treinen and Chapin, 1991, and Ku et al., 1993.

In a two-year study conducted by Weir and Fischer, 1972, different boron doses were administered in the daily diet to a group of laboratory rats. At high boron doses, rats exhibited coarse hair, scaly tails, hunched posture, abnormally long toenails, shrunken scrotum, inflamed eyelids and bloody eye discharge. The absolute weights of testes were significantly lower than in controls (EFSA, 2004). The estimated boron dose at which risk to humans may exist is based on animal experiments because no human data is available. The non-carcinogenic reference dose (RfD) is 0.2 mg $kg^{-1}day^{-1}$, according to the analysis carried out by the US EPA in 2004; this amount represents 0.2 mg of boron per kilogram per day.

The World Health Organization recommends a boron concentration limit of 2.4 mg L^{-1} for drinking water (WHO, 2011). Nevertheless, in the European Union the limit is set at 1.0 mg L^{-1}. Japan uses the same limit as the EU, but in other countries such as New Zealand and Israel the permissible values are 1.4 mg L^{-1} and 1.5 mg L^{-1}, respectively. In the United States there are no federal regulations and permissible levels are determined by each State (e.g. Florida = 0.63 mg L^{-1}, California = 1.0 mg L^{-1}, and Minnesota = 0.6 mg L^{-1}). Saudi Arabia is the only country that uses the World Health Organization guide limit; Canada and Australia have permissible boron levels for drinking water of 4 mg L^{-1} and 5 mg L^{-1}, respectively (Hilal et al., 2011). Spain follows EU policy for drinking water (1 mg L^{-1}) and establishes a maximum permissible boron concentration in industrial effluents of 3 mg L^{-1} (Royal Decree 130/2003).

1.4 THE PROBLEM: HIGH BORON CONCENTRATION IN WATER BODIES

High levels of boron in water sources have two main causes: natural and anthropogenic. Boron reaches the hydrosphere through the erosion of rocks; however, water boron levels have increased due to pollution caused by industrial growth. The erosion of rocks containing boron may increase the concentration of this element in rivers and lakes. In some South American rivers, boron concentrations of between 4 and 26 mg L^{-1} have been recorded, due to their proximity to natural deposits (Rodriguez-Guerrero et al., 2009; Smallwood, 1998) but mining activities (anthropogenic actions) in the last decades have accelerated this type of pollution, as is the case of the Simav river in Turkey, which passes through the main areas of borate reserves of this country (Okay et al., 1985).

Boron compounds are widely used in the manufacturing of glass, soaps, detergents, pesticides, cosmetics and agricultural fertilizers. They can also be used in the preservation of food, in lumber treatment, in the synthesis of high energy fuel, in catalysis, and in the manufacturing of cutting fluids.

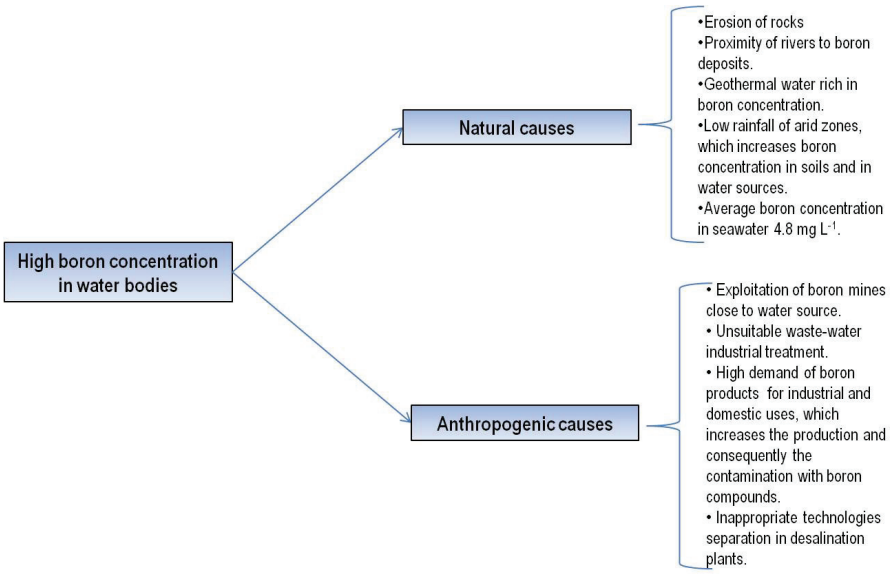

Figure 1.5. Causes of high boron levels in water bodies.

Figure 1.5 summarizes the main causes of high boron concentrations in water. A very serious problem is encountered in the final stages of sewage treatment and in seawater desalination, where boron concentrations exceed the limit established in European legislation (1 mg L^{-1}); this is a particular concern because the treated water is intended for human consumption. In the case of seawater, high salinity is generally associated with high boron content. High salinity is found in hot climates in areas such as the Red Sea, the Persian Gulf, the Caribbean Sea and the Mediterranean Sea. Reverse osmosis technology and thermal processes are currently used to remove boron from water, but further research is required because these technologies have high operating and maintenance costs.

Wyness et al., 2003 presented a review of boron surface water quality based on EU data provided by national environment and river authorities. They found that borate concentrations in surface waters vary throughout Europe, from less than 0.01 mgB L^{-1} to more than 1 mgB L^{-1}; this variation is due to both natural and anthropogenic factors (Neal et al., 1998). Table 1.3 shows a summary of boron concentration levels in consumable water for selected European countries. The concentration levels are different for each country, and the highest values are recorded in Portugal, Spain, France and Belgium.

In Spain, boron concentration in rivers is generally below 0.2 mgB L^{-1}, but concentrations in excess of 1 mgB L^{-1} have been recorded in some southern and eastern areas, particularly to the west of the Jucar river in the Valencian Community (Figure 1.6), where untreated industrial wastewater from a range of applications (mainly textile, paper and canned vegetable factories) is discharged into the river. These industries use boron compounds in their production processes: in textile factories, decaborane is normally used as a mothproofing agent and sodium perborate is used for fabric bleaching (it is also used in the manufacture of soaps, detergents and deodorants); in the food industry, boron trifluoride is commonly used in food packaging.

Table 1.3. Summary of boron concentration data for European countries

Country	No. of monitoring Points	Date coverage	Total samples	Percentages of values greater than 1 (mgB L^{-1})
Austria	30	1998-2000	712	0.0%
Belgium	651	1998-2000	5056	1.1%
Finland	463	1995	463	0.0%
France	25	1995-2000	1304	1.8%
Germany	197	1980-1995	197	1.0%
Ireland	185	1999-2000	185	0.5%
Italy	64	1998-1999	926	0.0%
Netherlands	9	1986-1999	1842	0.0%
Portugal	8	1999-2000	129	11.6%
Spain	328	1991-2000	4272	2.5%
United Kingdom	98	1974-2000	22329	0.004%

Table adapted from the literature (Wyness et al., 2003).

For the specific case of Catalonia (Figure 1.7), data on boron concentrations in surface waters over the period 2008-2013 provided by the Catalan Water Agency were thoroughly analyzed; boron concentrations in the outflow from water purifiers is not controlled and no specific technologies are installed to deal with possible contamination. Figure 1.7 shows the maximum boron concentrations (mg L^{-1}) registered for each river in Catalonia over the last four years.

In general, the main Catalan rivers appear to have high water quality and low boron concentrations; nevertheless, concentrations recorded at some points in the Anoia river were ten times higher than those found in the other rivers for the same period (a maximum of 1.9 mg L^{-1} was registered by the Catalan Water Agency). This is principally due to the proximity of industries which use boron in their production chains (mainly paper, leather and ceramics) and discharge wastewater into the river. In the leather industry, sodium tetraborate (borax) is used as a reagent for tanning; in the paper industry, sodium borohydride is widely employed as a bleaching agent for paper pulp; in the ceramic industry, boric oxide is a component of glazes and sodium tetraborate is a component of enamels and porcelain. Further research is required to identify possible solutions in the case of high levels of boron contamination.

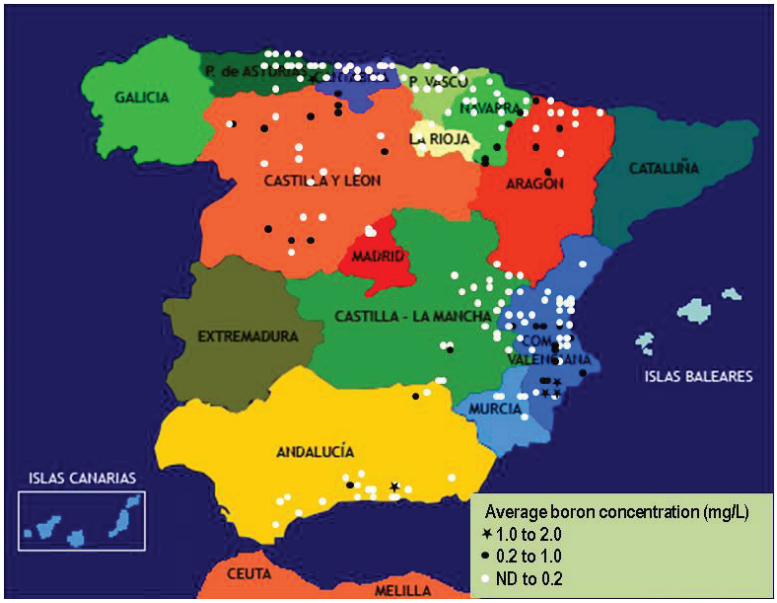

Figure 1.6. Distribution of boron concentrations in Spain.

Figure adapted from the literature (Wyness et al., 2003).

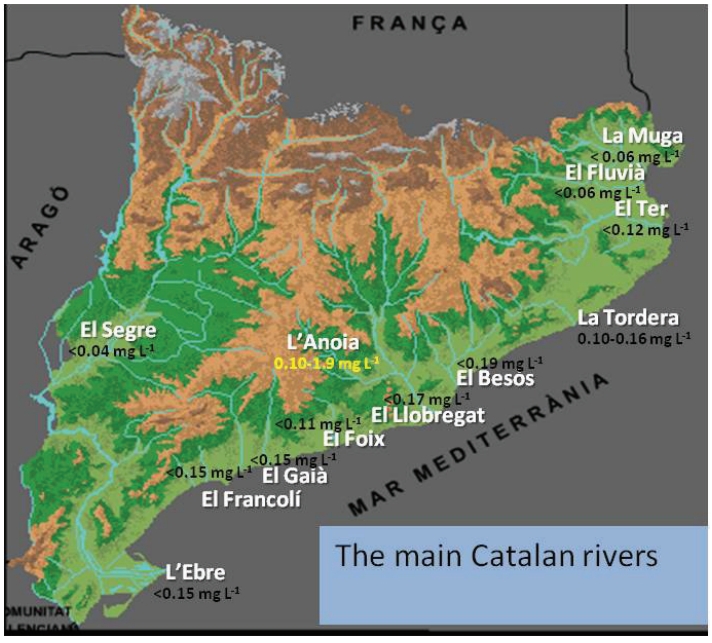

Figure 1.7. Distribution of boron concentrations in Catalan rivers (2008-2013).

In short, the problem created by boron excess in water may come from different sources. In order to avoid a contamination with this element due to its toxic effect in humans and plants, this research aims to provide a viable alternative to remove efficiently the boron content in water by using the biosorption technique employing biopolymers and composites as adsorbents.

1.4.1 A review of existing boron removal technologies

In the last decade many techniques have been used for boron removal, including electrodialysis (Yazicigil and Oztekin, 2006) precipitation (Itakura et al., 2005), chemical coagulation and electrocoagulation (Yilmaz et al., 2007; Koparal, et al., 2002), complexation/nanofiltration (Dosoretz et al., 2006), phytoremediation (Del Campo-Marin and Gideon, 2007), ion exchange (Simonnot et al., 2000; Kabaya et al., 2004), reverse osmosis (Prats et al., 2000; Cengeloglu et al., 2008) and adsorption with different materials (Öztürk and Kavak, 2005; Kavak, 2009).

Boron separation technologies currently used around the world are mainly employed in seawater purification (desalination processes). According to Tagliabue et al., 2014, boron levels have been substantially reduced by thermal desalination (based on multi-stage flash (MSF) or multi-effect distillation (MED)) and membrane processes (including reverse osmosis (RO), ultrafiltration (UF), microfiltration (MF) and nanofiltration (NF)). Although these technologies are widely used for water desalination in many countries, they generate high energy consumption (Ghaffour et al., 2013); and many of the membranes used for boron separation are not effective enough to reach acceptable concentration levels. Consequently, alternative approaches have been developed, at both the industrial and laboratory scales: Cengeloglu et al., 2008 investigated boron removal through reverse osmosis membranes, BW-30 (FILMTEC) and AG (GE Osmonics). Their experimental results indicated that the effectiveness of boron removal from the feed water depends mainly on the type of membrane, the pH and the operating pressure. They also found that boron is effectively removed at high pH (pH 11) and that increasing the operating pressure increases the percentage of separation.

Figure 1.8 (adapted from Ghaffour et al., 2013) shows the main desalination technologies in current use around the world; more than 60% of the total is carried out using membrane process and 34.2% is performed using thermal processes. According to Ghaffour et al., 2013, these figures change constantly due to the on-going expansion of the desalination market.

It was estimated in 2010 that global water desalination capacity was 64 million m^3 day^{-1} (Ghaffour et al., 2013), but this value is expected to increase by more than 50% (to 98 million m^3 day^{-1}) in the coming years due to rising demand for water and by the significant fall in desalination costs thanks to technological improvements that make the process more cost-competitive. To achieve a more cost-competitive process, hybrid systems were proposed (Kabay et al., 2013), which combine two or more processes to raise desalination efficiency and lower costs (the removal uptake obviously depend on the feed water, since seawater is more difficult to desalinate than brackish water).

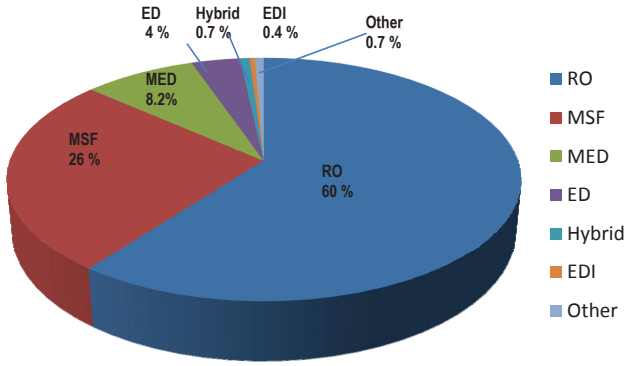

Figure 1.8. Desalination technologies in current use.

Adapted from the literature (Ghaffour et al., 2013).

Processes such as electrodialysis and electrocoagulation continue to be developed, despite their high energy consumption: Yazicigil and Oztekin, 2006 used an electrodialysis process with anion exchange membranes for boron separation from aqueous solutions. Several variables such as pH, current density, membrane type and concentration of different types of salt solutions were evaluated. Maximum boron removal was obtained under conditions in which the maximum current was applied at pH 9. Yilmaz et al., 2007 performed a quantitative comparison of electrocoagulation and chemical coagulation for boron removal. Using aluminum chloride as a coagulant, they found that electrocoagulation removes a greater percentage of boron under the same operating conditions. In optimal operating conditions (pH 8 and aluminum concentration 7.45 g L^{-1}), 94% of boron was removed by electrocoagulation, compared to 24% by chemical coagulation.

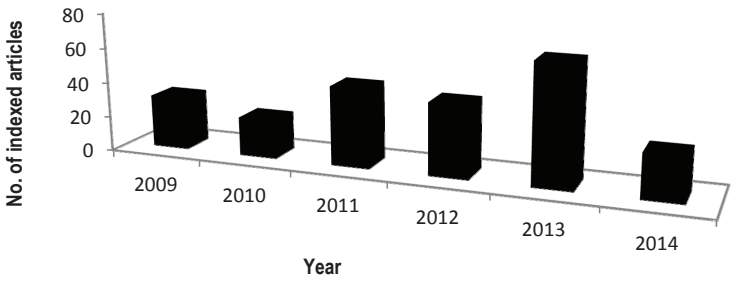

Figure 1.9 Number of published articles (indexed in Scopus) on boron removal.

Due to increased concern in various countries with efficient alternatives for boron removal from water, research output on this subject has increased in the last five years, as shown in Figure 1.9. From 30 Scopus-indexed publications in 2009, the figure grew to 68 in 2013, with a total of 231 indexed articles published as of April 2014 (for the period 2009-2014). Output is expected to increase further in the coming years, and in the period January-April 2014 alone the number of published articles equaled to total for the whole of 2009. Fifty-one international patents were registered in the period 2009-2013, most of them for adsorption and membrane processes.

It should be noted that adsorption has been widely regarded as a good boron removal solution over the last five years (Figure 1.10) and is the subject of the largest proportion of published articles; 35.5% of the Scopus-indexed publications considered here deal with adsorption, 26.8% with membrane processes, 10.4% with hybrid membrane-sorption processes, and 27.3% with other techniques such as electro-coagulation, phytoremediation, liquid-liquid extraction, chemical coagulation and precipitation.

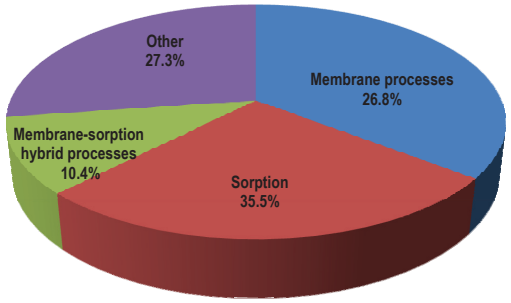

Figure 1.10. Boron removal techniques addressed in published research over the last decade.

Adsorption has become particularly important in this field due to the low cost of the adsorbents used; thus, materials that are treated as waste in many industrial processes can be reutilized to separate/recover boron from water. Studies using sepiolite (Öztürk and Kavak, 2004), siral-30 and pural (Seki et al., 2006), bentonite (Karahan et al., 2006), red mud (Cengeloglu et al., 2007), ash (Öztürk and Kavak, 2005) and impregnated carbon (Kluczka et al., 2007) have been performed.

Rhom & Haas (now The Dow Chemical company) has developed a boron-selective ion exchange resin (BSR) consisting of a macro-porous polystyrene matrix bearing N-methyl-D-glucamine functional groups. The operation mechanism of this resin can be summarized as follows (Tagliabue et al., 2014): i) borate ion complexation by two sorbitol groups releasing protons in solution; ii) proton capture by tertiary amine sites that behave as weakly basic anion exchangers, thus preventing pH decrease. In addition, two steps must to be carried out for resin regeneration (Tagliabue et al., 2014): i) acid washing (normally HCl or H_2SO_4 solutions) to elute chemisorbed boron as boric acid; ii) basic washing (generally NaOH or ammonia solutions) to convert ammonium into amine groups and to sweep resulting salts.

Simonnot et al., 2000 investigated boron removal from water using a continuous system with Amberlite IRA-743. They concluded that the retention of boron is not pH- or ionic strength-dependent in the intervals studied but also explained that the resin is well suited to removing boron from aqueous solutions. Minimizing the amount of chemicals required for BSR regeneration is a key factor in large-scale implementation (Tagliabue et al., 2014); it has been observed that higher stirring speeds in BSR batch experiments increases the initial boron removal rate. Kabay et al., 2008 investigated the performance of BSRs for boron removal from seawater RO permeate. Seawater samples with a boron concentration of 5.1 mg L^{-1} and ion exchange resins (Dowex 02, Diaion CRB-XUS 43594.00) containing groups of N-methyl-D-glucamine were evaluated; the optimal amount of resin was 1 g L^{-1} and equilibrium was reached at 30−45 min for Dowex and at around 20−30 min for Diaion.

Some authors such as Cengeloglu et al., 2008 have investigated the use of industrial waste sludge (red mud), which is rich in silica and aluminum, for the adsorption of boron from aqueous solutions, in order to find a feasible alternative for the removal of boron compounds from industrial effluents. They examined the performance of neutralized red mud as an adsorbent as a function of variables such as pH (2-7), adsorbent mass dose (1-8 g L^{-1}), initial boron concentration (12-200 mg L^{-1}) and contact time (20-200 min). The results indicated that boron uptake increases as pH is increased; equilibrium was reached within 20 min.

Kavak, 2009 investigated boron adsorption by using calcined alunite; a full factorial design (two level) was performed to examine the influence of temperature (25−45 ºC), pH (3−10) and mass of adsorbent dose (0.5 g and 1 g of adsorbent to 25 ml of solution). The results indicated that these factors affect boron removal: boron uptake increases when pH and the amount of sorbent are increased but decreases with increasing temperature. The optimum conditions were found at pH 10, adsorbent mass 1 g and temperature 25 °C; the maximum adsorption capacity obtained was 3.39 mg g^{-1}.

Similarly, Östürk and Kavak, 2005 investigated boron adsorption using coal ash (fly ash); the effect of pH, initial boron concentration, temperature, adsorbent mass dose and the presence of foreign ions on adsorption capacity was studied. Fly ash was found to be an effective adsorbent for removing boron from aqueous solutions; the optimum operating conditions in a batch system were obtained at pH 2 and 25 °C, and the highest adsorption capacity obtained was 20.9 mg g^{-1}. The Langmuir isotherm equation fitted well to the experimental equilibrium data and the pseudo-second-order model gave a better fit than the pseudo-first-order model in the kinetic study.

Chong et al., 2009 studied boron adsorption from ceramics industry effluents using a waste ash from the manufacturing process of palm oil (palm oil mill boiler, POMB). Particle size was found to have an effect on sorption capacity: a lower adsorbent particle size improved the boron removal. The best operating conditions were obtained with a particle size of 0.5 mm, 40 g of adsorbent in 300 ml of effluent (without pH adjustment), and an agitation speed of 100 rpm for 1 h. Boron concentration was reduced from 15 mg L^{-1} to 3 mg L^{-1}. The purpose of this research was to identify a feasible alternative for boron removal from water and to provide an application for residual ash from POMB in countries where palm oil production is abundant.

The use of metal hydroxides has also been considered as a possible solution for boron recovery; De la Fuente García-Soto and Muñoz, 2006 and 2009 studied boron adsorption using magnesium oxide as sorbent and

found that MgO has alkaline properties that improve adsorption at basic pH: Boron uptake rose as temperature and pH were increased.

Yurdakoc et al., 2005 studied boron adsorption using aluminum oxide (Al_2O_3)-based materials. A full factorial design was used to investigate the influence of three main factors on the adsorption process: pH (5.7−9.5), temperature (298−318 K) and type of adsorbent (Siral 30 and Pural 30). It was found that the interaction between the type of adsorbent and temperature positively contributes to the removal of boron from aqueous solutions. Siral 30 was more efficient than Pural 30 as an adsorbent for boron removal, and adsorption capacity rose as temperature and pH were increased.

Although studies of adsorption process have become more frequent in the last decade, the use of biopolymers as an adsorbent for boron recovery has received little attention in the literature. Published articles report the possibility of using cotton cellulose (Liu et al., 2007) or chitosan modified with N-methyl-D-glucamine (Sabarudin et al., 2005), sugars (Matsumoto et al., 1999) and polyols (Dydo et al., 2012). Wei et al., 2011 obtained a high boron sorption capacity (3.25 mmol g^{-1}) with N-Methyl-D-glucamine grafted on chitosan (CTS-MG material) and highlighted the low cost of the natural polymer support for the preparation of new sorbents for selective boron removal, since chitosan can be obtained from crustacean shells.

Among the biopolymers which are attracting the greatest interest are polysaccharides. These renewable resources are major structural components of the walls of marine crustaceans, plants algae and microorganisms and provide an extensive range of glycosidically linked structures over some 40 different monosaccharides. They may also provide carbon and energy reserves for many types of cells or can be excreted as plant exudates or as microbial exopolysaccharides.

Polysaccharides comprise different types of biopolymers produced universally among living organisms. In this research, alginate (from algae) and chitosan (from crustacean shells) have been considered due to their easy availability, cost-effectiveness and flexibility, making them suitable for a wide range of industrial applications.

1.4.2 Alginates

1.4.2.1 Brief historical review

Alginates are polysaccharide cell-wall constituents of brown algae (*Phaeophyceae),* an organic polymer derivative of alginic acid first obtained in the 1880s from British kelp by E.C.C. Stanford, a Scottish chemist who described in his patent the preparation of alginic acid from brown algae, initially believing that the structure contained nitrogen. Atsuki and Tomoda, 1926 and Schimdt and Vocke, 1926 studied the structure of alginic acid and discovered that it was formed by uronic acid.

World War II boosted the alginate industry; production units were set up in Scotland and California using local wrack and kelp. After the war, other production units were constructed close to natural seaweed beds in Norway, France, Germany, Japan and, more recently, China. The main raw materials were obtained in California (*Macrocystis pyrifera*, giant kelp), from north-eastern Atlantic kelps and wracks (*Ascophyllum nodosum*, *Laminaria hyperborea* and *L. digitata*), and from *Durvillaea* and other kelps in the southern

hemisphere. In China, the kelp *Saccharina japonica,* introduced from Japan in the 1950s and grown on ropes in the Yellow Sea, was used as the main source for the production of crude alginates. Over two million wet tons of this kelp are grown by mariculture in China, making it the largest maricultural crop in the world by far.

Alginate exports increased from 100 tons in 1954 to 300 tons in 1960; today, annual alginate production is around 5000 tons (dry weight) in Norway alone (Meland and Rebours, 2012). Figure 1.11 shows the locations of the main harvest areas of brown seaweeds in the world.

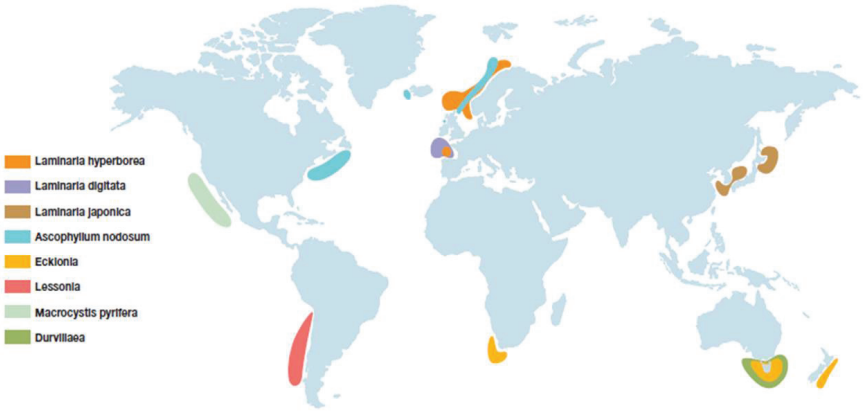

Figure 1.11. Brown seaweeds used for alginate extraction and harvest areas.

Figure provided by FMC Biopolymer.

In 1955, a chromatography study by Fissher and Dörfel revealed the presence of an uronic acid different to mannuronic acid in the hydrolysates of alginic acid. This new compound was named L-guluronic acid, and a quantitative method for the determination of mannuronic and L-guluronic acid was developed. Alginates can thus be defined as chain-forming heteropolysaccharides made up of blocks of β-D-mannuronic acid and L-guluronic acid. The composition of these blocks depends on the extraction procedures, which probably affect alginate quality, and on the species used for extraction, since not all large brown algae have sufficient quantities of alginates to merit exploitation: *Sargassum muticum*, for example, which is an adventive species from Japan that has recently arrived in the Atlantic and Mediterranean, contains only 16−18% alginates.

A high quality alginate forms strong gels and gives thick aqueous solutions. A good raw material for alginate extraction should obviously give a high yield. Although global production currently focuses on the harvesting of brown seaweeds (*Ascophyllum, Ecklonia, Durvillaea, Macrocystis, Laminaria, Lessonia*, and to a lesser extent *Sargassum)* (Painter, 1983), it has been demonstrated that several bacteria from the genera Azobacter and Pseudomonas can also produce alginate (Donati and Paoletti, 2009; Gorin and Spencer 1966; Govan et al., 1981). In algae (*Phaeophyceae*) they can constitute up to 40% of the dry matter from the cell wall and provides the seaweed with its mechanical strength and flexibility, in addition to acting as a water reservoir, preventing dehydration when the seaweed is exposed to air (Donati and Paoletti, 2009). Alginate is obtained

from bacteria (such as *Azobacter Vinelandii* and *Pseudomonas aeruginosa*) as an exocellular polymeric substance with similar characteristics to alginate obtained from algal (Rehm, 2002).

1.4.2.2 Uses of alginates

Alginate is one of the most versatile biopolymers in nature; it is widely used in industry and has a variety of applications. Alginates are used on the basis of a number of properties (McHugh, 2003): i) They are soluble in water and can be used to increase the viscosity of aqueous solutions; ii) They form stable gels. When sodium alginate comes into contact with divalent ions, such as calcium ions, the calcium displaces the sodium from the alginate and holds the long alginate molecules together to create a gel. Alginate gels are thermally stable, unlike Agar gels, so the solution does not need to be heated and the resulting gel does not melt when heated; iii) They are able to form films and fibers of calcium alginates.

The properties of alginates make them suitable for various branches of industry: i) In the food industry they are used as thickeners, emulsifiers and stabilizers and can improve the texture, body and sheen of foods such as yoghurts (McHugh, 2003). In chocolate milk, the cocoa can be kept in suspension by an alginate/phosphate mixture; ii) In the pharmaceutical industry they are used as fixing agents in the manufacture of medicinal tablets. In some cases, the active component is placed in a calcium alginate bead, which has been verified as a feasible drug delivery method in humans (Xing et al., 2003); iii) In the textile industry they are used as thickeners for dye pastes. Alginates have grown in importance in recent years since the conventional thickeners, such as starch, react with the dyes and give lower color yields. According to McHugh, 2003, alginates improve this process because they do not react with the dyes and easily wash out of the finished textile; iv) In other applications alginates are used as stabilizers in waterborne paints, for prostheses and dental impressions, and as binders for salmon and other fish feeds in the aquaculture industry.

In water treatment, calcium alginate beads have been used to remove heavy metals from contaminated water. Papageorgiu et al., 2006 evaluated the use of calcium alginate beads from *Laminaria digitata* to remove heavy metals (Pb^{+2}, Cd^{+2} and Cu^{+2}) from aqueous solutions. The results indicated that mannuronic acid is responsible for the ion-exchange mechanism; pH was found to have a significant effect on the process, with maximum sorption capacity reached at pH 4.5. The maximum sorption uptake followed the order $Pb^{+2} > Cu^{+2} > Cd^{+2}$. There is a competitive mechanism between H^{+} and metal ions that results in increased sorption with increasing pH.

Deze et al., 2012 synthesized porous calcium alginate aerogel beads for the effective sorption of Cu^{+2} and Cd^{+2} from aqueous solutions. The process was evaluated in a batch system and the maximum sorption capacities were 127 mg g^{-1} for Cu^{+2} and 245 mg g^{-1} for Cd^{+2}. The porosity of the material was influenced by the drying method; when supercritical drying was used, the aerogel sorbent consisted of a fibril network with a large surface area (419 m^2 g^{-1}).

The residue of alginate extraction (from *Sagassum filipendula*) has recently been used by Bertagnolli et al. 2014 to remove chromium(VI) and chromium(III) from aqueous solutions. The residue was found to be a suitable, cost-effective and easily available adsorbent for chromium uptake. Among the main conclusions, the

authors highlighted that the biosorption of Cr(VI) is a complex process involving carboxyl groups, amino and sulfonic groups in which the hexavalent chromium ions are simultaneously sorbed and reduced to trivalent chromium ions. The maximum sorption capacities were 0.64 mmol g^{-1} for Cr(III) and 0.82 mmol g^{-1} for total chromium species.

It is noteworthy that alginates, due to their biodegradability, have also been used to synthesize innovative composite materials for the removal of contaminants from water, with a view to improving on the adsorption rates of traditional adsorbents. Soltani et al., 2014 removed lead(II) ions from aqueous solutions using silica nanopowders/alginate composite. Kumar et al., 2013 compared the adsorption efficiencies of activated carbon, barium alginate and modified carbon/barium alginate to remove Victoria Blue dye from aqueous solutions; the results confirmed that the composite may improve removal efficiency for this contaminant and is an eco-friendly solution to the problem.

1.4.2.3 Structure of alginates

Alginates are polymers whose monomer units are uronic acids (sugars where the CH_2OH group has been replaced by a COOH group). One of the units derived from D-mannose is D-mannuronic acid, the other is L-guluronic acid. The main difference between these units is the spatial conformation, which causes a structural difference between polyhedral blocks (Figure 1.12). Haug and SmidsrΦd, 1965, Haug et al., 1966 and Haug and Larsen, 1966 concluded that alginates are copolymers consisting of (1,4)-linked β-D mannuronic acid (M) and α-L-guluronic acid (G) residues of widely varying composition and sequence. Alginates can be regarded as blocks composed of homopolymeric regions of M and G, named M- and G-blocks, respectively (see Figure 1.4), which alternate around the whole structure forming MG blocks. It was further explained by Painter et al., 1968 and Larsen et al., 1970 that alginates are a conformation of many repetitions of these blocks with no regular repeating unit and, in all cases studied, the distribution of monomers along the polymer structure could not be described by Bernoullian statistics. As explained by SmidsrΦd and Draguet, 1996, the variability in monomer block structures strongly affects the physical-chemical and rheological properties of the polymer. M-block regions correspond to linear chains while G-blocks have a loop-shaped structure. Figures 1.13 and 1.14 show the structure and distribution of M- and G-blocks; four possible glycosidic linkages can be present in alginates: diequatorial (MM), diaxial (GG), axial-equatorial (GM) and equatorial-axial (MG). The diaxial linkages in G-blocks (GG) are responsible for the stiffness of the polymer chain.

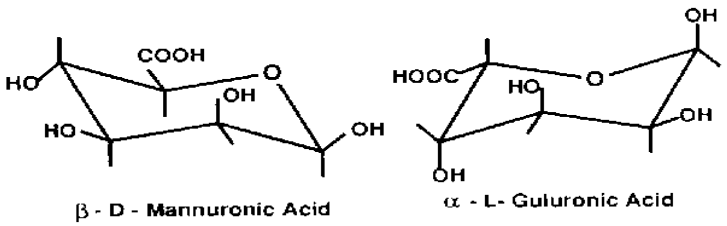

Figure 1.12. Units conforming alginic acid.

Figure 1.13. MM homopolymer blocks.

Figure 1.14. GG homopolymer blocks.

1.4.2.4 Gelling properties of alginates

The polysaccharides derived from seaweeds, such as alginates, agars, carrageenans and furcelleran, can form gels under certain conditions (Rees, 1972; Morris, 1985); standard commercial grades of alginate form gels in acidic conditions since the pKa values for mannuronic and guluronic acids are 3.38 and 3.68, respectively. Alginate gels are generally softer than calcium gels, which are of particular interest for a wide range of industrial applications; propylene glycol alginate (PGA), produced by the reaction between the carboxylic group (of the alginic acid) with propylene oxide, is soluble in acid medium and is therefore widely used as an emulsifier, stabilizer and thickener in food products (commercially known as E-405) (FMC Biopolymer).

However, interest in calcium (as divalent ions) gels has increased in recent years because calcium salts are cheap, readily available, and non-toxic for human consumption; the most widely used are calcium carbonate, calcium nitrate, chloride and calcium phosphate. Calcium ions must be released slowly into the alginate solution, which is achieved by using a calcium salt of low solubility. Is should be noted that the characteristics of alginate gels vary according to the percentages of G-block and M-block regions in different species of algae. Commonly, alginates with a high proportion of G-blocks form rigid gels, whereas alginates with mainly M-blocks are softer and more elastic; alginate obtained from *Laminaria hyperborea*, which has a high percentage of polyguluronic segments, forms rigid gels with low water-binding capacity and tendency to syneresis (water loss by exudation of the gel process, produced by contraction). By contrast, alginate from *Macrocystis pyrifera* or *Ascophyllum* forms elastic gels, has a low tendency to syneresis and the ability to undergo deformation (McHugh, 2003).

Grants et al., 1973 proposed that when two chains of G-blocks are aligned side by side a diamond-shaped structure is formed, which has suitable dimensions to accommodate a calcium ion, forming a dimeric structure. This model, known as the egg-box model, was proposed to explain the gelling properties of alginates by reacting with divalent metal ions. The buckled chain of guluronic acid units is associated with a corrugated egg-box form with interstices in which the calcium ions may pack and be coordinated (McHugh, 2003). The extended analogy states that the strength and selectivity of cooperative binding is determined by the comfort with which 'eggs' of a particular size may pack in the 'box', and with which the layers of the box pack with each other around the eggs (Grant et al., 1973; McHugh, 2003). The structure of the guluronic acid chains gives distances between carboxyl and hydroxyl groups which allow a high degree of coordination of the calcium (McHugh, 2003). Magnesium ions are smaller and thus do not form gels (McHugh, 2003; McDowell, 1977).

Based on the observations of Grant et al., 1973, calcium ions reacting with G-blocks (*L-guluronic acid*) can be found, as bridges between negatively charged groups reacting with calcium ions to form the dimeric structure, similar to an eggs box (Figure 1.15).

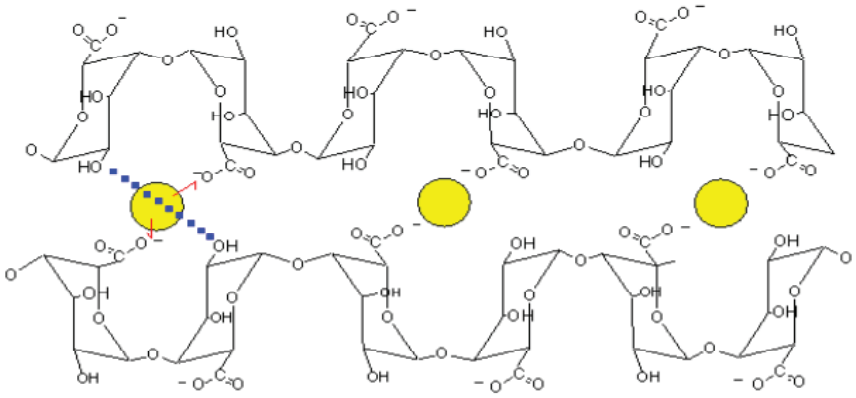

Figure 1.15. Structure of calcium alginate gel presented by Grants et al.,1973.

1.4.2.5 Alginate production processes

The chemistry of the processes used to produce sodium alginate from brown seaweeds seems to be very simple; the main drawback lies in the handling of the raw materials. To extract the alginate from algal, the seaweeds must be broken into pieces and washed with an alkali solution (usually sodium carbonate); the alginate dissolves as sodium alginate and a very thick slurry is produced, which also contains the unwanted insoluble residue (mainly cellulose). In many processes this viscous solution is forced through a filter cloth in a filter press, but the insoluble residues are very small and can quickly clog the filter cloth. Therefore, a filter aid is normally used, which holds most of the fine particles away from the surface of the filter cloth and enhances the filtration step.

There are currently two commercial methods for obtaining sodium alginate, as shown in Figure 1.16 (provided by McHaug et al., 2003). The first method, related to the calcium alginate process, is advantageous because calcium alginate can be precipitated in a fibrous form which can be readily separated and converted into alginic acid. In the second method, related to the alginic acid process, no calcium alginate is formed and alginic acid is precipitated directly from sodium alginate solution; as a result, a gelatinous precipitate is formed which is difficult to separate from the resulting solution and it causes loss of alginic acid. In addition, in the second process the water content is often high and an alcohol solution must be used (as a solvent) for sodium alginate conversion, which increases the operating costs of the process.

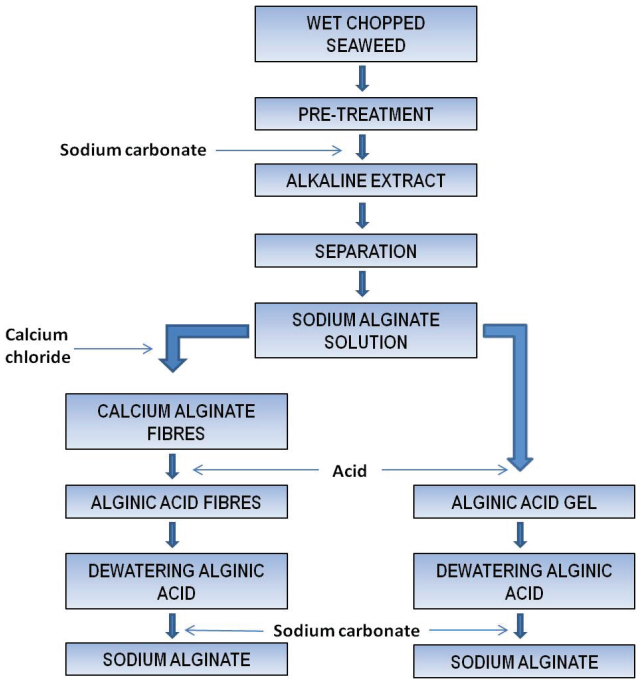

Figure 1.16. Production processes of sodium alginate.

Figure provided by McHugh, 2003.

1.4.3 Chitosan

Chitin is the second most omnipresent natural polysaccharide after cellulose and is composed of β(1→4)-linked 2-acetamido-2-deoxy-β-D-glucose. It can be found in a wide range of natural sources such as crustaceans, insects, fungi and mollusks and is often considered a cellulose derivative, even though it does not occur in cellulose-producing organisms. Chitin is structurally identical to cellulose but has acetamide groups (-$NHCOCH_3$) at C-2 positions.

Chitosan is a natural carbohydrate biopolymer obtained by deacetylation of chitin and is the main derivative of chitin. It is a linear polymer of α(1→4)-linked 2-amino-2-deoxy-β-D-glucopyranose, which is a copolymer of N-acetylglucosmine and glucosamine. Chitosan has begun to attract considerable attention not only for its

potential as an under-utilized resource but also as a very promising new functional biomaterial in various fields thanks to recent progress in chitin chemistry. The main difference between chitosan and chitin is the acetyl content of the polymer; chitosan is poly [β-(1-4)-2-amino-2deoxy-D-glucopyranose] and chitin is poly [β-(1-4)-2-acetamido-2deoxy-D-glucopyranose] (Figure 1.17).

Chitosan is an abundant, renewable biopolymer which has excellent properties of biodegradability, non-toxicity and bio-compatibility. The reaction of chitosan is considerably more versatile than that of cellulose due to the presence of NH_2 groups (Dutta et al., 2004).Various efforts have been made to prepare functional derivatives of chitosan by chemical reactions.

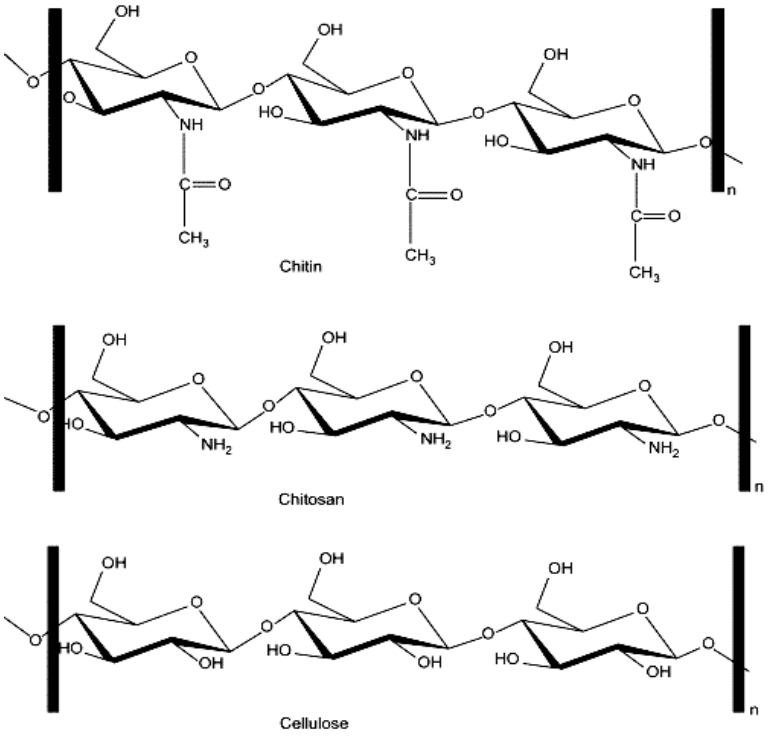

Figure 1.17. Structure of chitin, chitosan and cellulose.

1.4.3.1 Properties of chitosan

Most the natural polysaccharides, e.g. cellulose, alginic acid, pectin, dextran, agar, etc., are neutral or acidic, whereas chitin and chitosan are highly basic polysaccharides. As such, chitin and chitosan have gained increasing commercial interest due to their biodegradability, adsorption, and ability to form films and to chelate metal ions.

The main properties of chitosan are as follows:

Physical-chemical properties

- Chelating and complexing properties.
- Rigid D-glucosamine structure, high crystallinity and hydrophilicity.
- Capacity to form intramolecular hydrogen bonds, high viscosity.
- Forms salts with organic and inorganic acids.
- Weak base; the deprotonated amino group acts as powerful nucleophile (pka = 6.3).
- Insoluble in water or in alkaline solutions at pH levels above 6.5 and not soluble in organic solvents.
- Soluble in dilute aqueous acidic solutions; dissolves readily in dilute solutions of most organic acids, including acetic, formic, tartaric and citric acids.
- Numerous reactive groups for chemical activation and crosslinking.

Polyeclectrolyte properties (at acidic pH)

- Film-forming ability.
- Entrapment and adsorption properties, filtration and separation.
- Flocculating agent, interacts with negatively charged molecules.
- Cationic biopolymer with high charge density.

1.4.3.2 Chitosan processing

The main sources of chitin are the shell wastes of shrimp, lobster and crab. According to Dutta et al., 2004, chitosan is a natural resource waiting for a big market. The US Department of Commerce reported in 1973 that over 150,000 million tons of chitin were produced as processing waste from shellfish, clams, oysters, krill, squid and fungi.

Chitin and chitosan are commercially manufactured by a chemical method. Crab and shrimp are deproteinized by treatment with NaOH solution (3-5% w/w). The resulting product is neutralized and calcium is removed by treatment with HCl solution (3-5% w/w) at room temperature to form a white or slightly pink precipitate of chitin. N-deacetylation of chitin is performed by treatment with an aqueous 40-45% NaOH solution and the precipitate is washed with water. The crude sample is dissolved in aqueous 2% w/w acetic acid and the insoluble material is removed. The resulting clear supernatant solution is neutralized with aqueous NaOH solution to form a purified sample of chitosan as a white precipitate (Hirano, 1997).

CHAPTER II

SCOPE OF THE WORK

In this chapter the scope of the work and the specific objectives of the investigation are presented.

2.1 SCOPE OF THE WORK

The present thesis is focused to the study of the separation and recovery of boron by sorption processes using biopolymers and composites as sorbents.

The removal of boron from natural waters to achieve permissible concentration levels is important as boron is toxic to humans and plants. Thus, new sorbent materials are proposed based on biopolymers (alginate and chitosan) that are easy available, easy to manipulate and environmentally friendly.

2.1.1 Objectives

- Preparation of beads based on alginate biopolymers and characterization using spectroscopic techniques.
- Study in a batch system of boron sorption on alginate beads. Equilibrium studies: Determination of the contact time required to reach equilibrium; determination of the maximum sorption capacity; study of the pH influence, effect of alginate concentration in beads and influence of foreign ions on sorption capacity. Fitting of the sorption isotherms.
- Kinetic study of alginate beads as a sorbent for boron removal: Effect of stirring speed and pH influence on kinetic profiles. Fitting of the experimental data.
- Evaluation of alginate beads for boron removal from aqueous solutions using a fixed-bed system. Study of the influence on breakthrough curves; varying the feed flow into the column and varying the amount of adsorbent. Fitting of the experimental data.
- Synthesis and characterization of new composites of biopolymers (alginate and chitosan) and metal hydroxides (chiNi(III); chiFer(III); CAAl).
- Study of boron sorption in a batch system using the novel synthesized composites. Equilibrium studies: Determination of the contact time required to achieve equilibrium; determination of the

maximum sorption capacity; study of the pH influence, the effect of metal concentration in beads and the influence of ion strength on sorption capacity. Fitting of the sorption isotherms.

- Kinetic study of the novel composites in boron removal: Effect of the stirring speed and pH on kinetic profiles. Fitting of the experimental data.
- Desorption studies of sorbents, to provide reusable and environmentally-friendly materials.
- Application for boron recovery with real samples of Mediterranean seawater.

This thesis has been evaluated and accepted by the commission of the Doctoral School of the Universitat Politècnica de Catalunya to be presented as a compendium of publications and is structured in the following manner:

Paper I

In this paper, calcium alginate beads were characterized and evaluated as a sorbent for boron removal in a batch system; the effects of pH, initial boron concentration in the beads and stirring time were evaluated. NMR was used to determine the ratio of mannuronic and guluronic acid present in the raw sodium alginate used for sorbent production, and FTIR was used to characterize the calcium alginate beads, in order to demonstrate the interaction between boron and the sorbent. The Langmuir and Freundlich models were used to fit the equilibrium data and pseudo-first-order and pseudo-second-order models were used to adjust the kinetic experimental data.

Paper II

In this paper, the best operating conditions were determined for calcium alginate beads used as a sorbent for boron removal in a batch system. A full factorial design (2^4) and statistical software (Minitab.15) were used; the effect of the main parameters on the adsorption process was investigated: pH (3-10), concentration of alginate in the beads (1.6-3.2% w/w), bead size (1.6-2.4 mm) and initial boron concentration (50-1000 mg L^{-1}).

Paper III

Boron removal using calcium alginate beads in a fixed-bed system was evaluated in this paper. The breakthrough curves were obtained as a result of the variation of pH, inlet boron concentration, feed flow rate, mass of adsorbent and column diameter. The results were evaluated using the Bohart-Adams model to adjust the experimental data and to determine the characteristic column parameters required for process design.

Paper IV

In this paper, principal component analysis (PCA) was used to perform a comparative analysis of different equilibrium isotherms obtained by varying the percentage of alginate in the adsorbent beads. Partial least

squares (PLS) modeling was used to characterize the effect of the experimental variables (initial boron concentration, adsorbent mass, pH, column diameter, column depth and superficial flow velocity) on the adsorption efficiency of the process.

Paper V

This paper is devoted to the development of a novel composite containing chitosan and nickel (II) hydroxide [chiNi(II)] and to its evaluation for boron recovery from aqueous solutions. This novel material was characterized using SEM, FTIR, TGA and pHpzc techniques. Equilibrium parameters were calculated and the effect of immobilized $Ni(OH)_2$ on sorption capacity was tested. Diffusion constants of kinetic profiles were obtained; desorption study and thermodynamic parameters were presented.

Paper VI

This paper presented an approach for the application of a novel chitosan/Iron(III) hydroxide [chiFer(III)] material for boron separation from Mediterranean seawater in a continuous system; several adsorption-desorption cycles were performed to evaluate the efficiency of the adsorbent and the Thomas, Yoon and Nelson, and Bohart-Adams models were evaluated to adjust the experimental results.

Paper VII

In this paper, a novel composite of calcium alginate and alumina (CAAl) was synthesized and characterized. Techniques including SEM and TGA were used to characterize the composite material; the effect of equilibrium parameters (pH, temperature, adsorbent dosage) on sorption capacity was investigated. A desorption study was performed and the thermodynamic parameters such as enthalpy change, entropy change and Gibbs free energy change were determined.

Paper VIII

In this paper the effect of different sodium salts on the effectiveness of calcium alginate beads was evaluated. Three alginates with different compositions of guluronic and mannuronic acid were used for boron recovery and their effects were investigated. Equilibrium isotherm data were evaluated by the Langmuir and Freundlich models and maximum sorption capacity was compared with the performance of a commercial ion-exchange resin, Amberlite IRA-743.

CHAPTER III

EXPERIMENTAL PROCEDURE

This chapter describes the materials and general methods used to carry out this work which are not described in detail in the individual research articles.

3.1 PROPERTIES OF RAW MATERIALS USED FOR SORBENT PREPARATION

3.1.1 Alginates

The alginates used in this research were supplied by PANREAC QUIMICA SA (Barcelona, Spain) as sodium alginate [CAS-number (9005-38-3)], which is commercialized as a powder material with the following technical specifications:

- Loss on drying at 105 ºC: 15%.
- Residue on ignition: 30%.
- Heavy metals (as Pb): 0.004%.

In the current work, sodium alginate was used as the raw material to synthesize the adsorbents; it was previously characterized by NMR (chapter IV and paper 1) in order to determine the composition of M- and G-groups (mannuronic and guluronic acids, respectively).

3.1.2 Chitosan

The chitosan used in this work was supplied by Aber Technologies (Plouvien, France) as a flaked material (Figure 3.1).

The chitosan flakes were previously characterized by Ruiz et al., 2001 using FTIR and SEC (coupled with a differential refractometer and multi-angle laser light-scattering photometer) to determine the deacetylation degree and the molecular mass of the polymer, which were 87% and 125000 g mol^{-1}, respectively.

Figure 3.1. Chitosan flakes (particle size G2< 250 µm) provided by Aber Technologies (France).

3.2 PREPARATION OF INNOVATIVE SORBENT MATERIALS

In this section, the procedure for preparing the new sorbent materials for boron removal is presented.

3.2.1 Calcium alginate (CA) beads

Different calcium alginate beads were produced by preparing solutions of sodium alginate at different concentrations (3.2, 2.4, 2.0 and 1.6% w/w). The solutions were kept under continuous agitation at 800 revolutions per minute (rpm) until complete dissolution of the alginate in distilled water (Figure 3.2). In order to dissipate the air bubbles in the solution (which appeared as a result of the strong agitation used to dissolve the sodium alginate), the stirring speed was decreased slowly to 50 rpm over a period of 2 h. Then, the alginate solution was added dropwise to a 0.05 M calcium nitrate solution (coagulant solution) using a peristaltic pump.

In order to produce gel beads of a regular size, a peristaltic pump (WATSON-MARLOW 323) was used, fitted with a thin hose which has a nozzle in the tip to facilitate the formation of liquid drops (Figure 3.3). The nozzle must be at a distance of approximately 15 cm from the coagulant solution and the pump must operate at 8 rpm to ensure that beads with a regular diameter (2.4$\pm$1 mm) are formed. The slow contact between the drops of alginate solution and the calcium nitrate solution (which is in continuous agitation) allows the formation of calcium alginate beads that are not soluble in water.

To produce beads of different sizes, different flows of alginate drops were used by increasing the pump speed to 20 rpm introducing an air current at the nozzle tip.

The final beads (Figure 3.4) were stored in the same coagulant solution at 5 ºC for at least 24 h before use. Prior to the experiments, the beads were washed with distilled water to remove the excess surface calcium nitrate.

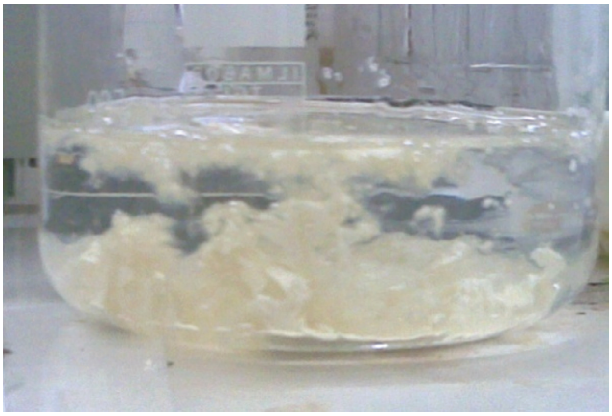

Figure 3.2. Sodium alginate solution 2% w/w.

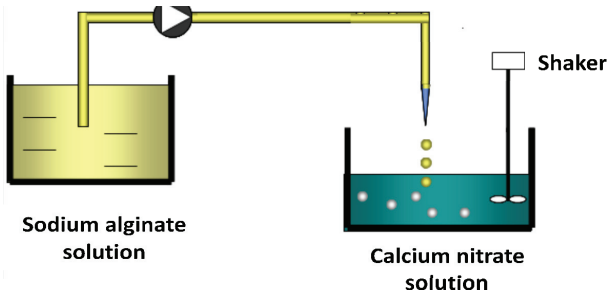

Figure 3.3. Schematic view the alginate bead production system.

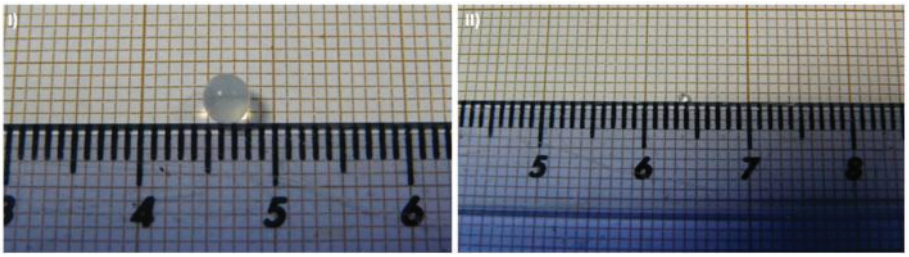

Figure 3.4. Calcium alginate beads of different diameters: I) 2.4 mm; II) 1.6 mm.

3.2.2 Composite of calcium alginate and alumina (CAAl)

Following the same procedure used for CA production, a solution of sodium alginate (2% w/w) was prepared. This solution was kept under continuous agitation (800 rpm) for 3 hours until complete dissolution of alginate. The installation system was the same as used for CA production. Alginate/alumina composites were prepared by adding a known mass of alumina into the alginate solution to produce a mixture of 2% w/w. The resulting alginate/alumina solution was continuously stirred at 100 rpm and was added dropwise into a 0.05 M calcium nitrate solution with the peristaltic pump.

The beads were stored in the same coagulant solution at 5 ºC for 24 h before use. The final CAAl composite was expected to be slightly whiter than CA due to the presence of alumina.

3.2.3 Composite of chitosan and nickel (II) hydroxide [chiNi(II)]

The chitosan solution, with a concentration of 1% w/w, was prepared by dissolving 1 g of chitosan in 1% w/w acetic acid solution and stirring for at least 3 h. A known amount of $Ni(NO_3)_2.6H_2O$ powder was mixed in 120 mL of 1 M HCl solution and stirred continuously until complete dissolution. Then, 640 g of chitosan solution 1% w/w was mixed with nickel(II) solution by vigorous stirring for 120 minutes. The chitosan-nickel(II) mixture was added dropwise by syringe and using a peristaltic pump into an aqueous solution of sodium hydroxide (1 M) under magnetic stirring to facilitate the formation of microsphere composites of chitosan/nickel (II) hydroxide (Figure 3.5).

In order to compare the effectiveness and stability of the composites, different masses of $Ni(NO_3)_2.6H_2O$ were employed:

- B40: 40 g of $Ni(NO_3)_2.6H_2O$, 120 mL of 1 M HCl solution and 640 g of chitosan 1% w/w.
- B10: 10 g of $Ni(NO_3)_2.6H_2O$, 30 mL of 1 M HCl solution and 640 g of chitosan 1% w/w.
- B5: 5 g of $Ni(NO_3)_2.6H_2O$, 15 mL of 1 M HCl solution and 640 g of chitosan 1% w/w.

The composites were stirred continuously for 6 h at room temperature (20°C), then filtered and intensively washed with distilled water to remove the excess of nickel traces present on the surface. Finally, the composites were washed with ethanol and kept at room temperature (25 ºC) for 48 h to dry.

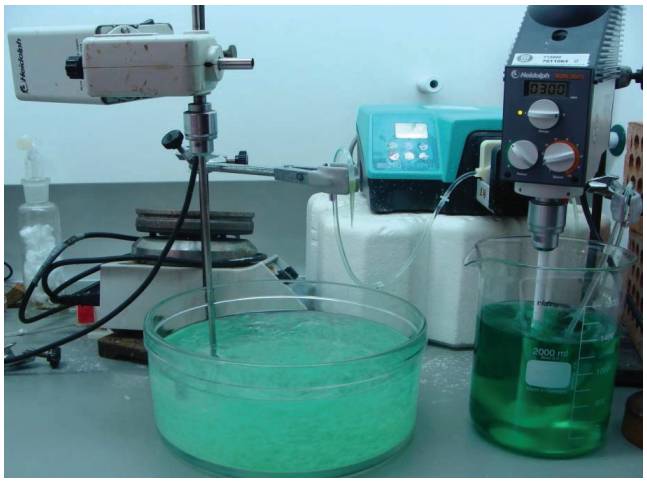

Figure 3.5. Installation system for [chiNi(II)] and [chiFer(III)] materials.

3.2.4 Composite of chitosan and iron (III) hydroxide [chiFer(III)]

The procedure to prepare the [chiFer(III)] composite was similar to the one used for [chiNi(II)] production; nevertheless, the iron (III) solution was prepared by dissolving 20 g of $FeCl_3.6H_2O$ powder in 60 mL of HCl solution (1 M). The resulting wet beads were washed with abundant distilled water prior to the experiments (Figure 3.6). In order to compare the influence of the drying method, the samples were dried using two different techniques: (i) air drying (ordinary method), in which the wet beads of chiFer(III) were washed with ethanol and then kept at room temperature (20 ºC) for 48 h to dry; and (ii) freeze drying, in which the adsorbent was dried with a freeze dryer (Bioblock Scientific Christ) at 223 K and 0.01 mbar.

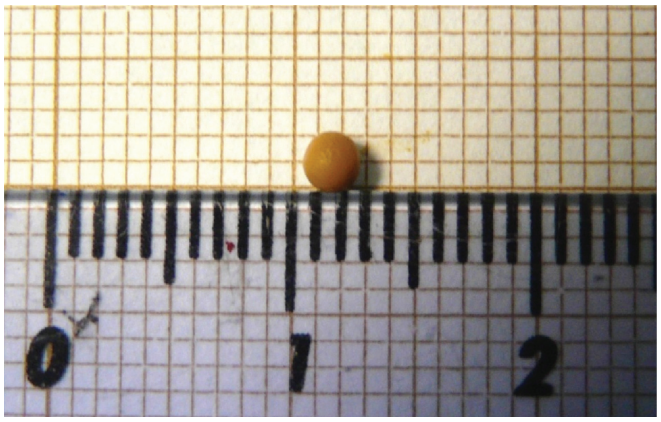

Figure 3.6. Novel [chiFer (III)] composite material.

3.3 ANALYTICAL METHODS FOR BORON QUANTIFICATION

The boron solutions used in this work were prepared from boric acid provided by Merck AG (Germany), which has the followings specifications:

- Water solubility: 46.5 g L^{-1} (at 20 ºC).
- Melting point: 171 ºC (decomposition).
- Molar mass: 61.83 g mol^{-1}.
- Density: 1.44 g cm^{-3} (at 20 ºC).
- Bulk density: 400–600 kg cm^{-3}.
- pH value: 3.8–4.8 (33 g L^{-1}, H_2O, 20 ºC).
- Vapor pressure: 2.7 hPa (at 20 ºC).

In the present work, the boron content of the samples was determined by the azomethine-H method using ultraviolet-visible absorption spectroscopy (UV-Vis), atomic absorption spectroscopy (AAS) and inductively coupled plasma (ICP).

3.3.1 Azomethine-H/UV-Vis method

The azomethine-H method was used in this thesis in conjunction with UV-Vis as an effective and inexpensive technique for boron determination (De la Fuente García-Soto, 2000), at a wavelength of 415 nm as reported in the literature (Mohammed et al., 2014). A UV-SHIMADZU spectrophotometer was used.

Azomethine-H corresponds to 8-hydroxy-1-(salicylideneamino)-3,6-naphthalenedisulfonic acid, a Schiff base of salicylaldehyde and H-acid (1-amino-8-naphthol-3,6-disulfonic acid) shown in equation 3.1. It is a light orange colorimetric reagent commonly used in spectrophotometric determination of boron.

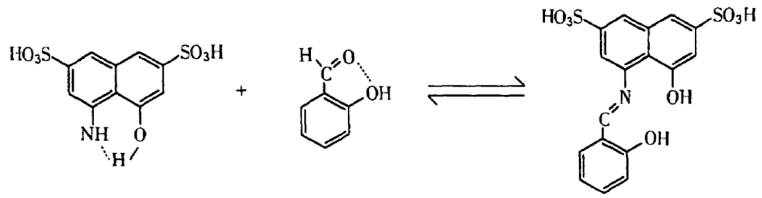

3.1

In aqueous media, the reaction between boron species and azomethine-H is reversible, forming a chelate complex of yellow color with a molar absorptivity of 1.01 x 10^4 at 415 nm. The reaction depends on the pH of the aqueous medium and reaches its maximum rate at pH 5.2, according to De la Fuente García-Soto, 2000. Therefore, a pH-adjusting buffer solution is necessary to control the optimum operating conditions. In this case, a buffer solution consisting of acetic acid, ammonium acetate and ethylenediaminetetraacetic acid (EDTA) was used.

Figure 3.7 shows the possible complexes of boric acid and azomethine-H. Matsuo et al., 2004 studied the complexation reaction between boric acid and azomethine-H using the ^{11}B NMR method; it was suggested that the 1:1 bis-chelate complex containing B-N bonding (Figure 3.7.II) is the chelate most likely to be formed in this interaction.

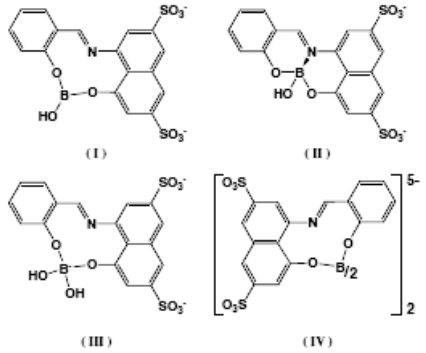

Figure 3.7. Possible complex of boric acid with azomethine-H. I) 1:1 monochelate complex of trigonal boric acid. II) 1:1 bis-chelate complex with tetrahedral boron. III) 1:1 monochelate complex with tetrahedral boron. IV) 1:2 chelate complex.

Figure provided by Matsuo et al., 2004.

Experimental procedure of azomethine-H

In this work, the following procedure was used:

To prepare the azomethine-H solution, 1 g of azomethine-H and 2 g of ascorbic acid were dissolved in 50 mL of hot bi-distilled water at a temperature below 70 ºC, then diluted to 100 mL with bi-distilled water in a volumetric flask.

A buffer solution was prepared by dissolving 100 g of ammonium acetate in 160 mL of glacial acetic acid and 20 mL of bi-distilled water. After dissolution, 5 g of EDTA disodium salt was added and the pH was adjusted to 4.5 by adding acetic acid or ammoniac.

In a volumetric flask, a stock standard solution of boron was prepared by adding a known amount of boron, 1.5 mL of buffer solution and 1.5 mL of azomethine-H. Calibration samples were prepared by taking aliquots from the stock solution and leaving them to stand for 120 minutes to allow reaction between the azomethine-H and boron. Then, using the UV-equipment, a sample was placed into the Quartz cells and the absorbance was measured in the spectrophotometer at 415 nm.

3.3.2 Inductively coupled plasma (ICP)

Inductively coupled plasma atomic emission spectrocopy (ICP-AES) was used in this work for the determination of boron content and trace metals in solution. The analyses were performed at the

corresponding wavelengths using HORIBA Jobin Yvon equipment (France): 249.7 nm for boron, 221.6 nm for nickel, 248.3 nm for iron and 309.3 nm for aluminum.

ICP-AES is commonly used for the detection of trace metals in environmental samples. ICP technology uses a plasma source in which the energy is supplied by electric currents generated by electromagnetic induction.

ICP comprises a very high temperature excitation source that efficiently desolvates, vaporizes, excites and ionizes atoms; molecular interference is greatly reduced but not completely eliminated. When a time-varying electric current is passed through the coil it creates a time-varying magnetic field around it, which induces an azimuthal current in the rarefied gas (argon, helium, etc.) to form plasma.

ICP equipment normally includes the following components (Ruiz, 2002):

- Sample introduction system (nebulizer)
- High frequency generator
- Transfer optics and spectrometer
- Computer interface

The elements to be analyzed must be in solution. In the case of the ICP-AES equipment used in this work (Figure 3.8), the ICP torch consists of 3 concentric quartz glass tubes, and a radiofrequency (RF) generator (typically of 1–5 kW and 27–41 MHz) produces an oscillating current in an induction coil, which in turn generates an oscillating magnetic field.

The magnetic field sets up an oscillating current in the ions and electrons of the rarefied gas (argon was used in this work). Argon gas flowing through the torch is ignited with a Tesla unit that creates a discharge arc through the argon flow to start the ionization process; this is ionized in the intensity of the electromagnetic field. A stable temperature of 7000–10000 K is generated by the collisions of atoms.

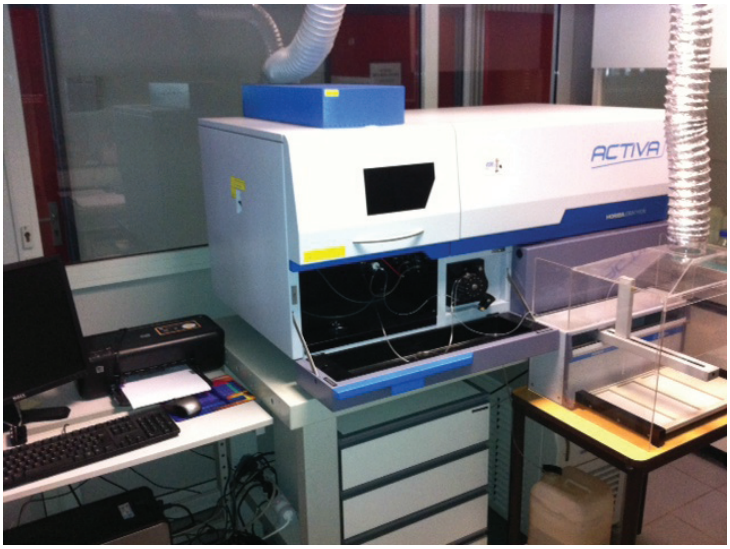

Figure 3.8. ICP-AES equipment used for boron analysis.

Then, a peristaltic pump delivers an aliquot of the sample into the nebulizer and into the flow of plasma support gas. The sample collides with the electrons and charged ions in the plasma and is itself broken down into charged ions at the characteristic wavelength of the element involved. The light emitted is converted to an electrical signal by the photomultiplier in the spectrometer; the intensity of an electron signal is compared to previous intensities (which have been obtained using known boron concentrations in the calibration curve). Each element will have specific wavelengths in the spectrum that can be used for analysis.

3.3.3 Atomic absorption spectroscopy (AAS)

This technique is based on the capacity of atoms to absorb light emission at a characteristic wavelength; AAS uses the wavelengths of light absorbed by an element to determine its concentration in the solution. Boron solutions were analyzed at a wavelength of 249.7 nm with a Varian AA240FS spectrophotometer (Australia) and using a lamp current of 20 mA (acetylene fuel and nitrous oxide support).

The sample must be atomized before analysis (it is converted into ground state free atoms in the vapor state); a lamp of the same element emits a beam of electromagnetic radiation from excited atoms, which is passed through the vaporized sample (Royal Society of Chemistry). The radiation induces the wavelengths to be absorbed by the atoms of the element in the sample (analyte); a fraction of this radiation is adsorbed, which is proportional to the amount of atoms in the analyte.

Consecutively, the intensity of this absorption is compared with the calibration curve to calculate the element concentration. A typical absorption spectrometer needs three main components: a light source; a sample cell to produce gaseous atoms, and a means of measuring the specific light absorbed (Royal Society of Chemistry).

Figure 3.9. AAS equipment.

3.4 ANALYTICAL TECHNIQUES USED FOR THE CHARACTERIZATION OF MATERIALS

3.4.1 Fourier transform infrared spectroscopy (FTIR)

Fourier transform infrared spectroscopy is an effective tool for identifying types of chemical bonds and the functional groups of the materials synthesized in the current work. It is one of the most useful techniques for identifying organic or inorganic chemical components and, though not particularly sensitive, can be applied to the analysis of solids, liquids and gases as a first step in combination with other more sensitive techniques.

The main objective of any absorption spectroscopy technique (FTIR, UV-Vis spectroscopy, etc.) is to measure the amount of light absorbed at a fixed wavelength. Molecular bonds vibrate at various frequencies depending on the elements and the type of bonds; frequencies are specific to a given bond. Infrared spectroscopy is based on the fact that the molecules have frequencies at which rotate and vibrate; that is, rotation and molecular vibration have discrete energy levels (normal vibrational modes). These energies are determined by the shape of the potential energy surfaces, the masses of the atoms, and the associated vibronic coupling.

A simplified diagram of an FTIR spectrometer is shown in Figure 3.10. The source emits infrared radiation that is passed through the sample. A Michelson interferometer (consisting of a beamsplitter, a fixed mirror and a movable mirror) encodes the radiation by creating a periodic intensity pattern. The movable mirror adjusts the distance between itself and the beamsplitter. When the light from the fixed mirror recombines with the light from the movable mirror, a phase shift between the two beams causes interference in the resulting beam. Therefore, the intensity of the beam varies sinusoidally between a maximum intensity (at 0º phase difference) and a minimum intensity (at 180º phase difference). The sample absorbs some of the infrared radiation at characteristic frequencies according to its bond strength and structure. The transmitted part of the beam then enters the detector for final measurement (the detectors are specially designed to measure these signals) (Ruiz, 2002).

A computer processes the data obtained from the detector; Fourier transform methods are used to calculate the spectrum absorbance values. The final absorbance data are presented to user for interpretation.

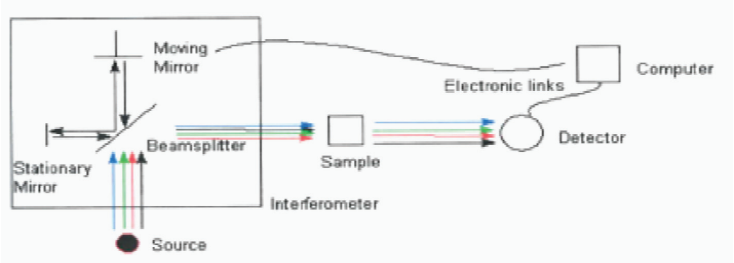

Figure 3.10. Diagram of FTIR instrumentation.

Figure provided by Ruiz, 2002.

3.4.2 Thermogravimetric analysis (TGA)

Thermogravimetric analysis was used to determine the mass variation of the composite materials as a function of temperature. This calculation is useful for characterizing the thermal stability of the materials.

Thermogravimetric analysis requires a high degree of precision in three measurements: mass change, temperature, and temperature change. Therefore, the basic instrumental requirements for TGA are a precision balance with a pan loaded with the sample, and a programmable furnace. The furnace can be programmed either to heat at a constant rate or to heat the sample such as to produce a constant mass loss with time. In the current research, a PerkinElmer 6 TGA instrument was used to characterize the materials and analyses were performed under a nitrogen flow of 20 ml min^{-1} at a heating rate of 10 ºC min^{-1}.

The main advantages of this technique are summarizes as follows:

- TGA can measure the mass variation of a material (organic or inorganic), either as a function of increasing temperature, or isothermally as a function of time, in a nitrogen, helium or air atmosphere or even in vacuum.
- TGA can provide information about physical phenomena, such as second-order phase transitions, including vaporization, sublimation, absorption, adsorption and desorption.
- TGA is commonly used to measure the weight of fiberglass and inorganic fill materials in plastics, laminates, paints and composite materials by burning off the polymer resin. The fill materials can then be identified by XPS, which commonly identifies TiO_2, $CaCO_3$, $MgCO_3$, Al_2O_3, $Al(OH)_3$, $Mg(OH)_2$ and silica.
- Samples can be analyzed in powder form or in small pieces (in order to keep the sample temperature close to the gas temperature).
- Inorganic materials, polymers, plastics, metals, ceramics, glasses and composites material can be analyzed.
- Temperatures usually range from 25 ºC to 900 ºC, giving a wide interval of analysis.
- Sample weights can range from 1 mg to 150 mg, with a sensitivity of 0.01 mg.
- TGA can be used to measure evaporation rates, such as the volatile emissions of liquid mixtures.
- TGA can help to identify organic materials by measuring the temperature of bond scissions in inert atmospheres or of oxidation in air or oxygen atmospheres.
- TGA can help to identify the fill materials added to some foods, such as silica gels and titanium dioxide.

3.4.3 Environmental scanning electron microscopy (ESEM)

Environmental scanning electronic microscopy was used in this work to capture images of the material surfaces and to determine the concentration of metals, through energy-dispersive X-ray (EDX) analysis of different sections of the composites, in order to verify homogeneous composition throughout the polymer matrix.

The ESEM technique was chosen due to the limitations of scanning electron microscopy (SEM), which requires a high vacuum sample medium and clean, dry and electrically conductive samples; non-conductive specimens must be coated with a conductive film to prevent charging. ESEM conserves the advantages of SEM but also removes the high vacuum constraint on the sample environment. Wet, oily, dirty, non-conductive samples may be examined in their natural state without modification or preparation. ESEM offers high-resolution secondary electron imaging in a gaseous environment of practically any composition, at pressures as high as 50 Torr and temperatures of up to 1500 ºC.

As shown in Figure 3.11, SEM equipment comprises an electron column (which creates a beam of electrons), a sample chamber (where the electron beam interacts with the sample), detectors (which monitor the signal resulting from the beam-sample interaction), and a viewing system (which builds and display an image from the signal). An electron gun at the top of the column generates the electron beam (an electrostatic field directs electrons, emitted from a very small region on the surface of an electrode, through a small spot called the crossover). The electrons emerge from the gun as a divergent beam. A series of magnetic lenses and apertures in the column focuses the beam into a demagnified image of the crossover. Near the bottom of the column a set of scan coils deflects the beam in a scanning pattern over the sample surface. The final lens focuses the beam into smallest possible spot on the sample surface (Kimseng and Meissel, 2001).

The beam exits the column into the sample chamber. As the beam electrons penetrate the sample, they give up energy, which is emitted from the sample in two common ways: as secondary electrons (SE) and backscattered electrons (BSE). Each emission mode is a signal from which an image can be created (Kimseng and Meissel, 2001).

An EDX analyzer is an accessory integrated into the scanning electron microscope that provides valuable element analysis and chemical characterization functionalities. It relies in the fact that each element has a unique atomic structure and a unique set of peaks on its X-ray spectrum.

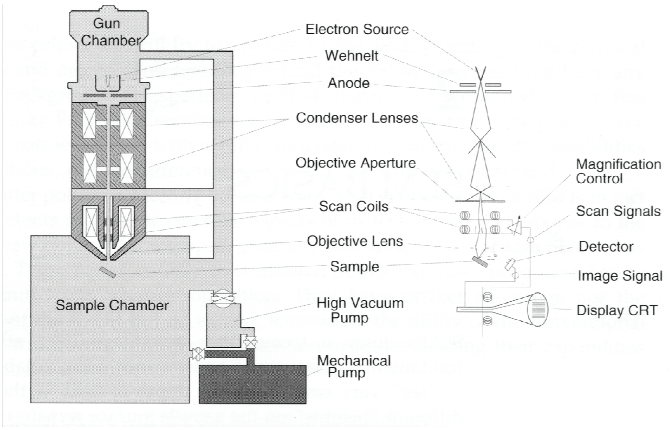

Figure 3.11. Schematic representation of a scanning electron microscope.

Figure provided by Kimseng and Meissel, 2001.

3.4.4 Nuclear magnetic resonance (NMR) spectroscopy

Nuclear magnetic resonance spectroscopy was used to characterize sodium alginate powder by determining mannuronic and guluronic block concentrations. The NMR ^{1}H spectra were recorded at 400 MHz on a Bruker spectrometer.

NMR spectroscopy is used to determine the content of a sample as well as the entire structure of an organic molecule (through combination with other techniques such as infrared and mass spectrometry methods). The technique is based on a physical phenomenon in which nuclei in a magnetic field absorb and re-emit electromagnetic radiation. This energy (at a specific resonance) depends on the strength of the magnetic field and on the magnetic properties of the atomic isotope.

The principle behind NMR (Figure 3.12) is that many nuclei have spin and all nuclei are electrically charged. If an external magnetic field is applied, an energy transfer is possible between the base energy and a higher energy level (generally a single energy gap). The energy transfer takes place at a wavelength that corresponds to radio frequencies; when the spin returns to its base level, energy is emitted at the same frequency. The signal that matches this transfer is measured in many ways and processed to yield an NMR spectrum for the nucleus in question.

The precise resonant frequency of the energy transition is dependent on the magnetic field at the nucleus; in general, the more electronegative the nucleus, the higher the resonant frequency. It is also dependent on the proton alignment; when protons are aligned with the external magnetic field, they are in a lower energy state, but when they are aligned with the external magnetic field, they are in a higher energy state.

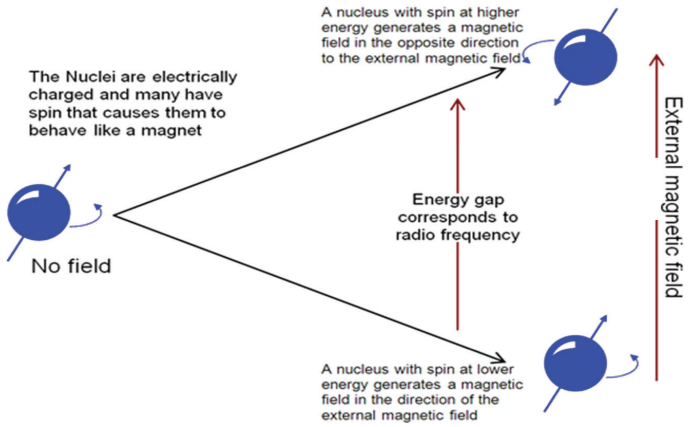

Figure 3.12. Basis of NMR spectroscopy.

3.4.5 Point of zero charge (pH_{pzc})

The point of zero charge of [chiNi(II)] composites was determined by potentiometric titration; the pHpzc is an isoeletric point on the material surface at which the total concentration of surface anionic sites is equal to the

total concentration of surface cationic sites. At pH values above this point, the surface has an anionic charge and may participate in cation attraction and cation exchange reactions. By contrast, at pH values below pH_{pzc}, the surface has a positive charge and will attract anions and participate in anion exchange reactions.

In this work, potentiometric experiments were used to determine the variation in the surface charge density σ_0 (C m^{-2}) of [chiNi(II)] sorbent as a function of pH at room temperature (20 ºC). Surface charge density was calculated as follows:

$$\sigma_0 = \frac{(C_A - C_B + [OH^-] - [H^+])F}{Sa} \quad (3.2)$$

where C_A and C_B are the concentrations (mol L^{-1}) of acid and base needed to reach a point on the titration curve, $[H^+]$ and $[OH^-]$ are the concentrations (mol L^{-1}) of H^+ and OH^-, F is Faraday's constant (96490 C mol^{-1}), S is the specific surface area of adsorbent (m^2 g^{-1}), and *a* is the concentration of adsorbent in the solution (g L^{-1}).

3.4.6 BET surface area and porosimetry studies

Nitrogen adsorption-desorption isotherms were performed to determine the specific BET surface area and the pore distribution of the sorbent materials, using a nitrogen adsorption apparatus (Micromeritics, TriStar 3000; Figure 3.13). Prior to nitrogen adsorption, the samples were dried and degassed with N_2 at 100 ºC for 6 h in order to clean the adsorbent surface of the materials. The samples were dried using two methods: i) air drying, in which the beads were washed with ethanol and then kept at room temperature (20 ºC) for 48 h to dry; and ii) freeze drying, in which the materials were freeze dried (Bioblock Scientific Christ) at 223 K and 0.01 mbar. The surface area, pore volume and pore diameter were determined by the BET method (Brunauer et al., 1938) and the pore size distribution was determined using the BJH model (Barret et al., 1951).

Figure 3.13 Micromeritics, TriStar 3000 equipment.

3.5 OUTLINE OF EXPERIMENTAL PROCEDURE

Although the experimental procedure is explained in detail in each article, this section provides complementary information to facilitate the reproducibility of the results.

Figures 3.14 and 3.15 show an overview of the experimental procedure used in this work for batch and continuous systems, respectively; for isotherm studies, a known volume of boron solution at different boron concentrations (and fixed pH) was mixed with a fixed mass of adsorbent for at least 72 h to ensure equilibrium. Then, an aliquot of adsorbate was withdrawn and the residual concentration was measured by ICP-AES, azomethine-H or atomic absorption. For kinetic studies, the aliquots were withdrawn at different times.

For a continuous system, different columns (with different diameters, ranging from 1.2 to 2.6 cm) were filled with known amounts of sorbent to obtain different columns depths (12, 15 and 18 cm). Boron solution (of a known initial concentration) was fed into the column using a peristaltic pump at different flow rates; the samples were regularly collected at different time points using a Gilson FC 203B fraction collector (United Kingdom), as shown in Figure 3.15, and the residual boron concentration was measured.

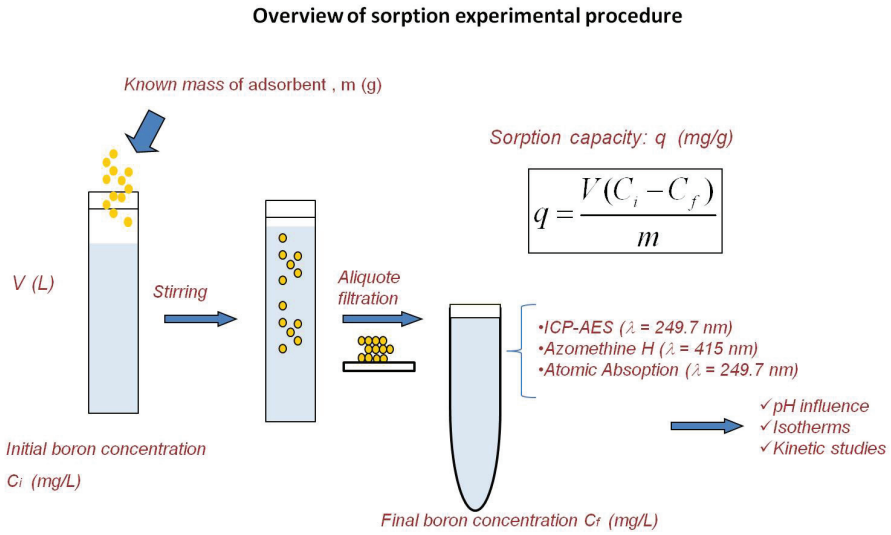

Figure 3.14. Overview of experimental procedure for batch system.

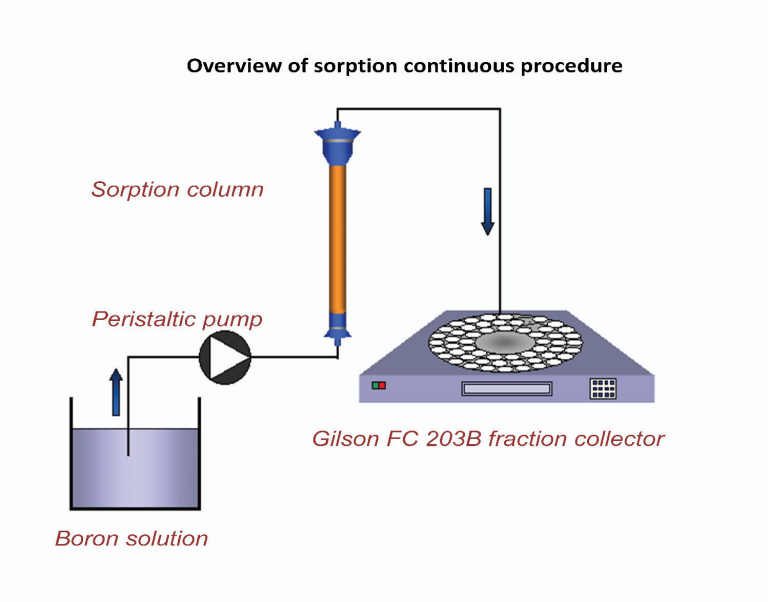

Figure 3.15. Experimental procedure for continuous system.

CHAPTER IV

GENERAL RESULTS AND DISCUSSION

4.1 BORON REMOVAL WITH ALGINATE BEADS IN A BATCH SYSTEM

4.1.1 Characterization of sodium alginate and calcium alginate beads

Sodium alginate used for bead preparation was characterized by NMR. The average molar composition of mannuronic (M-Blocks) and guluronic (G-Blocks) acid in the conventional alginate used throughout the research (provided by PANREAC) were 64% w/w and 36% w/w, respectively. In order to compare the effect on boron adsorption, varying the type and composition of alginates, two additional alginates were characterized (provided by ACROSS): LF 200S alginate was found to be the richest in G-blocks (70% w/w) and therefore the poorest in M-Blocks (30% w/w), while LF 240D alginate was found to contain 67% w/w M-blocks and 33% w/w G-blocks.

The calcium alginate (CA) beads were characterized using BET surface and porosimetry studies, FTIR, TGA and ESEM. The results suggest that CA is a mesoporous material, according to the IUPAC classification (2nm<pore size<50 nm); CA had a pore size of 34 nm, and a pore volume and BET surface area of 4.8 x 10^{-3} cm^3 g^{-1} and 0.6 m^2 g^{-1}, respectively. The FTIR results revealed the chemical interaction between the OH^- groups of the sorbent and boron species; TGA determined the temperature at which thermal decomposition of the CA material began (468 K), and the ESEM images were used to verify the roughness of the sorbent surface structure and the formation of cracks and folds during the drying processes.

4.1.2 Influence of pH

The pH of the solution plays an important role in the adsorption process. Higher levels of boron removal were achieved when the pH of the boron solutions was increased. The maximum boron uptake was obtained at pH 11. Between pH 3 and 5, carboxylic groups in the alginate formed a weak base that neutralized the acid solution; this was verified for the variation in the initial and final pH of boron solutions (a similar trend was also observed by Papageorgiou et al., 2006 and by Fiol et al., 2006). The pH and concentration determine the distribution of ionic forms of boron; the pKa for the equilibrium reaction is 9.2 (Barron et al., 1999):

$$B(HO)_3 + H_2O \leftrightarrow B(OH)_4^- + H^+ \quad (4.1)$$

The experimental results confirmed that the mechanism of boron separation with alginate beads is a chemical reaction between $B(OH)_3$ and $(BOH)_4^-$ with OH^- groups of the sorbent in cis position; at pH ≥ 9.2 the dominant species is tetrahydroxy-borate ions, and as pH increases the concentration of this species also increases and the adsorption process becomes more effective (reaching a maximum at approximately pH 11).

The interaction of boron removal with the CA material is schematically represented by the reaction with the OH^- groups of alginate and boron species:

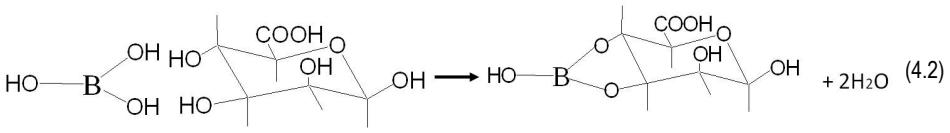

(4.2)

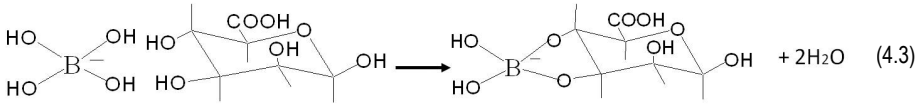

(4.3)

FTIR results verified this interaction through: i) Appearance of the band at 1204 cm^{-1} and the disappearance of the band at 1037 cm^{-1}, due to the reaction between OH^- groups of the C-O bond and boron species; ii) the appearance of the band at 1375 cm^{-1} (typical of B-O link), and iii) the appearance of the band at 1739 cm^{-1} which is consistent with the formation of boron esters groups. It was also detected a possible interaction between boron species and COO^- groups with the total disappearance and the reduction of the band at 1610 cm^{-1} at pH 6 and pH 9 respectively.

4.1.3 Determination of best sorption operating conditions

Boron removal from aqueous solutions was investigated using a 2^4 full factorial design. The effect of four parameters on sorption capacity was evaluated: pH, initial boron concentration, concentration of alginate in the beads, and size of the beads. A better sorption uptake was obtained with increasing initial boron concentration of solutions, increasing the pH, decreasing the alginate concentration in the sorbents beads and decreasing the size of the beads.

The effect of temperature was evaluated separately; the results verified the exothermic nature of the adsorption process, which means that boron removal on CA is favored at lower temperatures.

The influence of different types of alginates was also evaluated; boron uptake is not dependent on the variation in M- or G-block concentration; hydroxyl groups in both monomeric units appear to have easy access to boron species.

4.1.4 Sorption isotherms

Adsorption isotherms express the relation between the amount of adsorbate (mg) removed from the solution by unit of adsorbent mass (g) at constant temperature.

Sorption isotherms of boron onto alginate beads were performed at different pH (3, 6, 9, 10 and 11) and at different temperatures (293 K and 308 K). The equilibrium adsorption capacity increased as initial boron concentration increased; the shape of the isotherm curves indicated that sorption on CA was favorable (a plateau was formed at a high residual boron concentration). The equilibrium isotherms fitted very well to the Langmuir model; the maximum sorption capacity was obtained at pH 11 at room temperature (12 mmol g^{-1}). These promising results were compared with the results provided in the literature and show the CA material to be an eco-friendly alternative for boron removal.

4.1.5 Kinetic study

Sorption parameters (such as pH, stirring speed, temperature, concentration of M- and G-blocks) were examined to determine their influence on the kinetic profiles of boron adsorption with the CA material. It was found that sorption of boron onto CA is performed in two stages; adsorption was very fast in the initial stage and became slower as equilibrium was approached. The contact time to reach equilibrium was 20 min and was independent of stirring speed, pH and temperature; however, adsorption uptake was strongly affected by pH and temperature. It was verified that boron removal from aqueous solutions is favored at higher pH and lower temperature.

Two kinetic models, widely used for adsorption processes reported in the literature (pseudo-first-order and pseudo-second-order models), were used in the present study in combination with the intraparticle diffusion equation (Web and Morris, 1963) to examine the controlling mechanism of boron removal on CA. The results showed the pseudo-second-order model to give a better fit for the experimental data; in the literature, this model is usually associated with chemisorption processes.

The sorption process can be described by four consecutive steps: i) transport in the bulk of the solution; ii) diffusion across the liquid film surrounding the sorbent particles; iii) particle diffusion in the liquid; iv) sorption and desorption within the particle and on the external surface.

In the present work, the results indicated that intraparticle diffusion is not the only limiting step in boron uptake; resistance to film diffusion may affect the kinetics of boron uptake.

4.1.6 Effect of sodium salts

Sorption of boron on CA was found to be seriously influenced by the presence of sodium salts in the solution. Sorption capacity was reduced by more than 50% in the presence of sodium ions; these contribute to the swelling of the beads, promoting ion exchange between sodium in the solution and calcium ions in the sorbent, which weakens the egg-box structure.

4.2 EVALUATION OF ALGINATE BEADS FOR BORON SORPTION IN A FIXED-BED SYSTEM

4.2.1 Influence of sorption parameters

The effect on breakthrough curves of sorption parameters such as pH, inlet boron concentration, feed flow rate and adsorbent mass (through variations of column diameter and depth) were evaluated in a fixed-bed system. The results indicated that boron removal is dependent on all of the above parameters.

As expected, when a higher boron concentration was used a higher sorption capacity was obtained. At higher concentrations, the slope of the breakthrough curves increases, indicating better mass transfer. A similar trend was obtained by increasing the pH of the solutions; boron uptake rose from 3 mg g^{-1} to 9.9 mg g^{-1} when the pH was increased from 6 to 11. These results are in agreement with those obtained in the batch system. At lower flow rates, a higher sorption uptake was obtained; this is due to the fact that boron sorption is influenced by the residence time of the sorbate in the column, the diffusion of the sorbate into the pores, and the amount of active sites available in the adsorbent beads. The dependence on residence time is clear evidence that external and intraparticle diffusion are rate-controlling. The best operating conditions were found at high pH, high initial boron concentration, high column depth and low flow rate.

4.2.2 Fitting of the experimental data

The experimental results were well described by the Adams-Bohart and the Hutchins models; a good agreement was obtained with these models in order to calculate the design parameters. The partial least squares (PLS) technique was used to statistically correlate the main sorption variables with the sorption efficiency of the process; the statistical coefficients were determined and could be useful for predicting the theoretical efficiency of boron sorption in continuous systems.

4.3 DEVELOPMENT AND CHARACTERIZATION OF CHITOSAN AND ALGINATE-BASED COMPOSITES FOR BORON REMOVAL

In order to improve the sorption uptake in acidic-neutral medium, to improve the selectivity towards boron species and to enhance the mechanical properties of calcium alginate beads and raw chitosan, different composites were synthesized. The novel materials are based on an organic support (of alginate or chitosan) used to immobilize the inorganic material as metal hydroxides (which are demonstrated in the literature to be effective for boron removal, but with limiting handling capacity and low reusability in sorption processes when are used separately). These composites—calcium alginate/alumina (CAAl), chitosan/nickel(II) hydroxide [chiNi(II)], chitosan/iron(III) hydroxide [chiFer(III)]—have been evaluated under a wide interval of operating conditions.

4.3.1 Characterization

The composite materials were characterized by ESEM-EDX, TGA, FTIR and porosimetry studies. The ESEM images were used to compare the surface morphology, and EDX analysis was used to determine the

composition of several areas of the composites. As shown in Figure 4.1, CAAl exhibits a non-homogenous distribution of alumina around the polymer support; this is due to the initial immobilization technique used for this material, which consisted of the direct addition of metal hydroxide to the alginate solution followed by the co-precipitation of alginate/alumina in a calcium nitrate solution. The ESEM images clearly showed that this was not the most effective immobilization method. Nevertheless, it did not strongly affect the sorption properties of alginate and alumina.

The immobilization technique was improved using chitosan; the metal hydroxides were formed and trapped in situ by mixing the chitosan solution with a solution containing the metal ions and later through co-precipitation of the chitosan/metal solution with NaOH. Cross-sections of the materials were analyzed by EDX, which revealed a homogenous distribution of the metal hydroxide across the external and internal surfaces of the polymer.

Porosimetry studies indicated that these composites are essentially mesoporous materials. TGA studies indicated that the material can resist high temperatures, with thermal decomposition starting at 483 K for CAAl and around 531 K for [chiNi(II)] and [chiFer(III)]. FTIR spectra performed with the chitosan-based composites showed an interaction between boron and hydroxyl and amino groups. FTIR analysis recorded in the range 4000–400 cm^{-1} was used to verify the chemical interaction of boron with the hydroxyl and amino groups in the sorbent.

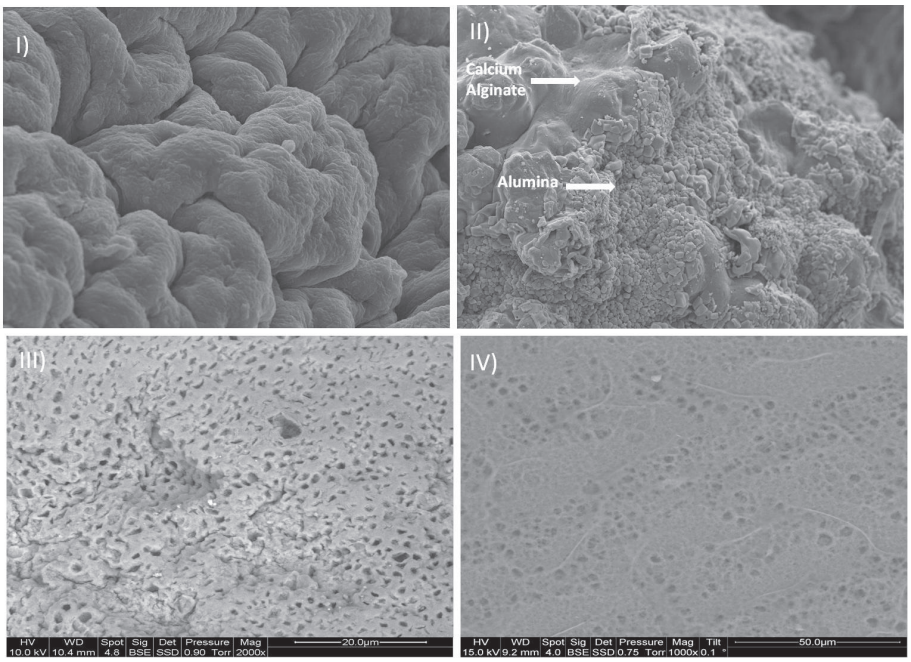

Figure 4.1. Surface morphology of adsorbent materials. I) CA. II) CAAl. III) [chiNi(III)]. IV) [chiFer(III)].

4.3.2 Effect of pH

The pH influence on boron removal was tested in the batch system; the results showed that CAAl improves boron sorption in neutral medium (i.e., pH 6–8), which contrasts with the results for alginate and alumina used separately. The maximum boron removal rate was still reached at pH 11, and the results suggest that CAAl can be used in a broader pH range than CA.

The best results using [chiNi(II)] were obtained in the range pH 6–9, which was found to be the best pH region for boron removal with this material. The pH of zero charge (pHpzc) was 6.57, which means that at pH above the pHpzc the surface becomes negatively charged and adsorption becomes favorable for the removal of $B(OH)_3$ species; [chiFer(III)] showed the same trend.

4.3.3 Equilibrium study

The equilibrium studies verified the effect of pH, initial boron concentration and temperature on boron uptake. The best sorption capacity was 12 mmol g^{-1} (at pH 11) for CAAl and 5.6 mmol g^{-1} (at pH 7) for [chiNi(II)]. The experimental data were well described by the Langmuir equation.

In the current work, temperature increase had a negative influence on boron removal; the process is exothermic. High enthalpy change values calculated from the Van't Hoff equation support the hypothesis that sorption on CA and CAAl follows a chemisorption process. On [chiNi(II)] and [chiFer(III)] composites, however, the mechanism of interaction with boron species is the result of a combination of electrostatic forces and chemical sorption. The interaction with metal hydroxides can be summarized by the following equations:

pH < 9.2

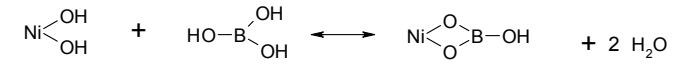
(4.4)

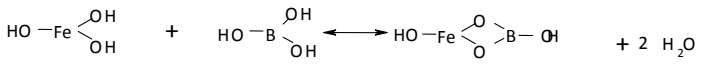
(4.5)

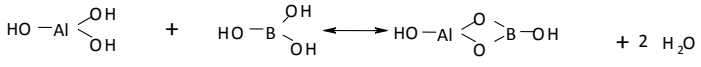
(4.6)

pH ≥ 9.2

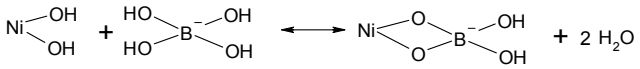
(4.7)

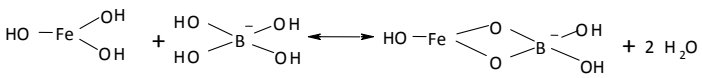
(4.8)

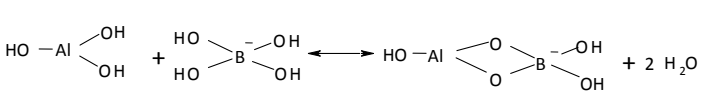
(4.9)

This mechanism takes place if the distances between hydroxyl groups in the sorbent are similar (or of the same order of magnitude) to those for boric acid and borate ions. Amino groups have also been found to interact with boron on chitosan; previous experiments with chitosan beads were used to determine the maximum sorption capacity, which was 0.3 mmol g^{-1} (in agreement with the literature; Wei et al., 2011).The results indicated that sorption uptake at pH 7 followed the order [chiNi(II)] > [chiFer(III)] ≈ CAAl > CA > chitosan. Table 4.1 shows the maximum sorption capacity reported in the literature (for a batch system); CA seems to be a good alternative at high pH and [chiNi(II)] is suitable for neutral medium.

Table 4.1. Comparison of boron sorption capacities for several adsorbents

Adsorbent	T(K)	pH	q (mmol.g^{-1})	Ce (mmol L^{-1})	Authors
CA	293	11	12	320	This work
CAAl	293	11	12	320	This work
Calcined magnesite tailing	318	6	6.1	50.9	Kipçak and Özdemir, 2012
NanoFe	298	8.3	6.01	2.78 10^{-2}	Zelmanov and Semiat, 2014
[chiNi(II)]	298	7	5.68	231.3	This work
Fe-impregnated GAC	298	8.3	4.63	2.78 10^{-2}	Zelmanov and Semiat, 2014
CTS-MG	298	7	3.25	17	Wei et al., 2011
Polymer-supported Iminodipropylene glycol functions	298	6.0 - 6.5	3	*430.0	Senkal and Bicak, 2003
ATG	303	8.8	2.25	14.1	Morisada et al., 2001
GlyPSF	303	7	2.09	87.9	Meng et al., 2012
Polymer-supported 2-hydroxylethylamino glycol functions	298	7.4	1.82	*485.0	Gazi and Bicak, 2007
Si-MG	298	7	1.54	0.2	Xu et al., 2012
TG	303	8.8	1.05	14.3	Morisada et al., 2011
Amberlite IRA-743	298	7	0.71	8	Wei et al., 2011
Fly ash	318	10	0.64	7.7	Polowczyk et al., 2013
CCTS	298	7	0.39	8	Wei et al., 2011
Calcined alunite	298	10	0.31	16.7	Kavak, 2009
Al-WTRs	298	8.3	9.07x10^{-2}	7.4	Irawan et al., 2001
Palm oil mill boiler bottom ash	298	8	4.35x10^{-2}	1.2	Chong et al., 2009

*Initial boron concentrations (mmol L^{-1}).

4.3.4 Kinetic study

In all cases, the experimental data fitted well with the pseudo-second-order model. Two stages were identified from the kinetic profiles: fast initial sorption followed by a slow-rate step as equilibrium was approached. The air-drying method used for sorbent preparation was found to influence on the kinetic profiles of the composites materials; the active sites in the wet and freeze dried beads are more easily accessible, hence the time taken to reach equilibrium is lower. In the case of [chiNi(II)], the time to reach the equilibrium was 17 h for wet and freeze dried beads versus 48 h for air-dried beads; and for CAAl this time was 0.3 h using wet beads and 3.3 h employing air-dried beads.

ESEM images indicated that air-drying method influence on the morphology of the sorbents beads: some folds were observed over entire surfaces (and small cavities or pores were found between these folds); it affects the accessibility to the active centers and the diffusion properties. The intraparticle diffusion and resistance to film diffusion may affect the control of uptake kinetics; the diffusion coefficients calculated by Crank's equation followed the order: Wet beads > freeze-dried beads > air-dried beads.

4.3.5 Effect of NaCl

In order to determine the influence of ionic strength on the effectiveness of the composites, sodium chloride was added to the boron solution up to a concentration of 40 g L^{-1}. At this high concentration, boron uptake on CAAl changed drastically and the ion exchange between the Na^{+} (from the solution) and Ca^{+2} ions (from the adsorbent) collapsed the egg-box structure of the alginate beads. By contrast, the sorption uptake on [chiNi(II)] composites did not change, which enabled us to evaluate the performance of this material with seawater samples.

4.4 TOWARDS AN INDUSTRIAL APPLICATION FOR BORON RECOVERY

4.4.1 Desorption in a batch system

The composite materials developed in this work were evaluated in sorption-desorption cycles in order to provide efficient sorbents with high reusability and easy to elute.

In the batch system, pH was found to be a critical parameter and the loaded material was eluted by changing the pH of the aqueous medium in contact with the surface of the sorbent. Desorption of CAAl was effectively achieved using water at pH 7 (the sorption step was performed at pH 11). The results for [chiNi(II)] indicated that desorption can be performed with a dilute solution of NaOH (0.01 M), i.e. water at pH 12. This material can be reused at least five times with no change in boron uptake, which represents a major advantage over commercial ion-exchange resins that require more expensive eluents for sorbent regeneration.

4.4.2 Adsorption-desorption cycles in a continuous system with real samples of Mediterranean seawater

A good sorbent, particularly for large-scale application, must be recyclable in order to be competitive; [chiFer(III)] composites were evaluated in a continuous system with seawater samples of natural pH 8.3 and a boron concentration of 4.2 mg L^{-1}.

The sorption step was performed at a flow rate of 3 mL min^{-1} and the results confirmed that this composite is effective for boron recovery from seawater; five adsorption-desorption cycles were performed, the molar ratio between the mass of adsorbed boron in the five consecutive cycles and the mass of Iron(III) hydroxide present in the adsorbent beads was 10.7 $mmol_B$ (mol $_{Fe(OH)3}$)$^{-1}$. The governing mechanism is similar to the one observed for [chiNi(II)]. Boron was recovered from the loaded sorbent using a 0.01 M NaOH solution.

GENERAL CONCLUSIONS

This work contributes to the improvement of boron separation by sorption technique; it focuses on the development of innovative composite materials (alginate and chitosan-based) and the evaluation of their suitability for boron recovery from aqueous solutions.

Based on the results of the study, calcium alginate (CA) beads and the composites synthesized during this thesis—calcium alginate/alumina (CAAl), chitosan/$Ni(OH)_2$ [chiNi(II)], and chitosan/$Fe(OH)_3$ [chiFer(III)]—appear to be efficient and promising sorbents for boron separation.

The adsorption of boron on calcium alginate beads is influenced by the pH and the initial boron concentration of the solutions. Tetrahydroxy borate ions [$B(OH)_4^-$] are the boron species most effectively removed by calcium alginate beads: when pH is increased, boron adsorption also increases, due to the interaction between the OH^- groups of the boron species and the OH^- groups present in the alginate.

Fourier transform infrared spectroscopy confirmed the formation of boron esters groups. Boron adsorption on alginate beads can be described by Langmuir isotherms, with a maximum adsorption capacity of 12 mmol g^{-1} reached in an alkaline medium.

Experimental kinetics studies demonstrated that equilibrium with calcium alginate beads can be reached in the first 20 minutes; the results are adequately described by the pseudo-second-order model. Statistical studies with a full factorial design demonstrated that the best sorption capacity was achieved at high pH (10–11), at high initial boron concentration (1000 mg L^{-1}) and with the smallest bead size (1.6 mm). The results of the isotherms at different alginate concentrations in beads show that there is no significant difference in adsorption capacity at concentrations in the range 1.6–3.2%.

The results of dynamic studies with alginate beads were consistent with those obtained in the batch system; the best sorption uptake was achieved at high pH (11), at high initial boron concentration, increased column depth and at the lowest flow velocity. The breakthrough curves were described by the Adams-Bohart model; maximum boron removal was 55% under optimal operating conditions. The use of the PLS technique enabled a partial adjustment between experimental parameter values (initial boron concentration, C_0; mass of adsorbent, m; volume of the column Vc; flow rate, Q; pH) and adsorption rate.

In order to improve sorption uptake in neutral medium, different composites were synthesized and evaluated; CAAl, [chiNi(II)] and [chiFer(III)] may substantially improve boron removal in acidic-neutral pH region in comparison with alginate beads (CA). The experimental data conformed to the Langmuir isotherm model. The results of kinetics studies showed that the experimental data are a better fit to the pseudo-second-order

model; sorption uptake at pH 7 was improved in the following order: [chiNi(II)] > [chiFer(III)]≈CAAl > CA > chitosan.

The effect of temperature was evaluated for CA, CAAl and [chiNi(II)]; sorption was found to be temperature-dependent: the exothermic nature of the adsorption process was verified, according to which an increase in temperature decreases the sorption capacity of sorbents; high values of enthalpy changes (ΔH^o) calculated by the Van't Hoff equation indicated that sorption on CA and CAAl follows a chemisorption process. On the [chiNi(II)] and [chiFer(III)] composites, however, the mechanism of interaction with boron species is a combination of physical and chemical processes. The reaction between OH^- groups and the cis-diol groups of the composite and the electrostatic forces between $B(OH)_3$ species and the adsorbent surface (at $pH>pH_{pzc}$) were identified as the main responsible in boron removal; sorption uptake was better than achieved by chitosan alone.

Desorption studies were performed to verify the reusability of the sorbent materials. High efficiency was achieved with distilled water at pH 7 using CA and CAAl, and with a dilute solution of NaOH (0.01M) using the [chiNi(II)] and [chiFer(III)] composites. More than 70% of boron was recovered from the CA and CAAl sorbents, and 70–90% was recovered from the loaded [chiNi(II)] composites in five successive adsorption-desorption cycles in a batch system, with no significant change in sorption uptake (in the range 80–100%). This represents a clear advantage over other commercial resins reported in the literature, which require more expensive and chemically aggressive eluents whose sorption capacity decreases with each new operational cycle.

The influence of foreign ions on boron sorption was investigated; the results showed that the presence of Na^+ ions induces swelling of the calcium alginate beads by ion-exchange process with Ca^{+2}, collapsing the egg-box structure.

On the [chiNi(II)] composite, ionic strength had a weak influence on boron sorption; the concentration of sodium chloride was increased to 40 g L^{-1} and only a slight reduction (approximately 10%) was observed at high salt concentration. This opened the possibility of using the adsorbent for boron recovery from seawater: real samples from the Mediterranean Sea, tested in a batch system, demonstrated that salinity does not influence sorption capacity.

In this sense, it has been manufactured a more stable, efficient, and cost-effective material (since 1 ton of $Fe(OH)_3$ is considerably less expensive than 1 ton of $Ni(OH)_2$) and with fewer secondary risks (such as possible contamination with metal ions in the case of nickel release from the polymeric matrix of the adsorbent). Thus, drawing on the experience gained with the [chiNi(II)] composite, [chiFer(III)] was synthesized in collaboration with the Centre des Matériaux des Mines d'Alès (École des Mines d'Alès-France), following the same innovative immobilization in situ technique. SEM-EDX analysis showed a homogeneous distribution of iron(III) hydroxide across the whole polymeric matrix structure (made of chitosan) of the composite; porosity studies revealed that [chiFer(III)] is a mesoporous material. This novel material was tested in a continuous system with real samples of seawater; the molar ratio calculated as the amount of adsorbed boron in the five adsorption cycles and the mass of iron(III) hydroxide, was 10.7 $mmol_B(mol\ Fe(OH)_3)^{-1}$.

The [chiFer(III)] composite can be effectively reused at least five times using MilliQ-water of pH 12 (0.01 M NaOH solution), with no significant change in sorption uptake in consecutive sorption cycles. Crucially, this opens the door to future research to devise an environmentally-friendly process.

REFERENCES

- Acuña, M., Los suelos como fuente de boro para las plantas, Revista UDO Agrícola 1(5) (2005) 10-26.
- Anderson, D.L., Kitto, M.E., McCarthy, L., Zoller, W.H., Sources and atmospheric distribution of particulate and gas-phase boron, Atmos. Environ. 28 (8) (1994) 1401-1410.
- Argust, P., Distribution of boron in the environment, Biol. Trace Elem. Res. 66 (1998) 131-143.
- Atsuki, K., Tomoda, Y., Studies on seaweeds of Japan I. The chemical constituents of Laminaria, J. soc. Chem. ind. Japan 29 (1926) 509-517.
- Barret, E.P., Joyner, L.G., Halenda, P.P., The determination of pore volume and area distributions in pourous substances. I. Computations from nitrogen isotherms, J. Am. Chem. Soc. 73 (1951) 373–380.
- Barron, D., Buti, S., Ruiz, M., Barbosa, J., Evaluation of acidity constants and preferential solvation in tetrahydrofuran-water mixtures, Polyhedron 18 (1999) 3281-3288.
- Bertagnolli, C., Da Silva, M.G., E. Guibal, Chromium biosorption using the residue of alginate extraction from Sargassum Filipendula, Chem. Eng. J. 237 (2014) 362-371.
- Brown, H., Wittig G., The nobel Prize in chemistry [on-line]. 1979. [Retrieved: 28th June, 2014]. Available in:
  <http://www.nobelprize.org/nobel_prizes/chemistry/laureates/1979/index.html>
- Brunauer, S., Emmet, P.H., Teller, E., Adsorption of gases in multimolecular layers, J. Am. Chem. Soc. 60 (1938) 309–319.
- Capelle, K., Microdosage colorimétrique du bore dans les aciers par l'emploi du reactif a l'azomethine H, Anal. Chim. Acta 25 (1961) 59-68.
- Cengeloglu, Y. Tor, A., Arslan, G., Ersoz, M., Gezgin, S., Removal of boron from aqueous solution by using neutralized red mud, J. Hazard. Mat. 142 (2007) 412-417.
- Cengeloglu, Y., Arslan, G., Tor, A., Kocak, I., Dursun, N., Removal of boron from water by using reverse osmosis, Sep. Purif. Technol. 64 (2008) 141–146.
- Chapin, R., Ku, W., Kenney, M., The effects of dietary boron on bone strength in rats, Fund. Appl. Toxicol. 35 (1997) 205-215.
- Chong, M.F., Lee, K.P., Chieng, H.J., Ramli, I.I., Removal of boron from ceramic industry wastewater by adsorption-flocculation mechanism using palm oil mill boiler (POMB) bottom ash and polymer, Water Res. 43 (2009) 3326-3334.
- Cox, C., Boric acid and borates, Journal of pesticide reform 24 (2) (2004) 10-15.
- Culver, B., Shen, P., Taylor, T., The relationship of blood- and urine-boron to boron exposure in borax-workers and the usefulness of urine-boron as an exposure marker, Environ. Health Persp. 102 (7) (1994) 133-137.
- De la Fuente García-Soto, M.M., Diseño y desarrollo de un sistema de tratamiento para la eliminación de boro en vertidos industriales. Doctoral thesis, Escuela Técnica Superior de Ingenieros Industriales, Madrid, 2000.
- De la Fuente García-Soto, M.M., Muñoz Camacho, E., Boron removal by means of adsorption with magnesium oxide, Sep. Purif. Technol. 48 (2006) 36–44.
- De la Fuente García-Soto, M.M., Muñoz Camacho, E., Boron removal by means of adsorption processes with magnesium oxide — Modelization and mechanism, Desalination 249 (2009) 626–634.
- Del Campo Marin, C., Gideon, O., Boron removal by the duckweed Lemna gibba: A potential method for the remediation of boron-polluted waters, Water Res. 41 (2007) 4579 – 4584.
- Deze, E.G., Papageorgiou, S.K., Favvas, E.P., Katsaros, F.K., Porous alginate aerogel beads for effective and rapid heavy metals sorption from aqueous solutions: Effect of porosity in Cu^{+2} and Cd^{+2} ion sorption, Chem. Eng. J. 209 (2012) 537-546.
- Dixon, R., Sherins, R., Lee, I., Assessment of environmental factors affecting male fertility. Environ Health Persp. 30 (1979) 53-68.

- Dixon, R.L., Lee, I.P., Sherins, R.J., Methods to assess reproductive effects of environmental chemicals: Studies of cadmium and boron administered orally, Environ. Health Persp. 13 (1976) 59-67.
- Donati, I., Paoletti, S. Material properties of alginates. In: Rehm, B.H.A. (Eds). Alginates: Biology and applications. Berlin: Springer-Verlag, 2009, 1-53, ISBN 978-3-540-92678-8
- Dosoretz, C., Geffen, N., Semiat, R., Eisen, M., Balazs, Y., Katz, I., Boron removal from water by complexation to polyol compounds, J. Membrane Sci. 286 (2006) 45-51.
- Draize, J., Kelley, E., The urinary excretion of boric acid preparations following oral administration and topical applications to intact and damaged skin of rabbits, Toxicol. Appl. Pharma. 1 (1959) 267-276.
- Dutta, P., Dutta, J., Tripathi, V., Chitin and chitosan: Chemistry, properties and applications, J. Sci. Ind. Res. India 63 (2004) 20-31.
- Dydo, P., Nems, I., Turek, M., Boron removal and its concentration by reverse osmosis in the presence of polyols compounds, Sep. Purif. Technol. 89 (2012) 171-180.
- European Food Safety Authority (EFSA), Opinion of the scientific panel on dietetic products, nutrition and allergies on a request from the commission related to the tolerable upper intake level of boron (sodium borate and boric acid), the EFSA Journal 80 (2004) 1-2.
- Fail, P., George, J., Seely, J., Reproductive toxicity of boric acid in CD-1 Swiss mice: Assessment using the continuous breeding protocol. Fund. Appl. Toxicol. 17 (1991) 225-239.
- Field, E., Price, C., Marr, M., Final report on the developmental toxicity of boric acid (CAS No. 10043-35-3) in CD-1-Swiss Mice. National Toxicology Program, Public Health Service, U.S. Department of Health and Human Services, Research Triangle Park, NC; NTP Final Report No. 89-250, 1989.
- Fiol, N., Escudero, C., Poch, J., Villaescusa, I., Prelimanary studies on Cr(VI) removal from aqueous solution using grape stalk wastes encapsulated in calcium alginate beads in a packed bed up-flow column, React. Funct. Polym. 66 (2006) 795-807.
- Fisher, F.G., Dörfel, H., Die Polyuronsäuren der Braunalgen (Kohlenhydrate der Algen), Z. Physiol. Chem. 302 (1955) 186-203.
- FMC Biopolymer, A word of possibilities lies Just below the surface [on-line]. Alginates [Retrieved: 26th June, 2014]. Available in: <http://www.fmcbiopolymer.com/Portals/Pharm/Content/Docs/Alginates.pdf>
- Fortuny, A., Coll, M.T., Kedari C.S., Sastre A.M., Effect of phase modifiers on boron removal by solvent extraction using 1,3 diolic compounds, J. Chem. Biotechnol. 89 (2014) 858-865.
- Gazi, M., Bicak, N., Selective boron extraction by polymer supported 2-hydroxylethylamino propylene glycol functions, React. Funct. Polym. 67 (2007) 936-942.
- Gazi, M., Shahmohammadi, S., Removal of trace boron from aqueous solution using iminobis-(propylene glycol) modified chitosan beads, React. Funct. Polym. 72 (2012) 680-686.
- Ghaffour, N., Missimer, T.M., Amy, G.L., Technical review and evaluation of the economics of water desalination: current and future challenges for better water supply sustainability, Desalination 309 (2013) 197-207.
- Gorin, P.A., Spencer, J.F., Exocellular alginic acid from Azotobacter vinelandii, Can. J. Chem. 44 (1966) 993-998.
- Govan, J.R., Fyfe, J.F., Jarman, T.R., Isolation of alginate-producing mutants of Pseudomonas fluorescens, Pseudomonas putida, and Pseudomonas mendocina, J. Gen. Microbiol. 125 (1981) 217-220.
- Grant, G., Morris, E., Rees, D., Smith, P., Thom, D., Biological interactions between polysaccharides and divalent cations: the egg-box model. FEBS Lett. 32(1) (1973) 195-198.
- Guibal E., Figuerola-Piñol, A., Ruiz, M., Vincent T., Jouannin C., Sastre, A.M., Immobilization of cyphos ionic liquids in alginate capsules for Cd(II) sorption, Separ. Sci. Technol. 45 (2010) 1935-1949.
- Harvey, S.C., Antiseptics and disinfectants; fungicides, ectoparasiticides. In: Goodman, L.S., Gilman, A., A.G. Gilman, Koelle, G.B. (Eds). Pharmacological basis of therapeutics. Toronto: Macmillan, 1975, 994.
- Haug, A., Larsen, B., A study on the constitution of alginic acid by partial acid hydrolysis, Proc. Int. Seaweed Symp. 5 (1966) 271-277.

- Haug, A., Larsen, B., SmidsrΦd O., A study of the constitution of alginic acid by partial hydrolysis, Acta Chem. Scand. 20 (1966) 183-190.
- Haug, A., SmidsrΦd, O., Fractionation of alginates by precipitation with calcium and magnesium ions, Acta Chem. Scand. 19 (1965) 1221-1226.
- Heindel, J., Price, C., Field, E., Developmental toxicity of boric acid in mice and rats, Fund. Appl. Toxicol. 18 (1992) 266-277.
- Hilal, N., Kim G.J., Somerfield C., Boron removal from saline water: A comprehensive review, Desalination 273 (2011) 23-25.
- Hirano S., N-acyl, N-arylidene and N-alkylidene chitosans, and their hydrogels, chitin handbook. In: Muzzarelli, R. A. A. and MG Peter, M.G. (Eds). Italy: European chitin society, 1997,71-76
- Ho, Y.S., McKay, G., Sorption of dye from aqueous solution by peat, Chem. Eng. J. 70 (1998) 115-124.
- Institute for Evaluating Health Risks (IEHR), An assessment of boric acid and borax using the IEHR evaluative process for assessing human developmental and reproductive toxicity of agents. Reprod. Toxicol. 11 (1997) 123-160.
- Irawan, C., Liu, J.C., Wu, C.C., Removal of boron using aluminum-based water treatment residuals (Al-WTRs), Desalination 276 (2011) 322-327.
- Itakura, T., Sasai, R., Itoh, H., Precipitation recovery of boron from wastewater by hydrothermal mineralization, Wat. Res. 39 (2005) 2543-2548.
- Jansen, J., Andersen, J., Schou, J., Boric acid single dose pharmacokinetics after intravenous administration to man, Arch. Toxicol. 55 (1984) 64-67.
- John, M.K., Chuah, H.H., Neufeld, J.H., Application of improved azomethine-H method to the determination of boron in soils and plants, Anal. Lett. 8 (1975) 559-568.
- Kabay, N., Koseoglu, P., Yavuz, E., Yuksel, U., Yuksel, M., An innovative integrated system for boron removal from geothermal water using RO process and Ion exchange-ultrafiltration hybrid method, Desalination 316 (2013) 1-7.
- Kabaya, N., Yılmaza, I., Yamacb, S., Samatyab, S., Yuksela, M., Yukselb, U., Ardab, M., Sa_glama, M., Iwanagac, T., Hirowatarid, K., Removal and recovery of boron from geothermal wastewater by selective ion exchange resins. I. Laboratory tests, React. Funct. Polym. 60 (2004) 163–170.
- Karahan, S., Yurdakoc, M., Seki, Y., Yurdakoc, K., Removal of boron from aqueous solution by clays and modified clays, J. Colloid Interf Sci. 293 (1) (2006) 36–42.
- Kavak, D., Removal of boron from aqueous solutions by batch adsorption on calcined alunite using experimental design, J. Hazard. Mater. 163 (2009) 308–314.
- Kimseng, K., Meissel, M., Environmental Scanning Electron Microscope [on-line]. 2011. [Retrieved: 28th June, 2014]. Available in: <http://www.calce.umd.edu/TSFA/ESEM.pdf>
- Kipçak, I., Özdemir, M., Removal of boron from aqueous solution using calcined magnesite tailing, Chem. Eng. J. 189-190 (2012) 68-74.
- Kluczka, J., Ciba, J., Trojanowska, J., Zolotajkin, M., Turek, M., Dydo, P., Removal of boron dissolved in Water, Environm. Progress 26 (1) (2007) 71-77.
- Koparal, A.S., The removal of salinity from produced formation by conventional and electrochemical methods, Fresen. Environ. Bull. 12A (11) (2002) 1071–1077.
- Krauskopf, K.B. Geochemistry of micronutrients. In: Mortvedt, J.J., Giordano, P.M., Lindsay, W.L. (Eds.). Micronutrients in Agriculture. Madison: Soil Science Society of America, 1972.
- Ku, W., Chapin, R., Moseman, R., Tissue disposition of boron in male Fischer rats. Toxicol. Appl. Pharma. 111 (1991) 145-151.
- Ku, W., Shih, L., Chapin, R., The effects of boric acid (BA) on testicular cells in culture. Reprod. Toxicol. 7 (1993) 321-331.
- Ku, W.W., Chapin, R.E., Mechanism of the testicular toxicity of boric acid in rats: In vivo and in vitro studies, Environ. Health Persp.71 (1994) 99-105.

- Kumar, M., Tamilarasan, R., Sivakumar, V., Adsorption of Victoria blue by carbon/Ba/alginate beads: Kinetics, thermodynamics and isotherm studies, Carbohyd. Polym. 98 (2013) 505-513.
- Lagergreen, S., Zur theorie der sogenannten adsorption gelöster stoffe: Kungliga Svenska Vetenskapsakademiens, Handlingar 24 (1898) 1-39.
- Larsen, B., SmidsrΦd O., Painter, T. J., Haug A., Calculation of the nearest-neighbour frequencies in fragments of alginate from the yields of free monomers after partial hydrolysis, Acta Chem. Scand. 24 (1970) 726-728.
- Linder, R., Strader, L., Rehnberg, G., Effect of acute exposure to boric acid on the male reproductive system of the rat, J. Toxicol. Environ. Health 31 (1990) 133-146.
- Lipscomb, W.N., Nobel Lecture: The Boranes and their relatives [on-line]. 1976. [Retrieved: 28th June, 2014]. Available in: <http://www.nobelprize.org/nobel_prizes/chemistry/laureates/1976/lipscomb-lecture.html>
- Liu, R., Ma, W., Jia, C., Wang, L., Li, H.Y., Effect of pH on biosorption of boron onto cotton cellulose, Desalination 207 (2007) 257-267.
- Matsumoto, M., Matsui, T., Kondo, K., Adsorption mechanism of boric acid on chitosan resin modified by saccharides. J. Chem. Eng. JPN. 32(2) (1999) 190-196.
- Matsuo, H., Miyazaki, Y., Takemura, H., Matsuoka, S., Sakashita, H., Yoshimura, K., 11B NMR study on the interaction of boric acid with Azomethine H, Polyhedron 23 (2004) 955-961.
- McDowell, R.H., Properties of alginates. 4th. London: Alginate Industries Ltd., 1977, 67.
- McHugh, D.J., A guide to the seaweed industry. Roma: FAO Fisheries technical paper, 44, 2003. ISBN 92-5-104958-0
- Meacham, S.L., Hunt, C.D., Dietary boron intakes of selected populations in the United States. Biol. Trace Elem. Res. 66 (1998) 65–78.
- Meland, M., Rebours, C., Short description of the Norwegian seaweed Industry, Bioforsk FOKUS 7(2) (2012) 275-277.
- Mellor, J.W. Mellor's comprehensive treatise on inorganic and theoretical chemistry. New York: Longman, 1980.
- Meng, J., Yuan, J., Kang, Y., Zhang, Y., Du, Q., Surface glycosylation of polysulfone membrane towards a novel complexing membrane for boron removal, J Colloid Interf. Sci. 368 (2012) 197-207.
- Mohammed, Y.I., Garba, K., Umar, S., Analytical determination of boron in irrigation water using azomethine-H: Spectrophotometry, IOSR Journal of Applied chemistry 7 (2014) 47-51.
- Morisada, S., Ogata, T., Kim, Y.H., Nakano, Y., Adsorption removal of boron in aqueous solutions by amine-modified tannin gel, Water Res. 45 (2011) 4028-4034.
- Morris, V.J., Food gels-roles played by polysaccharides, Chem. Ind. (1985) 159-164.
- Nadav, N., Boron removal from seawater reverse osmosis permeate utilizing selective ion exchange resin, Desalination 124 (1999) 131–135.
- Naghii, M., Samman, S., The boron content of selected foods and the estimation of its daily intake among free-living subjects, J. Am Coll. Nutr. 15(6) (1996) 614-619.
- Naghii, M., Samman, S., The effect of boron supplementation on the distribution of boron in selected tissues and on testosterone synthesis in rats, Nutr. Biochem. 7 (1996) 507-512.
- Neal C., Fox, K.K. Harrow, M.L., Neal M., Boron in the major UK rivers entering the North Sea. Sci. Total Environ. 210-211 (1998) 41–52.
- NTP (National Toxicology Program). Toxicology and carcinogenesis studies of boric acid (CAS No. 10043-35-3) in B6C3F1 mice (feed studies). Public Health Service, U.S. Department of Health and Human Services [on-line]; NTP TR-324,1987. [Retrieved: 8th January, 2010]. Available in: <http://cfpub.epa.gov/ols/catalog/advanced_bibliography.cfm?&FIELD1=SUBJECT&INPUT1=Carcinogenicity%20testing&TYPE1=EXACT&LOGIC1=AND&COLL=&SORT_TYPE=MTIC&start_row=201>

- Oishi K., Maehata, Y., Removal properties of dissolved boron by glucomannan gel, Chemosphere 91 (2013) 302-306.
- Okay, O., Güçlü, H., Soner, E., Balkan, T., Boron pollution in the Simav river, turkey and various methods of boron removal, Water Res. 9(7) (1985) 857-862.
- Öztürk, N., Kavak, D., Adsorption of boron from aqueous solutions using fly ash: Batch and column studies, J. Hazard. Mater. 127 (2005) 81–88.
- Öztürk, N., Kavak, D., Boron removal from aqueous solutions by adsorption on waste sepiolite and activated waste sepiolite using full factorial design, Adsorption 10 (2004) 245–257.
- Painter, T.J., Algal polysaccharides. In: Aspinall GO (Eds). The polysaccharides. New York: Academic, 1983, 196-286.
- Painter, T.J., SmidsrΦd O., Haug A., A computer study of the changes in composition-distribution occurring during random depolymerisation of a binary linear heteropolysaccharide, Acta Chem. Scand. 22 (1968) (1637-1648).
- Papageorgiou, S., Katsaros, F., Kouvelos, E.P., Nolan, J.W., Le Deit, H., Kanellopoulos, N. K., Heavy metal sorption by calcium alginate beads from Laminaria digitata. J. Hazard. Mater. B137 (2006) 1765–1772
- Polowczyk, I., Ulatowska, J., Kozlecki, T., Bastrzyk, A. Sawikski, W., Studies on removal of boron from aqueous solution by fly ash agglomerates, Desalination 310 (2013) 93-101.
- Power, P., Woods, W. The chemistry of boron and its speciation in plants, Plant Soil 193(1-2) (1997) 1-13.
- Prats, D., Chillon-Arias, M. F., Rodriguez-Pastor, M., Analysis of the influence of pH and pressure on the elimination of boron in reverse osmosis, Desalination 128 (2000) 269-273.
- Price, C., Field, E., Marr, M. Developmental toxicity of boric acid (CAS No. 10043-35-3) in Sprague Dawley rats. National Toxicology Program, Public Health Service, U.S. Department of Health and Human Services, Research Triangle Park, NC; NTP Report No. 90-105 (and Report Supplement No. 90-105A), 1990.
- Price, C., Marr, M., Myers, C. Determination of the no-observable-adverse-effect level (NOAEL) for developmental toxicity in Sprague-Dawley (CD) rats exposed to boric acid in feed on gestational days 0 to 20, and evaluation of postnatal recovery through postnatal day 21 [final report]. Research Triangle Institute, Center for Life Science, Research Triangle Park, NC; RTI Identification No. 65C-5657-200, 1994.
- Price, C., Marr, M., Myers, C., The developmental toxicity of boric acid in rabbits, Fund. Appl. Toxicol. 34 (1996b) 176-187.
- Price, C., Strong, P., Marr, M., Developmental toxicity NOAEL and postnatal recovery in rats fed boric acid during gestation, Fund. Appl. Toxicol. 32 (1996a) 179-193.
- Rainey, C.J., Nyquist, L.A., Christensen, R.E., Strong, P.L., Culver, B.D., Daily boron intake from the American diet, J. Am. Diet. Assoc. 99 (1999) 335–340.
- Rees, D.A., Polysaccharide gels, a molecular view, Chem. Ind. (1972) 630-636
- Rehm, B.H.A. Alginates from bacteria. In: Vandamme, E. J., De Baets, S., Steinbüchel, A. (Eds.).Biopolymers: Polysaccharides I - Polysaccharides from prokaryotes. Weinheim: Wiley-VCH verlag GmbH, 2002, 179-210, ISBN 3-527-30226-3.
- Rodriguez-Guerrero, M.J., Muñoz-Camacho, E., Bernal-Pita da Veiga, M.A., Estudio comparativo de la tolerancia al boro de dos variedades de pimiento (*Capsicum annuum L.*), Revista UDO Agricola 9 (3) (2009) 509-516.
- Romheld, V., Marschner H., Function of micronutrients in plants. In: Mortvedt, J.J. (Eds.). Micronutrients in Agriculture. 4th. Madison: Soil Society of America, 1991, 297-328.
- Ruiz, M., Development of techniques based on natural polymers for the recovery of precious metals. Doctoral thesis, Universitat Politecnica de Catalunya, Barcelona, 2002.
- Ruiz, M., Sastre, A.M., Zikan, M.C., Guibal, E., Palladium sorption on glutaraldehyde crosslinked chitosan in fixed-bed systems, J. Appl. Polym. Sci. 81 (2001) 153–165.
- Sabarudin, A., Oshita, K., Oshima, M., Motomizu, S., Synthesis of cross-linked chitosan possesing N-

methyl-D-glucamine moiety (CCTS-NMDG) for adsortion/concentration of boron in water samples and its accurate measurement by ICP-MS and ICP-AES. Talanta 66 (2005) 136-144.

- Santé Canadá, Santé de l'environnement et du milieu de travail. Le Bore [on-line]. Canada, 1990. [Retrieved: 6th August, 2014]. Available in:<http://www.hc-sc.gc.ca/ewh-semt/pubs/water-eau/boron-bore/index-fra.php#Recommandation>
- Schmidt, E., Vocke, F., Zur Kenntnis der Polyglykuronsäuren, Chem. Ber. 59 (1926) 1585-1588.
- Schou, J., Jansen, J., Aggerbeck, B., Human pharmacokinetics and safety of boric acid, Arch. Toxicol. 7 (1984) 232-235.
- Schubert, D. Borates in industrial use. In: Roesky, H.W., Atwood, D.A (Eds). Structure and bonding. Berlin: Springer-Verlag 105 (2003) 1- 40.
- Schucker, G.D., Maglioca, T.S., Su, Y.S., Spectrophotometric determination of boron in siliceous materials with Azomethine H, Anal. Chem. Acta 75 (1975) 95-100.
- Seal, B., Weeth, H., Effect of boron in drinking water on the male laboratory rat, Bull Environ Contam. Toxicol. 25 (1980) 782-789.
- Seki, Y., Seyhan, S., Yurdakoc, M., Removal of boron from aqueous solution by adsorption on Al_2O_3 based materials using full factorial design, J. Hazard. Mater. B138 (2006) 60–66.
- Senkal, B.F., Bicak, N., Polymer supported iminodipropylene glycol functions for removal of boron, React. Funct. Polym. 55 (2003) 27-33.
- Siegel, E., Wason, S., Boric acid toxicity, Pediatr. Clin. North Am. 33 (1986) 363-367.
- Simonnot, M.O, Castel, C., Nicolai, M., Rosin, C., Sardin, M., Jauffret, H., Boron removal from drinking water with a boron selective resin: is the treatment really selective?, Water Res. 34 (2000) 109-116.
- Smallwood, C., Boron. WHO. Guidelines for Drinking Water Quality. 2nd, 1998, 15-29.
- SmidsrΦd O., Draget, K.I., Alginates: chemistry and physical properties, Carbohydr. Eur. 14 (1996) 6-13.
- Soltani, R.D., Khorramabadi, G.S., Khataee A.R., Jorfi S., Silica nanopowders/alginate composite for adsorption of lead (II) ions in aqueous solutions, Journal of the Taiwan institute of Chemical Engineers 45 (2014) 973-980.
- Stanford, E.C.C. New substance obtained from some of the commoner species of marine algae; Algin, Chem. News 47 (1883) 254-257.
- Tagliabue, M., Reverberi A. P., Bagatin R., Boron removal from water: needs, challenges and perspectives, Journal of cleaner production 77 (2014) 56-64.
- Treinen, K., Chapin, R., Development of testicular lesions in F344 rats after treatment with boric acid, Toxicol. Appl. Pharm. 107 (1991) 325-335.
- U.S. Department of the Interior and U.S. Geological Survey, Mineral commodity Summaries [on-line]. Virginia, 2006. [Retrieved: 6th August, 2014]. Available in: <http://minerals.usgs.gov/minerals/pubs/mcs/2006/mcs2006.pdf>
- U.S. Department of the Interior and U.S. Geological Survey, Mineral commodity Summaries [on-line]. Washington, 2007. [Retrieved: 6th August, 2014].. Available in: <http://minerals.usgs.gov/minerals/pubs/mcs/2007/mcs2007.pdf>
- U.S. Department of the Interior and U.S. Geological Survey, Mineral commodity Summaries [on-line]. Washington, 2008. [Retrieved: 6th August, 2014]. Available in: <http://minerals.usgs.gov/minerals/pubs/mcs/2008/mcs2008.pdf>
- U.S. Department of the Interior and U.S. Geological Survey, Mineral commodity Summaries [on-line]. Washington, 2009. [Retrieved: 6th August, 2014]. Available in: <http://minerals.usgs.gov/minerals/pubs/mcs/2009/mcs2009.pdf>
- U.S. Department of the Interior and U.S. Geological Survey, Mineral commodity Summaries [on-line]. Washington, 2010. [Retrieved: 6th August, 2014]. Available in: <http://minerals.usgs.gov/minerals/pubs/mcs/2010/mcs2010.pdf>
- U.S. Department of the Interior and U.S. Geological Survey, Mineral commodity Summaries [on-line]. Virginia, 2011. [Retrieved: 6th August, 2014]. Available in:

<http://minerals.usgs.gov/minerals/pubs/mcs/2011/mcs2011.pdf>

- U.S. Department of the Interior and U.S. Geological Survey, Mineral commodity Summaries [on-line]. Virginia, 2012. [Retrieved: 6th August, 2014]. Available in: <http://minerals.usgs.gov/minerals/pubs/mcs/2012/mcs2012.pdf>
- U.S. Department of the Interior and U.S. Geological Survey, Mineral commodity Summaries on-line]. Virginia, 2013. [Retrieved: 6th August, 2014]. Available in: <http://minerals.usgs.gov/minerals/pubs/mcs/2013/mcs2013.pdf>
- U.S. Environmental Protection Agency (EPA), Toxicological review of boron and compounds. In Support of Summary Information on the Integrated Risk Information System (IRIS) [on-line]. Washington, DC, CAS No. 7440-42-8, 2004. [Retrieved: 5th June, 2010]. Available in:<http://www.epa.gov/ncea/iris/toxreviews/0410tr.pdf>
- Usuda, K., Kono, K., Orita, Y., Serum and urinary boron levels in rats after single administration of sodium tetraborate. Arch Toxicol. 72 (1998) 468-474.
- Vanderpool, R., Hof, D., Johnson, P., Use of inductively coupled plasma-mass spectrometry in boron-10 stable isotope experiments with plants, rats, and humans, Environ. Health Persp. 102 (7) (1994) 13-20.
- Weber, W.J., Morris, J. C., Kinetics of adsorption on carbon from solution, J. Sanit. Eng. Div. Proceed. Am. Soc. Civil Eng. 89 (1963) 31-59.
- Wei, Y.T., Zheng, Y.M., Chen, J.P., Design and fabrication of an innovative and environmental friendly adsorbent for boron removal, Water Res. 45 (2011) 2297-2305.
- Weir, R., Fisher, R., Toxicological studies on borax and boric acid, Toxicol. Appl. Pharma. 23 (1972) 351-364.
- WHO, Environmental health criteria 204: boron. Geneva, Switzerland: World Health Organization, 1998.
- Wilding, J., Smith, W., Yevich, P., The toxicity of boron oxide, Am. Ind. Hyg. Assoc. J. 20 (1959) 284-289.
- Woods, W.G., An introduction to boron: history, sources, uses, and chemistry. Environ. Health Persp. 102 (7) (1994) 5-11.
- World Health Organization, Guidelines for drinking-Water quality, fourth ed., Geneva, 2011.
- Wyness, A.J., Parkman R.H., Neal C., A summary of boron surface water quality data throughout the European Union, Sci. Total Environ. 314-316 (2003) 255-269.
- Xing, L., Dawei C., Liping X., Rongqing Z., Oral colon-specific drug delivery for bee venom peptide: development of a coated calcium alginate gel beadsentrapped liposome. J Control Release 93 (2003) 293–300.
- Xu, L. Liu, Y. Hu, H. Wu, Z. Chen, Q., Synthesis, characterization and application of a novel silica based adsorbent for boron removal, Desalination 294 (2012) 1-7.
- Yazicigil, Z., Oztekin, Y., Boron removal by electrodialysis with anion-exchange membranes, Desalination 190 (2006) 71–78.
- Yilmaz, A.E., Boncukcuoğlu, R., Kocakerim, M.M., A quantitative comparison between electrocoagulation and chemical coagulation for boron removal from boron-containing solution, J. Hazard. Mater. 149 (2007) 475-481.
- Yoshimura, K., Kariya, R., Tarutani, T., Spectrophotometric determination of boron in natural waters and rocks after specific adsorption on sephadex gel, Anal. Chim. Acta 109 (1979) 115-121.
- Yurdakoç, M., Seki, Y., Yurdakoç, K., Kinetic and thermodynamic studies of boron removal by Siral 5, Siral 40 and Siral 80, J. Colloid Interf. Sci. 286 (2005) 440-446.
- Zelmanov, G., Semiat, R., Boron removal from water and its recovery using iron (Fe+3) oxide/hydroxide-based nanoparticles (NanoFe) and NanoFe-impregnated granular activated carbon as adsorbent, Desalination 333 (2014) 107-117.

ANNEX I

SORPTION OF BORON ON ALGINATE GEL BEADS

Attention¡¡

M. Ruiz, C. Tobalina, H. Demey-Cedeño, J. A. Barron-Zambrano, A. M. Sastre. *Sorption of boron on alginate gel beads*. Reactive and Functional Polymers, 73 (2013) 653-657.

Pages 70 to 76 of the thesis are available at the editor's web

http://www.sciencedirect.com/science/article/pii/S1381514813000266

DOI: doi:10.1016/j.reactfunctpolym.2013.01.014

ANNEX II

BORON REMOVAL FROM AQUEOUS SOLUTIONS BY CALCIUM ALGINATE BEADS

ATTENTION¡

M. Ruiz, J.A. Barron-Zambrano, H. Demey, A. M. Sastre. *Boron removal from aqueous solutions by calcium alginate beads*. EMChIE 2010 Conference Proceedings, Vol. 2, pp.783-791. In: Dewil, R., Appels, L., Hulsmans, A. (Eds). Leuven (2010) ISBN: 9789081548601.

Pages 78 to 88 of the thesis, as part of the publication

EMChIE 21010 Conference Proceeding : [Mechelen, Belgium 17-19 May 2010] / edited by Raf Dewil, Lisa Appels & Ann Hulsman. Belgium : Acco Leuven, 2010. 2 vol. Powder technology, adsorption, advanced oxidation processes, process technology

are available at the UPC Library, permanent URL

http://cataleg.upc.edu/record=b1371824~S1*cat

ANNEX III

BORON REMOVAL FROM AQUEOUS SOLUTIONS USING ALGINATE GEL BEADS IN FIXED-BED SYSTEMS

Research Article

Received: 5 May 2013 Revised: 6 July 2013 Accepted: 15 July 2013

(wileyonlinelibrary.com) DOI 10.1002/jctb.4361

Boron removal from aqueous solutions using alginate gel beads in fixed-bed systems

Hary Demey-Cedeño,[a] Montserrat Ruiz,[a*] Jesús Alberto Barron-Zambrano[a] and Ana Maria Sastre[b]

Abstract

BACKGROUND: A column sorption study was carried out using calcium alginate gel beads as adsorbent for the removal of boron from aqueous solutions. The breakthrough curve was obtained as a function of pH, initial concentration of boron, feed flow rate, adsorbent mass and column diameter. The breakthrough capacity values and adsorption percentage of calcium alginate gel for boron were calculated. Column data obtained at different conditions were described using the Adams–Bohart model and bed-depth service time (BDST), derived from the Adams–Bohart equation to predict breakthrough curves and to determine the characteristic column parameters required for process design.

RESULTS: The maximum adsorption percentage of boron on calcium alginate gel beads using an initial concentration of boron of 50 mg L^{-1} at pH 11 and room temperature (20±1°C) was calculated to be 55.14%.

CONCLUSION: The results indicated that calcium alginate can be used in a continuous packed-bed column for boron adsorption. The optimal conditions for boron adsorption were obtained at high pH, higher initial boron concentration, increased column depth and lower flow velocity.

Keywords: sorption; boron; alginate; removal

INTRODUCTION

The increase in our knowledge of boron science in recent years has been of great importance both commercially and environmentally. Boron enters the hydrosphere naturally through the erosion of rocks, but its presence in water is increasingly attributed to pollution caused by industrial growth. Boron is an essential trace element for plant growth and human health but in excessive quantities it can affect human reproduction and lead to diseases of the nervous system. Boron has many industrial applications, particularly in the manufacturing of glass, detergents, ceramics and catalysts, but it is also used for its preservative and refrigerant properties. In all of these uses, boron is mainly released into the environment through industrial wastewater discharge. In recent years, boron has been identified as an essential element in chemical processes. In the natural environment, it is found mainly as boric acid or borates. In aqueous solutions at a boron concentration below 270 mg L^{-1}, boric acid is very weak and acts as a Lewis acid, as shown below:

$$B(HO)_3 + 2H_2O \leftrightarrow B(HO)_4^- + H_3O^+; \quad pK_a = 9.23 \qquad (1)$$

where the acid dissociation constant is pKa = 9.23.[1] The relative concentration of the tetrahydroxyborate anion increases with increasing pH and becomes the dominant species at pH 9.2. However, at higher concentrations and with increasing pH, especially above pH 11, polynuclear ions such as $[B_3O_3(OH)_5]^{2-}$ and $[B_4O_5(OH)_4]^{2-}$ form.[2] Formation of these species is a direct result of boron's tendency to form complexes with electron-donor species including oxygen, which attaches to the boron itself.[3]

Boron's electrophilicity and tendency to form esters through condensation with compounds bearing hydroxyl groups, including B-OH, make it particularly suitable for widespread industrial use. The increased presence of boron in the natural environment has led to the creation of guidelines that establish recommended limits for boron content in water used for irrigation and human consumption. According to the World Health Organization (WHO),[4] the guideline value for boron concentration in drinking water is 2.4 mg L^{-1}. Alongside this, the need for new sources of drinking water has led to the development of desalination processes for obtaining potable water from seawater. The boron content of seawater is approximately 5 mg L^{-1}, and after desalting

* *Correspondence to: M. Ruiz, Universitat Politècnica de Catalunya, EPSEVG, Department of Chemical Engineering, Av. Víctor Balaguer, s/n, 08800 Vilanova i la Geltrú, Spain. E-mail: montserrat.ruiz@upc.edu*

a *Universitat Politècnica de Catalunya, EPSEVG, Department of Chemical Engineering, Av. Víctor Balaguer, s/n, 08800 Vilanova i la Geltrú, Spain*

b *Universitat Politècnica de Catalunya, Department of Chemical Engineering, ETSEIB, Diagonal 647, 08028 Barcelona, Spain*

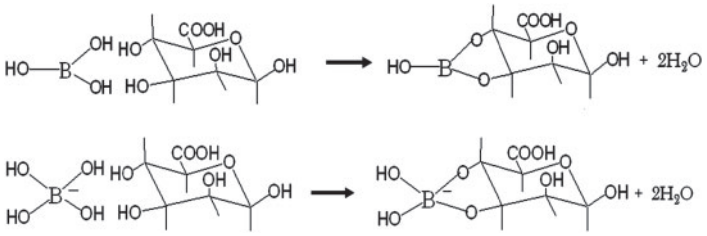

Figure 1. Possible interactions of boric acid and tetrahydroxyborate with diol groups of alginate.

the resulting water still has high boron content, making it unsuitable for human consumption and, in certain cases, even for use in irrigation. It is therefore unsurprising that recent years have seen numerous efforts to develop new processes for removing boron from water, including reverse osmosis membranes,[5] ionic exchange resins,[6] anion exchange membranes,[7] electrocoagulation and chemical coagulation.[8] Many of these methods are effective, but the high cost involved makes them difficult to apply at the industrial level. Another removal technique that deserves special attention is adsorption. The adsorption process has become particularly important in this field due to the low cost of the adsorbents used to separate/recover boron from water, many of which are waste materials from a range of industrial processes. Studies using Sepiolite,[9] Siral-30 and Pural,[10] bentonite,[11] red mud,[12] ash,[13] and impregnate carbon[14] have been carried out for this purpose. However, the use of biopolymers for boron adsorption has received little attention in the last decade. The literature describes the possible use of cotton cellulose[15] or chitosan modified with N-methylglucamine,[16] sugars,[17] polyols,[18] and calcium alginate gel beads.[19] However, although all of these studies discuss adsorption capacity or adsorption rate, none describes a continuous examination of the industrial application of the adsorbent. Consequently, this paper evaluates the use of calcium alginate gel beads in fixed-bed systems under several experimental conditions as a potential adsorbent for industrial-scale removal of boron from wastewater. Calcium alginate was chosen as the adsorbent because it is a polymer rich in hydroxyl groups. Alginates are linear unbranched polymers containing β-(1→4)-linked D-mannuronic acid (**M**) and α-(1→4)-linked L-guluronic acid (**G**) residues. The pKa values for mannuronic and guluronic acid are 3.38 and 3.65, respectively. Alginate gelation takes place when divalent cations (usually Ca^{2+}) interact ionically with blocks of guluronic acid residues, resulting in the formation of a three-dimensional network which is usually described by an 'egg-box' model.[20] The presence of OH^- groups enables the formation of complexes by reaction of boron compounds (Fig. 1). Obtaining a model to accurately describe the dynamic behaviour of the adsorption process in a fixed-bed system is inherently difficult. Although several models based on fundamental mass-transport mechanisms – including external film, and pore and surface diffusion – have been proposed, their application involves the use of complex numerical methods to solve a number of differential equations. To make the process easier, various simple mathematical models have been proposed for predicting the dynamic behaviour of the column, including the Adams–Bohart model and the bed-depth service time (BDST) design model,[21] which is derived from the Adams–Bohart equation. These simplified models are used in this study to optimize boron sorption on calcium alginate gel beads.

EXPERIMENTAL

Materials

Sodium alginate was supplied by Panreac as a power material. Boron solutions were prepared from boric acid (supplied by Merck) in demineralized water. The pH of each solution was adjusted using concentrated solutions of HCl and NaOH. HCl, NaOH and calcium nitrates were supplied by Panreac.

Synthesis of calcium alginate gel beads

For bead production, a solution of sodium alginate at 2% w/w was prepared. This solution was shaken at 800 rpm for a minimum of 5 h until completely homogenized. Next, the stirring speed was lowered to approximately 50 rpm to allow air to be dissipated and prevent the formation of air bubbles, which affect the manufacturing process. The viscous solution was then pumped and distributed drop-wise through a thin nozzle (diameter 0.6 mm) into a 0.05 mol L^{-1} calcium nitrate solution under continuous agitation. The alginate drops coagulated in the calcium nitrate solution and formed perfectly spherical beads with an average diameter of 2±0.2 mm.

Sorption studies in batch and column systems

The effect of initial pH on boron sorption by calcium alginate gel beads was examined in a batch system. Beads containing 0.7 g of alginate were contacted with 100 mL of the boron solution (50 mg L^{-1}) in flasks at the desired pH. The flasks were agitated on a shaker at 50 rpm and room temperature (20 ± 1°C) for 78 h, which is more than ample time for sorption equilibrium. Samples were then filtered through 1.2 μm filtration membranes and the boron content was analysed by the Azomethine-H method in a spectrophotometer (Varian UV-visible).[22] At the same time, the calcium release from the beads during the adsorption process was analysed by atomic absorption in a fast sequential atomic absorption spectrometer (Varian AA240FS).

For the study of sorption in continuous systems, columns of different diameters (1.2 and 1.6 cm) were filled with different amounts of the sorbent (0.39, 0.50, 1.44 and 3.5 g) to obtain different column depths (12, 15 and 18 cm) and fed with boron solutions (pH 6 and 11) at different flow rates (0.17 and 0.91 mL min^{-1}). Samples were regularly collected and analysed. Randomly, some breakthrough curves were duplicated, proving that experiments are reproducible (within an error lower than 7% in the breakthrough volume and with a similar breakthrough slope). Table 1 shows the different experimental conditions used for the column study.

Empirical modelling of breakthrough curves

The performance of packed beds is described through the concept of the breakthrough curve. Breakthrough curves are usually

Journal of Chemical Technology & Biotechnology published by John Wiley & Sons Ltd on behalf of Society of Chemical Industry.

Table 1. The effect of the operational parameters

Adsorption parameters									
Columnno.	C_0 (mg L^{-1})	*pH*	*m* (g)	*Z* (cm)	Ø (cm)	*Q* (mL min^{-1})	q_{total} (mg)	q_{eq} (mg g^{-1})	Boron removal (%)
pH									
I	59	**6**	0.50	15	1.6	0.91	1.53	3.03	24.18
II	59	**11**	0.50	15	1.6	0.91	4.93	9.86	38.01
Initial concentration of boron, C_0 (mg L^{-1})									
III	**10**	11	1.44	18	1.6	0.91	0.59	0.36	42.10
IV	**25**	11	1.44	18	1.6	0.91	2.99	2.07	43.56
V	**50**	11	1.44	18	1.6	0.91	5.29	3.88	55.14
Alginate mass, *m* (g)									
VI	59	11	**0.39**	12	1.6	0.91	3.89	9.96	30.74
II	59	11	**0.50**	15	1.6	0.91	4.93	9.86	38.01
Flow rate, *Q* (mL min^{-1})									
VII	10	11	3.50	18	2.6	**0.17**	1.59	0.45	32.44
VIII	10	11	3.50	18	2.6	**0.91**	1.51	0.45	29.90
Diameter, Ø (cm)									
III	10	11	1.44	18	**1.6**	0.91	0.59	0.36	42.10
VIII	10	11	3.50	18	**2.6**	0.91	1.51	0.45	29.90

expressed in terms of the ratio of effluent boron concentration to inlet boron concentration (C/C_0) as a function of time or effluent volume for a given bed height.[23] Effluent volume (V_{eff}) can be calculated as follows:

$$V_{eff} = Q\, t_{total} \tag{2}$$

where t_{total} and Q are the total flow time (min) and volumetric flow rate (mL min^{-1}), respectively. The area under the breakthrough curve (A), obtained by integrating the adsorbed concentration (C_{ad}; mg L^{-1}) versus t (min) plot, can be used to determine the total adsorbed boron quantity (maximum column capacity). The total adsorbed boron quantity (q_{total}; mg) in the column for a given feed concentration and flow rate is calculated as follows:

$$q_{total} = \frac{Q}{1000}\int_{t=0}^{t=t_{total}} C_{ad}\,dt \tag{3}$$

The total amount of boron fed to the column (m_{total}; g) is calculated from the following equation:

$$m_{total} = \frac{C_i Q\, t_{total}}{1000} \tag{4}$$

The total percentage removal of boron is determined from the ratio of total adsorbed quantity of boron (q_{total}) to the total amount of boron passing through the column (m_{total}):

$$Total\,removal\,\% = \frac{q_{total}}{m_{total}}100 \tag{5}$$

The sorption capacity of the column is defined as the total amount of boron sorbed (q_{total}) per gram of sorbent ($m_{sorbent}$) at the end of the total flow time:

$$q_e = \frac{q_{total}}{m_{sorbent}} \tag{6}$$

The fundamental equation describing the relationship between C/C_0 and t in a continuous system was established by Bohart and Adams[23] in 1920 and, although it was originally applied to a gas–solid system, it has been widely used to describe and quantify other systems. This model assumes that the sorption rate is proportional to the residual capacity of the solid and the retained species concentration and is used to describe the initial part of the breakthrough curve:[24,25]

$$\frac{C_t}{C_0} = \frac{\exp\left[kC_0 t\right]}{\exp\left[kN_0 Z/\upsilon\right] - 1 + \exp\left[kC_0 t\right]} \tag{7}$$

where N_0 is the volumetric sorption capacity (mg L^{-1}), and is equal to $q(C_0)(1-\epsilon)\rho/\epsilon$, where ρ represents the volumetric mass (mg L^{-1}) and ϵ is the column voidage, which varied between 0.77 and 0.83 with the beads used in this study. The average column voidage value was used for calculations. The parameter k is the kinetic constant (L mg^{-1} min^{-1}) and υ represents the linear flow velocity (cm min^{-1}) ($\upsilon = U_0/\epsilon$), U_0 is the superficial flow velocity (cm min^{-1}) ($U_0 = Q/S$), Q is the flow rate (cm^3 min^{-1}) and S is the cross-section area of the column (cm^2). The advantages of this model are its simplicity and its reasonable accuracy in predicting breakthrough under various conditions.

The linearized form of the Bohart and Adams model can be expressed as follows:

$$\ln\left[\frac{C_0}{C_t} - 1\right] = \ln\left[\exp\left(\frac{kN_o Z}{\upsilon}\right) - 1\right] - kC_0 t \tag{8}$$

where t is the service time of the breakthrough curve (min), N_0 is the volumetric sorption capacity (g L^{-1}), k is the kinetic constant (L mg^{-1} min^{-1}), Z is the depth of the bed (cm), C_0 (mg L^{-1}) is the initial boron concentration, C_t (mg L^{-1}) is the effluent boron concentration and v is the linear flow rate (cm min^{-1}).

Hutchins[26] (1973) proposed a linear relationship between the service time and the weight of the adsorbent. As the exponential term is usually much larger than unity, the unity term in the brackets on the right-hand side of Equation (4) is often neglected, leaving:

$$\ln\left[\frac{C_0}{C_t} - 1\right] = \frac{kN_o Z}{\upsilon} - kC_0 t \tag{9}$$

Solving the above equation for t,

$$t = \frac{N_o}{C_0 \upsilon} Z - \frac{1}{C_0 k} \ln\left(\frac{C_0}{C_t} - 1\right) \quad (10)$$

Equation (10) is the bed depth service time (BDST). According to this equation, the service time, t, and the bed depth, Z, can be correlated with the following process parameters: the initial solute concentration, the solution flow rate, the sorption capacity and the sorption rate constant.

Setting $t = 0$ and solving Equation (10) for Z yields

$$Z_0 = \frac{\upsilon}{kN_0} \ln\left(\frac{C_0}{C_b} - 1\right) \quad (11)$$

where Z_0, the critical bed depth, is the theoretical depth of sorbent required to prevent the sorbate concentration from exceeding the limit concentration C_b, defined as a limit concentration or a fixed percentage of the inlet concentration, generally 5%. The breakthrough point is the time required to reach this 5% concentration, while the exhaustion point is defined as the time at which the outlet concentration reaches 100% of the inlet concentration.

Another important parameter is the coefficient s_0, which is defined using the Hutchins equation. It represents the time required for the adsorption wave front to pass through the critical bed depth and is obtained from the following expression:

$$s_0 = \frac{1}{kC_0} \ln\left(\frac{C_0}{C_b} - 1\right) \quad (12)$$

The coefficient s is the slope of Equation (6). It represents the time required to exhaust a unit length of the column under the selected experimental conditions and with the limited outlet concentration:

$$s = \frac{N_o}{C_0 \upsilon} \quad (13)$$

The experimental curves were mathematically modelled through the Bohart–Adams model, Equation (8), using the Macro Solver from Microsoft Excel. From the theoretical breakthrough curves and according to Equation (9), the value of k can be obtained from the slope of the plot $\ln[C_0/C_t - 1]$ versus breakthrough time t, and the parameter N_0 from the intersection with the axis at time $t = 0$.

RESULTS AND DISCUSSION

Effect of initial pH-calcium release

The pH of adsorption medium is related to the adsorption mechanisms onto the adsorbent surface from water and reflects the nature of the interaction between the boron species in solution, the adsorptive sites of the adsorbent and the species present in the solution. In the low pH region most of the carboxylic acid groups in the alginate were in the form of –COOH, as the pKa of alginate is approximately 3.2. At this pH boron exits in a neutral form, showing no interaction with the adsorbent. Figure 2 shows that when working at acidic pH there is increased release of calcium ions into the solution. At acidic pH, the high concentration of protons in the solution causes an ion exchange between the protons and the calcium ions in the beads. The concentration of boric acid in the solution is much lower than the concentration of protons, so the flow of protons into the adsorbent prevents the adsorption of boron by the beads. From pH 4–5 calcium release remains practically constant. Calcium is released into the solution by diffusion, due to the difference in concentration of calcium ions between the interior of the beads and the calcium present in the solution. When the pH of the medium increases the carboxylic acid groups of the alginate are ionised. In the case of calcium alginate, the negative surface density is partially neutralized by the presence of calcium ions in the beads but it is interesting to note that the surface charge density increases as the solution's pH increases. At pH 6 and 8, boron exits predominantly in the neutral boric acid form. As the pH increases the concentration of protons in the solution decreases, allowing the boron to access the adsorbent more easily where it reacts with the hydroxyl groups in the alginate beads to form boron esters. At pH 9 and above the negatively charged form (borate) increases and the interaction between boron and the adsorbent increases (Fig. 2). The hydroxide groups in the solution are not attracted to the adsorbent, allowing the boron to be more easily adsorbed. Figure 2 shows that the maximum adsorption is produced at pH 11. Above pH 11, negatively charged polynuclear species can form and the negatively charged bead surface increases. Charge repulsion prevents the negatively charged borate species from interacting with the adsorbent, reducing the adsorption rate.

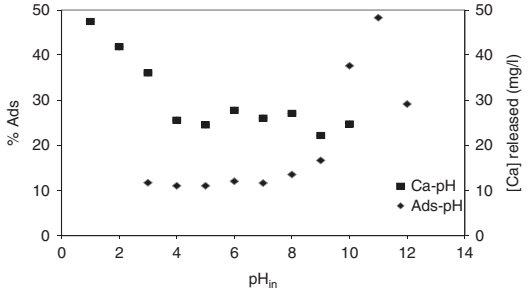

Figure 2. Influence of pH on the percentage adsorption by calcium alginate gel beads and in the calcium released to the solution during the process of adsorption (room temperate (20±1°C); initial concentration of boron, 50 mg L^{-1}; alginate mass, 0.7 g).

The column experiments were conducted at bed depth of 1.6 cm with a flow rate of 0.9 mL min^{-1}, initial concentration 10 mg L^{-1} at pH 6 and 11. The breakthrough curve C/C_0 versus V_{eff} at pH 6 and 11 is shown in Fig. 3. When pH was increased from 6 to 11, the breakthrough volume increased from 7.45 to 14.25 mL. Boron uptake at influent pH 6 and 11 was 3.03 and 9.87 mg g^{-1}, respectively, under these experimental conditions.

Effect of inlet boron concentration

The sorption breakthrough curves obtained by changing the inlet boron concentration from 10 to 50 mg L^{-1} at flow rate 0.91 mL min^{-1}, pH 11, column diameter 1.6 cm, column depth 18 cm and with 1.44 g of adsorbent are given in Fig. 4. The breakthrough curves became steeper and breakthrough volume decreased when boron concentration was increased from 10 to 50 mg mL^{-1}, as higher boron concentration leads to a higher boron loading rate which decreases the adsorption zone length due to the weaker driving force or lower mass-transfer flux from the bulk solution to the particle surface. The main effect is an increase in adsorption capacity with increasing boron concentration as shown in Table 1.

Journal of Chemical Technology & Biotechnology published by John Wiley & Sons Ltd on behalf of Society of Chemical Industry.

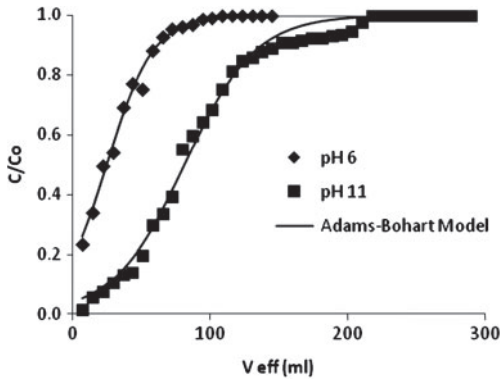

Figure 3. Comparison of the experimental data and predicted breakthrough curves obtained at different pH according to the Adams–Bohart model (room temperature (20±1°C); initial boron concentration 59 mg L^{-1}; flow velocity 0.91 mL min^{-1}; adsorbent mass 0.5 g; column depth 15 cm).

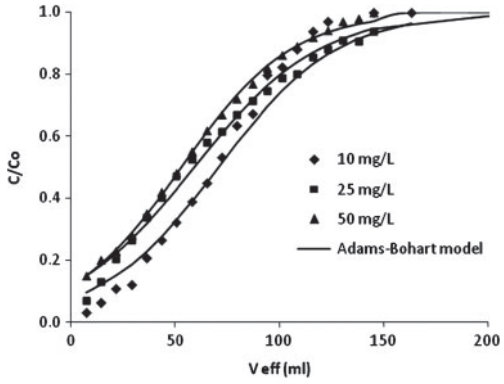

Figure 4. Comparison of the experimental data and predicted breakthrough curves obtained at different inlet boron concentrations according to the Adams–Bohart model (room temperature (20±1°C); pH 11; adsorbent mass, 1.44 g; flow rate, 0.91 mL min^{-1}; column depth, 18 cm).

Table 2 shows the standard Adams–Bohart and Hutchins coefficients of the BDST model calculated from Equations (8–10). The kinetic parameter k varies continuously with the concentration; when the inlet concentration increases a decrease of parameter k is observed. As expected, increasing the inlet concentration increases the volumetric capacity of the sorbent in the column from 1.12 to 4.24 g L^{-1}. The volumetric sorption capacity, N_0 (kg m^{-3}), is equal to $q(C_0)(1-\epsilon)\rho/\epsilon$, so N_0 is directly proportional to $q(C_0)$. When the adsorption capacity increases, the volumetric sorption increases. At higher concentrations the availability of boron species for the adsorption sites increases, leading to higher boron uptake. Boron concentration at column exhaustion increases with the initial concentration, reaching 0.36, 2.07, and 3.88 mg g^{-1} for concentrations of 10, 25, and 50 mg L^{-1}, respectively.

The critical bed length of the column increases from 10 to 25 mg L^{-1}, after which it stabilizes. The time required to exhaust a unit length of sorbent in the column (s) under the test conditions decreases continuously with increasing initial concentration. However, in the range of concentration used in this study the time required for the adsorption wave front to pass through the critical bed depth (s_0) remains constant.

Influence of column depth (sorbent amount) on breakthrough curves

Increasing the column depth is expected to affect the volume of the solution corresponding to an outlet concentration that is 50% of the inlet concentration. With a short column depth, the breakthrough point occurs at lower volume; increasing the depth of the column increases the contact time between the sorbent and the sorbate. As shown in Table 1, boron uptakes at different bed depths (12 and 15 cm) were 9.96 and 9.86 mg g^{-1}, respectively. The effect of column depth on the column parameters is shown in Table 2. Boron adsorption decreased with a longer bed, and the same tendency was observed for the volumetric capacity (N_0). Moreover, the breakthrough curves for the longer beds tended to be more gradual, as shown in Fig. 5; this means that a longer bed was more difficult to completely exhaust. Bed depth was found to increase breakthrough volume, which is seemingly due to the increase in the number of binding sites, which broadens the mass transfer zone. This increases the critical bed depth, Z_0, which represents the theoretical depth of the sorbent necessary to prevent the sorbate concentration from exceeding the limit concentration C_b. Increasing the depth of the bed also increases the surface area of the adsorbent, providing more binding sites for adsorption, which could lead to an increase in the rate of adsorption. In our case, the value of the parameter k obtained from the Adams–Bohart model, which is directly related to rate of adsorption, decreased from 0.7 to 0.6 (L mg^{-1} min^{-1}), respectively, when the adsorbent depth was increased from 12 to 15 cm. This result can be attributed to the fact that the calcium alginate gel beads are non-rigid, and can therefore produce packing in the initial part of the column. This packing may reduce the contact surface between the solution and the adsorbent in the initial part of the column, which contrasts with the use of rigid adsorbents and leads to increased diffusion problems in this part of the column and a consequent decrease in adsorption rate.

For this experimentation the value of U_0 (cm min^{-1}) is the same for the two columns (12 and 15 cm depth) that give the same value of υ. The initial concentration used for the two columns was 59 mg L^{-1}; based on these values, the value of s depends only on N_0, and an increase in N_0 leads to an increase in s, which is consistent with the experimental results.

Influence of superficial flow velocity on breakthrough curves

Figure 6 shows the effect of the superficial velocity on boron sorption breakthrough curves. As indicated in Table 1, at the lowest flow rate of 0.17 mL min^{-1}, relatively higher uptake was observed for boron sorption to immobilized calcium alginate gel beads. A much sharper breakthrough curve was obtained at lower flow rates. This behaviour is explained by the fact that boron sorption by calcium alginate gel beads is affected by insufficient solute residence time in the column, the diffusion of the solute into the pores of the biosorbent and the limited number of active sites and hydroxyl groups in the calcium alginate for sorption. The dependence of the rate parameter k on the flow velocity indicates that the external and intraparticle diffusion are rate-controlling.

Journal of Chemical Technology & Biotechnology published by John Wiley & Sons Ltd on behalf of Society of Chemical Industry.

Table 2. Influence of experimental conditions on the parameters of the Adams–Bohart and Hutchins models

	Bohart–Adams		Hutchins			
Operational parameters	$k\times10^{-3}$ (L mg^{-1} min^{-1})	N_0 (mg L^{-1})	Z_0 (cm)	s (min cm^{-1})	s_0 (min)	R^2
pH						
6	0.63	49.88	26.27	0.24	80.01	1
11	0.62	97.55	13.78	0.46	80.01	1
Initial concentration of boron						
10	3.68	10.99	20.50	0.31	80.01	1
25	1.23	22.04	24.94	0.31	80.01	1
50	0.70	47.62	24.82	0.27	80.01	1
Alginate mass						
0.39	0.65	110.42	11.48	0.55	80.01	1
0.50	0.62	97.55	13.78	0.46	80.01	1
Flow rate						
0.17	0.23	11.50	21.84	0.02	1177.7	1
0.91	0.67	10.49	44.66	0.11	439.46	1
Diameter						
1.6	3.6	10.99	20.50	0.31	80.01	1
2.6	0.67	10.49	44.66	0.11	439.46	1

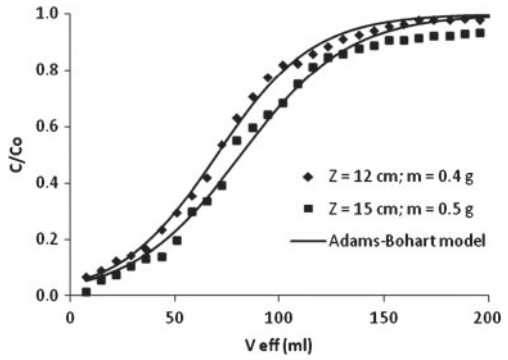

Figure 5. Comparison of the experimental data and predicted breakthrough curves obtained at different depths of the column according to the Adams–Bohart model (room temperature (20±1°C); pH 11; initial boron concentration 59 mg L^{-1}; flow rate 0.91 mL min^{-1}).

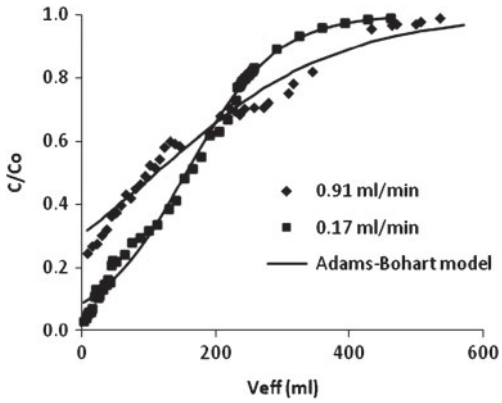

Figure 6. Comparison of the experimental data and predicted breakthrough curves obtained at different flow rates according to the Adams–Bohart model (room temperature (20±1°C); pH 11; initial boron concentration, 10 mg L^{-1}; mass adsorbent, 3.5 g; column depth, 18 cm; column diameter, 2.6 cm).

Influence of column diameter on breakthrough curves

Experiments were performed with different column diameters. Figure 7 shows two breakthrough curves obtained with the same column depth (2.6–18 cm, and 1.6–18 cm) and the same superficial flow velocity. The change in column diameter did not alter the breakthrough curves at *BV*o for the same column depth, as can be seen in Fig. 7, and the curves intersected at the breakthrough point (BV_0). The breakthrough point was defined as the point at which the effluent concentration was equal to $0.05C_0$. Increasing the column diameter for the same column depth increases the mass of the sorbent. As a result, the resistance to diffusion may limit the overall mass transfer and the adsorption efficiency. The kinetic parameter k decreases as the column diameter is increased, perhaps due to insufficient contact time and to dispersion effects. This finding is consistent with the previous results on the effect of the alginate mass. Although the larger amount of adsorbent in the wider column increases the dynamic adsorption capacity, the parameter N_0 decreases. For the same column depth, increasing the column diameter also increases the critical bed depth Z_0; consequently, a greater height is needed to prevent the sorbate concentration from exceeding the limit concentration C_b, and the time required to exhaust a unit length of the column (s) increases. Moreover, the slope of the breakthrough curve clearly shows that the column of diameter 1.6 cm was more efficient than the column of diameter 2.6 cm.

CONCLUSIONS

The biosorption of boron from aqueous solution on alginate gel beads was investigated in a continuous packed-bed column. The influence of several parameters on breakthrough curves such as pH, inlet boron concentration, column depth, flow rates and diameter of the column at room temperature (20±1°C) was studied. The

Journal of Chemical Technology & Biotechnology published by John Wiley & Sons Ltd on behalf of Society of Chemical Industry.

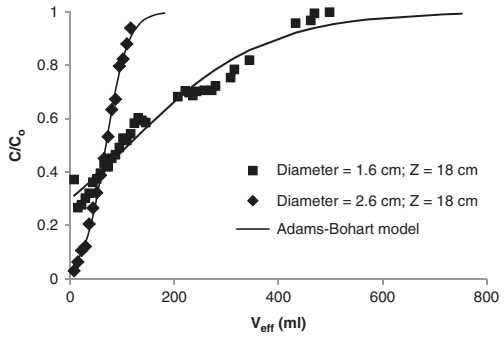

Figure 7. Comparison of the experimental and predicted breakthrough curves obtained at different diameters of the column according to the Adams–Bohart model (room temperature (20±1°C); pH 11). ■: Column diameter, 1.6 cm; flow rate, 0.91 mL min^{-1}; adsorbent mass, 1.44 g. ◆: Column diameter, 2.6 cm; flow rate, 0.91 mL min^{-1}; adsorbent mass, 3.50 g.

results showed that the removal yield of boron is dependent on all the above parameters. The best conditions for boron adsorption were obtained at high pH (the optimum value being pH 11), higher initial boron concentration, increased column depth and lower flow velocity.

The Adams–Bohart and Hutchins models were applied to experimental data from dynamic studies performed on a fixed column to predict the breakthrough curves and to determine the column kinetic parameters. The breakthrough curve is well described by the Adams–Bohart model for all of the experimental conditions analysed in this study.

With this study we have demonstrated that calcium alginate can be use as adsorbent for the removal of boron from aqueous solutions in fixed-bed systems and its application to industrial scale is possible.

ACKNOWLEDGEMENTS

This work was supported by the Spanish Ministry of Science and Innovation (Project no. CTQ 2011-22412).

REFERENCES

1 Pagznl M, Lemarchand D, Spivack A and Gaillardet J, A critical evaluation of the boron osotope pH proxy: the accuracy of ancient ocean pH estimates. *Geochim Cosmochim Acta* **69**:953–961 (2005).
2 Argust P, Distribution of boron in the environment. *Biologic Trace Element Res* **66**:131–143 (1998).
3 Power PP and Woods WG, The chemistry of boron and its speciation in plants. *Plant Soil* **193**:1–13 (1997).
4 WHO, Boron in drinking water, *WHO Guidelines for drinking-water quality*. World Health Organization (2011).
5 Cengeloglu Y, Arslan G, Tor A, Kocak I and Dursun N, Removal of boron from water by using reverse osmosis. *Sep Purif Technol* **64**:141–146 (2008).
6 Kabay N, Bryjak M, Schlosser S, Kitis M, Avlonitis S, Matejka Z, Al-Mutaz I and Yuksel M, Adsorption-membrane filtration (AMF) hybrid process for boron removal from seawater: an overview. *Desalination* **223**:38–48 (2008).
7 Yazicigil Z and Oztekin Y, Boron removal by electrodialysis with anion-exchange membranes. *Desalination* **190**:71–78 (2006).
8 Yilmaz, AE, Boncukcuoğlu R and Kocakerim MM, A quantitative comparison between electrogoagulacion and chemical coagulation for boron removal from boron removal containing solution. *J Hazard Mater* **149**:475–481 (2007).
9 Öztürk N and Kavak D, Boron removal from aqueous solutions by adsorption on waste sepiolite and activated waste sepiolite using full factorial design. *Adsorption* **10**:245–257 (2004).
10 Seki Y, Seyhan S and Yurdakoc M, Removal of boron from aqueous solution by adsorption on Al2O3 based materials using full factorial design. *J Hazard Mater* **B138**:60–66 (2006).
11 Karahan S, Yurdakoc M, Seki Y and Yurdakoc K, Removal of boron from aqueous solution by clays and modified clays. *J Colloid Interface Sci* **293**:36–42 (2006).
12 Cengeloglu Y, Tor A, Arslan G, Ersoz M and Gezgin S, Removal of boron from aqueous solution by using neutralized red mud. *J Hazard Mater* **142**:412–417 (2007).
13 Öztürk N and Kavak D, Adsorption of boron from aqueous solutions using fly ash: Batch and column studies. *J Hazard Mater* **B127**:81–88 (2005).
14 Kluczka J, Ciba J, Trojanowska J, Zolotajkin M, Turek M and Dydo P, Removal of boron dissolved in Water. *Environ Progress* **26**:71–77 (2007).
15 Liu R, Ma W, Jia C, Wang, L and Li HY, Effect of pH on biosorption of boron onto cotton cellulose. *Desalination* **207**:257–267 (2007).
16 Sabarudin A, Oshita K, Oshima M and Motomizu S, Synthesis of cross-linked chitosan possesing N-methyl-D-glucamine moiety (CCTS-NMDG) for adsortion/concentration of boron in water samples and its accurate measurement by ICP-MS and ICP-AES. *Talanta* **66**:136–144 (2005).
17 Matsumoto M, Matsui T and Kondo, K. Adsorption mechanism of boric acid on chitosan resin modified by saccharides. *J Chem Eng Japan* **32**:190–196 (1999).
18 Dydo P, Turek M, Ciba J, Trojanowska J and Kluczka J, Boron removal from landfill leachate by means of nanofiltrationn and reverse osmosis. *Desalination* **185**:131–137 (2005).
19 Ruiz M, Tobalina C, Demey H, Barron JA and Sastre AM, Sorption of boron on calcium alginate gel beads. *Reactive Funct Polymers* **73**:653–657 (2013).
20 Grant G, Morris E, Rees D, Smith P and Thom D, Biological interactions between polysaccharides and divalent cations. *FEBS Lett* **32**:195–198 (1973).
21 Ruiz M, Sastre AM, Zikan MC and Guibal E, Palladium sorption on glutaraldehyde-crosslinked chitosan in fixed-bed systems. *J Appl Polymer Sci* **81**:153–165 (2001).
22 Jaksic L, The spectrophotometric determination of boron in tourmalines. *J Serbian Chem Soc* **70**:255–260 (2005).
23 Shi J. Alves NM and Mano JF, Drug release of pH/Temperature-responsive calcium alginate/Poly(N-isopropylacrylamide) semi-IPN beads. *Macromol Biosci* **6**:358–363 (2006).
24 Kiran B and Kaushik A, Cyanobacterial biosorption of Cr(VI): application of two parameter and Bohart Adams models for batch and column studies. *Chem Eng J* **144**:391–399 (2008).
25 Barron-Zambrano J, Szygula A, Ruiz M, Sastre AM and Guibal E, Biosorption of Reactive Black 5 from aqueous solutions by chitosan: column studies. *J Environ Manage* **91**:2669–2676 (2010).
26 Hutchins RA, New method simplifies design of activated-carbon systems. *Chem Eng* **80**:133–138 (1973).

ANNEX IV

EQUILIBRIUM AND DYNAMIC STUDIES FOR ADSORPTION OF BORON ON CALCIUM ALGINATE GEL BEADS USING PRINCIPAL COMPONENT ANALYSIS (PCA) AND PARTIAL LEAST SQUARES (PLS)

ATTENTION ¡

M. Ruiz, L. Roset, H. Demey, S. Castro, A. M. Sastre, J. J. Pérez. *Equilibrium and dynamic studies for adsorption of boron on calcium alginate gel beads using principal component analysis (PCA) and partical least squares (PLS).* Materialwissenschaft und Werkstofftechnik, 44 (2013) 410-415.

Pages 100 to 106 of the thesis are available at the editor's web

http://onlinelibrary.wiley.com/doi/10.1002/mawe.201300144/abstract
DOI: 10.1002/mawe.201300144

ANNEX V

DEVELOPMENT OF A NEW CHITOSAN/NI(OH)$_2$-BASED SORBENT FOR BORON REMOVAL

ATTENTION¡

H. Demey, T. Vincent, M. Ruiz, A. M. Sastre, E. Guibal. Development of a new chitosan/Ni(OH)2-based sorbent for boron removal. *Chemical Engineering Journal,* 244 (2014) 576-586.

Pages 108 to 128 of the thesis are available at the editor's web

http://www.sciencedirect.com/science/article/pii/S1385894714000771

Doi:10.1016/j.cej.2014.01.052

ANNEX VI

BORON RECOVERY FROM SEAWATER WITH A NEW LOW-COST ADSORBENT MATERIAL

ATTENTION¡¡

H. Demey, T. Vincent, M. Ruiz, A. M. Sastre, E. Guibal. *Boron recovery from seawater with a new low-cost adsorvent material. C*hemical Engineering Journal, 254 (2014) 463-471

Pages 130 to 144 of the thesis are available at the editor's web

http://www.sciencedirect.com/science/article/pii/S1385894714006329

doi:10.1016/j.cej.2014.05.057

ANNEX VII

REMOVAL OF BORON FROM AQUEOUS SOLUTIONS USING A NEW COMPOSITE OF ALGINATE-ALUMINA

Elsevier Editorial System(tm) for Arabian Journal of Chemistry
Manuscript Draft

Manuscript Number: ARABJC-D-13-01762

Title: Removal of boron from aqueous solutions by a new adsorbent: Composite of alginate - alumina

Article Type: Original Article

Keywords: Boron, adsorption, composite, alginate, alumina, new adsorbent, desorption

Corresponding Author: Dr. Hary Demey,

Corresponding Author's Institution: Universitat Politecnica de Catalunya

First Author: Hary Demey, PhD student

Order of Authors: Hary Demey, PhD student; Montserrat Ruiz, PhD; Jesus-Alberto Barron-Zambrano, PhD; Alberto Canadell, PhD student; Ana Maria Sastre, Professor

Abstract: The present paper investigates the removal of boron from aqueous solutions by batch adsorption. Composite of alginate-alumina (CAAl) was manufactured and used as an adsorbent. The results were compared with the adsorption of boron on calcium alginate beads (CA) and alumina individually. The effects of parameters such as pH, temperature and adsorbent dosage on boron removal were investigated. The results confirm that calcium alginate beads (CA) exhibited a better adsorption capacity in a basic medium, and the composite alginate-alumina (CAAl) exhibits improved boron removal at acidic pH. Adsorption isotherm studies were also performed. The Langmuir and Freundlich isotherm models were applied and the experimental data were found to conform to the Langmuir isotherm model. The maximum sorption capacity was 132 mg.g-1 at pH 11 using calcium alginate beads (CA). Thermodynamic parameters such as change in free energy (ΔG0), enthalpy (ΔH0) and entropy (ΔS0) were also determined. The pseudo-first-order and pseudo-second-order kinetic model were tested to find the rate constants of adsorption. Kinetic experiments showed that boron adsorption onto composite alginate-alumina (CAAl) samples obeyed the pseudo-second order kinetics model. The desorption process was tested using distilled water, reaching values greater than 70%.

Suggested Reviewers: Khalid Elwakeel PhD
Assistant professor of environmental chemistry , Environmental Science Department, Faculty of Science. , Port-Said University, Port-Said, Egypt
khalid_elwakeel@yahoo.com
Expert in removal of metals using biopolymers

Isabel Villaescusa PhD
Chemical Engineering department, Universitat de Girona
isabel.villaescusa@udg.es
Expert in sorption process

Duygu Kavak Professor
Chemical Engineering department, Eskisehir Osmangazi University
dbayar@ogu.edu.tr
Expert in boron removal

Removal of boron from aqueous solutions by a new adsorbent: Composite of alginate - alumina

H. Demey[1*], M. Ruiz[1], J. A. Barron-Zambrano[1], A. Canadell[1], A. M. Sastre[2]

[1]Universitat Politècnica de Catalunya, EPSEVG, Department of Chemical Engineering, Av. Víctor Balaguer, s/n, 08800 Vilanova i la Geltrú, Spain,

[2]Universitat Politècnica de Catalunya, Department of Chemical Engineering, ETSEIB, Diagonal 647, 08028 Barcelona, Spain

*E-mail: hary.demey@upc.edu

Abstract

The present paper investigates the removal of boron from aqueous solutions by batch adsorption. Composite of alginate-alumina (CAAl) was manufactured and used as an adsorbent. The results were compared with the adsorption of boron on calcium alginate beads (CA) and alumina individually. The effects of parameters such as pH, temperature and adsorbent dosage on boron removal were investigated. The results confirm that calcium alginate beads (CA) exhibited a better adsorption capacity in a basic medium, and the composite alginate-alumina (CAAl) exhibits improved boron removal at acidic pH. Adsorption isotherm studies were also performed. The Langmuir and Freundlich isotherm models were applied and the experimental data were found to conform to the Langmuir isotherm model. The maximum sorption capacity was 132 $mg.g^{-1}$ at pH 11 using calcium alginate beads (CA). Thermodynamic parameters such as change in free energy (ΔG^0), enthalpy (ΔH^0) and entropy (ΔS^0) were also determined. The pseudo-first-order and pseudo-second-order kinetic model were tested to find the rate constants of adsorption. Kinetic experiments showed that boron adsorption onto composite alginate–alumina (CAAl) samples obeyed the pseudo-second order kinetics model. The desorption process was tested using

distilled water, reaching values greater than 70%.

Keywords: Boron, adsorption, composite, alginate, alumina, new adsorbent

1. Introduction

Boron compounds are used extensively in industrial applications, including many chemical processes, cosmetics manufacturing, leather production and welding and brazing of metals. Boric acid is used as a disinfectant and a food preservative due to its bactericidal and fungicidal properties. However, wastewater containing boron is introduced to the environment, altering agricultural harvests and causing several pollution problems. Although a trace amount of boron is fundamental for plant growth, at high concentrations, it can become harmful to both plants and animals (Morisada et al., 2011). According to the World Health Organization (WHO), the guideline value for the concentration of boron in drinking water is 2.4 $mg.L^{-1}$ (WHO, 2011).

Many researchers have reported the possibility of using a variety of methods to remove boron from wastewater and aqueous solutions. These methods include electrodialysis (Yazicigil and Oztekin, 2006), precipitation (Itakura et al., 2005), chemical coagulation and electrocoagulation (Erdem et al., 2007; Koparal, 2002), complexation/nanofiltration (Desortez et al., 2006), phytoremediation (Del campo-Marin and Gideon, 2007), ionic exchange (Simonnot et al., 2004; Kabay et al., 2008), reverse osmosis (Prats et al., 2000; Rodriguez-Pastor, 2001; Cengeloglu et al., 2008) and adsorption with various materials (Öztürk and Kavak, 2004; Seki et al., 2006; Karahan et al., 2006; Cengeloglu et al., 2007; Kavak, 2009; Öztürk and Kavak, 2005). Biosorption is an economical alternative technology for water treatment based on the properties of various types of inactive and dead biomass, which is easily available at a low cost, and is able to bind and concentrate hazardous ions from aqueous

solutions. The use of biopolymers for boron adsorption has received little attention over the last decade. Published papers report the possibility of using cotton cellulose (Liu et al., 2007) or chitosan modified with N-methylglucamine (Sabarudin et al., 2005), sugars (Matsumoto et al., 1999) and calcium alginate (Ruiz et al., 2013a; Ruiz et al., 2013b; Demey et al., 2013). Alumina is one of the most widely used adsorbents throughout the world. Bouguerra et al. (2008) compared the adsorption process using activated alumina with conventional reverse osmosis systems. Although alumina may adsorb boron, it is not clear whether the powder form can be reused, an important property for large industrial applications, along with effectiveness and ease of manipulation. This is the basic principle of adsorption.

While recent studies have shown that calcium alginate beads can adsorb boron from aqueous solutions (Ruiz et al., 2013a; Ruiz et al., 2013b; Demey et al., 2013), these authors did not present the results of desorption studies. Alginate is a biopolymer rich in hydroxyl groups, which can react with boron compounds to form esters. Alginate is a polysaccharide present in the cell-wall of brown algae (*Phaeophyceae algae*), which is abundant in seawater throughout the world. Alginate contains blocks of mannuronic and guluronic acid. While calcium alginate obtained from sodium alginate is not soluble in water, adsorbent beads can be used for water treatment. The main advantage of alginate is that it is produced by harvesting giant brown seaweed (some species like *Macrocystis pyrifera* may reach 45 m in length), a natural and renewable resource.

In this paper, beads of a new alumina based composite were prepared using a biopolymer alginate matrix that also facilitates the handling of alumina in the adsorption process. The main goal of this work was to investigate whether combining the two adsorbents can improve the capacity to adsorb boron from aqueous solutions and to study the possibility of regenerating these sorbents with a low cost eluent. The results were compared with the individual adsorption capacities of alumina and calcium alginate in a batch system.

2. Experimental

2.1 Materials

The boron solutions were prepared by dissolving boric acid (H_3BO_3, supplied by Merck) in distilled water. The pH of each solution was adjusted using HCl and NaOH before mixing with the adsorbent. Sodium alginate, calcium nitrate and alumina were supplied by Panreac.

2.2 Sorbent preparation

A solution of 2% w/w sodium alginate was prepared for the production of calcium alginate beads (CA). This solution was shaken at 800 rpm for a minimum of 5 hours to achieve complete homogenisation. Then, the stirring speed was reduced to about 50 rpm to allow the air to dissipate and to prevent the occurrence of air bubbles, making the bead manufacturing difficult. Then, the beads were dosed in a 0.05 M calcium nitrate solution under continuous agitation (Demey et al., 2013).

Alginate/alumina composites (CAAl) were prepared by adding a mass of alumina equivalent to 2% w/w into the alginate solution and stirring continuously before placing it in contact with a 0.05 M calcium nitrate solution. The gel beads produced in this way had an average diameter of 2.3±0.1 mm. The alumina used in this work was not activated alumina.

A given amount of gel beads (CA and CAAl, standard materials used in this work) were dried at room temperature (293 K, 1 atm) for 72 hours and the average diameter was measured as 0.8 mm.

2.3 Sorbent characterisation

2.3.1 Surface Images

Micrographs of alginate beads (CA) and composites of alginate-alumina (CAAl) were taken using a scanning electron microscope (Leitz, Laborluz 11, Germany) equipped with a video camera (Leica, DFC 420). Before observation, all samples were dried at 313 K for 24 hours

and then coated with gold to facilitate surface scanning at room temperature (293 K, 1 atm).

2.3.2 Thermogravimetric analyses

Thermogravimetric analyses were performed under a nitrogen flow of 20 mL.min^{-1} at a heating rate of 10 ºC.min^{-1}, within a temperature range of 30 to 800 ºC, using a Perkin-Elmer TGA 6 instrument. All samples were previously dried, and sample weights of about 20 mg were used to develop these experiments.

2.4 Batch sorption experiments

The initial pH values of boron solutions were adjusted from pH 3 to 12 by adding solutions of 0.1 M NaOH and 0.1 M HCl. Then, 0.7 g of sorbent was added to 100 ml of the 50 mg.L^{-1} boron solution at room temperature (20±1 ºC). After two days of agitation (150 rotations per min) in a reciprocal shaker, the solutions were forced through 1.2 µm filtration membranes and the filtrates were analysed using the azomethine-H method (Shanina et al., 1967). The concentration of boron in the solution was determined at 415 nm using a spectrophotometer (Varian UV-visible). The sorption capacity was obtained using a mass balance equation and expressed as mg of boron per g of sorbent (equation 1).

Sorption isotherms were obtained by mixing fixed amounts of adsorbent (0.7 g) at room temperature with fixed volumes of boron solutions (100 mL) at different boron concentrations (10 to 500 mg.L^{-1}). The initial pH of the boron solutions was adjusted to 11. After two days of agitation (150 rpm) to reach the adsorption equilibrium, samples were taken to determine the boron concentration using the azomethine-H method (Shanina et al., 1967).

To study the sorption kinetics, 250 mL of boron solution (50 mg.L^{-1}) at fixed pH (11) were mixed with 1.75 g of sorbent in a jar-test agitated system (150 rotations per min). Five mL samples were withdrawn at specified times and filtered through a 1.2 µm filtration membrane before analysis. The adsorption capacity of adsorbents and the percentage of adsorption were calculated according to equations 1 and 2:

$$q = \frac{V(C_0 - C_{eq})}{m} \quad (1)$$

$$\%Ads = \frac{(C_0 - C_{eq})}{C_{eq}}.100 \quad (2)$$

where % Ads is the percentage of boron removed from aqueous solutions, q is the sorption capacity of sorbents ($mg.g^{-1}$), C_0 is the initial boron concentration ($mg.L^{-1}$), C_{eq} is the liquid phase concentration at equilibrium ($mg.L^{-1}$), m is the mass of adsorbent (g) and V is the volume of the boron solution (L).

3. Modelling of sorption isotherms and kinetics

3.1. Sorption isotherms

The distribution of adsorbed species between the solid and the solution interface at equilibrium in adsorption processes is commonly represented by the Langmuir and Freundlich models. In the current study, these models were applied to determine the maximum sorption capacity of the adsorbent and its relationship with the mass of boron adsorbed. Langmuir and Freundlich isotherms are described by equations 3 and 4, respectively (Ruiz et al., 2005).

$$q = \frac{q_{máx} b C_{eq}}{1 + b C_{eq}} \quad (3)$$

$$q = K_F C_{eq}^{\ 1/n} \quad (4)$$

where *q* is the sorption capacity of sorbents ($mg.g^{-1}$), q_{max} is the maximum adsorption capacity of sorbents ($mg.g^{-1}$), and C_{eq} is the equilibrium concentration in the solution. In the Langmuir model (equation 3), *b* is related to the energy of adsorption ($L.mg^{-1}$). K_F and *n* are Freundlich adsorption constants, indicative of relative capacity and adsorption intensity, respectively.

3.2 Sorption kinetics

Experimental adsorption data can be described by several kinetic models. Pseudo-first-order (PFORE) (Lagergreen, 1898) and pseudo-second-order (PSORE) kinetic model (Ho and

McKay, 1998; McKay and Ho, 1999; Ho and Mckay 2000) were used to describe the effect of contact time and to understand the mechanisms governing boron adsorption by sorbents. These models are frequently used to describe the batch sorption system:

Pseudo first order rate equation (PFORE):

$$\frac{dq_t}{d_t} = K_1(q_1 - q_t) \quad (5)$$

Integrating for the boundary conditions t = 0 to t = t and q_t =0 to q_t = q_t:

$$\log(q_{eq} - q_t) = \log(q_{eq}) - \frac{K_1}{2.303}t \quad (6)$$

Pseudo second order rate equation (PSORE):

$$\frac{dq_t}{(q_{eq} - q_t)^2} = K_2 d_t \quad (7)$$

Integrating for the boundary conditions t = 0 to t = t and q_t =0 to q_t = q_t:

$$\frac{1}{q_t} = \frac{1}{K_2 q_{eq}^2} + \frac{1}{q_{eq}}t \quad (8)$$

where q_{eq} is the equilibrium sorption capacity (mg.g^{-1}), q_t is the sorption capacity (mg.g^{-1}) at any time t (min), and k_2 is the pseudo-second-order rate constant (g.mg^{-1}.min^{-1}).The parameters k_1 and k_2 are pseudo-constants depending on experimental conditions.

3.3 Effect of temperature

To evaluate the effect of temperature on boron removal, several kinetic experiments were performed at two different temperatures (293 K, 308 K) at pH 11 using CA and CAAl. The thermodynamic parameters such as standard entropy ($\Delta S°$), standard enthalpy change ($\Delta H°$) and free energy change were calculated using the Van't Hoff equation (9) (Kavak, 2009):

$$\ln K_C = -\frac{\Delta H°}{RT} + \frac{\Delta S°}{R} \quad (9)$$

Gibbs free energy change ($\Delta G°$) were determined using equations 10 and 11 (Kavak, 2009):

$$\Delta G° = -RT\ln K_C \quad (10)$$

$$K_C = \frac{C_S}{C_e} \quad (11)$$

where T is the solution temperature (K), R is the gas constant (8.314 J.mol-1.K^{-1}), K_c is the equilibrium constant, C_s is the amount of boron adsorbed per gram of adsorbent (mmol.g^{-1}), and C_e is the equilibrium boron concentration (mmol.L^{-1}).

4. Results and discussion

4.1 Composite characterisation

4.1.1 Scanning electron microscope, SEM

SEM micrographs are presented in Figures 1 and 2. These images were obtained to examine the topography and surface structure of the adsorbents. Figure 1.a and Figure 1.b demonstrate the roughness of the surface, and an examination of the SEM images indicates the presence of pores and some cracks that formed during the drying process. The surface of CAAl materials is different from that of the CA samples as shown in Figures 1.c and 1.d. Figure 1.c shows small alumina particles that are strongly attached to the calcium alginate, coating the surface. Some beads were fractured to observe the distribution of alumina inside the adsorbent (Figure 2). The alumina is not homogenously distributed throughout the beads, and the spectrum in the central portion of the material demonstrates the presence of calcium, carbon, oxygen, alumina, chloride and sodium ions, as expected as these are the main elements of the composite.

Figure 1. Adsorbent topography. 1.a CA surface at 90 X magnification, 20 kV. 1.b CAAl surface at 90 X magnification, 20 kV. 1.c CAAl surface at 1500 X magnification, 20 kV.

1.d CA surface, 1500 X magnification, 20 kV.

Figure 2. Cross-sectional area of CAAl materials.

4.1.2 TGA

Thermograms of CA and CAAl materials were captured to examine the degradation of these materials with temperature. TGA and derivative curves are presented in Figure 3.a and Figure 3.b, with similar results between the two samples, including a slight initial weight loss (4% for CA, 7% for CAAl) due to the presence of a small amount of residual water in the samples. These curves shows that the decomposition of the adsorbents begins at 195.4 ºC for CA with a remaining weight of 33 % and at 210.2 ºC for CAAl with a remaining weight of 57%. These results show that these sorbents could even be used for water treatment at high temperatures. The results suggest that CAAl is more thermally stable than CA at high temperature.

Figure 3. Thermogravimetric analyses. 3.a. TGA curve of CA. 3.b TGA curve of CAAl.

4.2 Influence of pH

To determine the best pH for the adsorption of boron onto adsorbents, the uptake of boron removal as a function of proton concentration was studied. The experiments were carried out over a pH range from 3 to 12. The results in Figure 4.a demonstrate that increasing pH increases the boron adsorption of CA. The maximum boron removal occurs at pH 11 using CA. Over the interval from pH 3-9, CAAl exhibited the best adsorption, greater than alumina and CA over the same interval. Over the interval of pH 9-12, CA exhibited the best results, with a maximum at pH 11, whereas adsorption by alumina decreased with increasing OH^- ion concentration.

These results suggest that the complexation reaction of boron species [$B(OH)_3$ and $B(OH)_4^-$ species] occurs with the OH^- groups in the cis position on the reagent surface (Demey et al.,

2013). Thus, in the case of CA between pH 9 and 11, the species of boron present in the solution can produce esters of borates with the OH^- groups present in alginates. In addition, increasing pH increases the concentration of hydroxyl ions in relation to the borate ions, and due to the competitiveness of these two species for adsorption sites, boron removal decreases at pH >11. However, a reaction still occurs between the borate ion and the reactive hydroxyl groups of the adsorbent reagent. This explains the decrease at pH >11.

The removal of boron by alumina from pH 3-9 can be attributed to the presence of hydrated oxygen in alumina and to the electrostatic interactions between the alumina surface and boron species. These results with alumina follow the same trend as those obtained by Seki et al., 2006, who studied boron adsorption with Al_2O_3-based materials and reported that pH had a negative influence on boron adsorption over the range studied here.

Figure 4. Influence of pH. 4.a Effect of boron removal using CA and CAAl. 4.b Variation in pH.

(pH_o=3-12, $[B]_{initial}$= 50 mg.L^{-1}, V = 100 ml, T_{room}, 1 atm)

Bouguerra et al., 2008 reported low adsorption of boron at higher pH values using activated alumina. The pH and concentration determine the distribution of ionic forms of boron; as the pKa for an equilibrium reaction of boric acid is 9.2 (equation 11) and the point of zero charge (pH_{pzc}) for different types of alumina is around 8.7-9.0 (Bouguerra et al., 2008), the surface of alumina is negatively charged at pH ≥ pH_{pzc}. Thus, anionic boron species [$B(HO)_4^-$] would have lower interactions with alumina and CAAl materials, and lower boron uptake is observed at pH ≥ 9 (Figure 4.a). Therefore, at pH > 9, the alginate present in the composite becomes the active material for boron adsorption.

$$B(HO)_3 + H_2O \leftrightarrow B(HO)_4^- + H^+ \qquad pKa = 9.2 \qquad (11)$$

Figure 4.b shows the impact of the variation of pH on the sorption process of boron solutions. The experimental points of the CA curve exhibited a slight increase in the equilibrium pH, especially over the pH interval 2-7. This suggests that calcium alginate has a type of 'buffering' effect, which may explain why boron removal was almost constant over this interval. At pH >7, the equilibrium pH of solutions did not vary with respect to initial pH. pH control is thus an important parameter for the interpretation of sorption data; for this reason, further experiments were carried out at pH 11 as the maximum boron removal was obtained at this pH.

The equilibrium pH for CAAl and alumina did not change at pH 7; nevertheless, equilibrium pH increased for pH < 7 and decreased slightly for pH > 7. This effect can be attributed to the known amphoteric character of alumina.

4.3 Effect of adsorbent mass

Figure 5 shows that the amount of boron removed increases with increasing adsorbent dose as expected, attributed to the increase in the total available surface area of adsorbents in contact with the adsorbate. Using boron concentrations of 5 $mg.L^{-1}$ at pH 7 (Figure 5.a), CAAl materials exhibited better boron uptake than CA, achieving about 40 % boron adsorption when 0.75 g of adsorbent was dosed and 50 % when 1.5 g was added.

Figure 5. Effect of adsorbent dosage on boron removal. 5.a Effect at 5 $mg.L^{-1}$ boron. 5.b Effect at 25 $mg.L^{-1}$ boron.

(pH_o=7, $[B]_{initial}$= 5 $mg.L^{-1}$, V = 100 mL, T_{room}, 1 atm)

The same trend was obtained using a boron concentration of 25 $mg.L^{-1}$, as seen in Figure 5.b. These concentrations (5 $mg.L^{-1}$ and 25 $mg.L^{-1}$) were evaluated to ensure the presence of monomeric species of boron. According to Morisada et al., 2011, at boron concentrations

below 270 mg.L^{-1}, boric acid acts as a weak and monobasic acid, making monoborate ions the dominant species in the solution (equation 11). Boron removal did not change significantly above an adsorbent dosage of 0.75 g/100 mL.

4.4 Adsorption isotherms

Figure 6 plots the sorption isotherm of boron. The results showed that the adsorption of boron decreased with increasing boron concentration. Maximum boron removal uptake was 50 % for boron concentrations < 10 mg.L^{-1}. CA and CAAl materials achieved similar boron removal, which could be due to the weak interaction between negatively charged alumina charged and anionic boron species at this pH, as explained above.

Figure 6. Boron adsorption isotherms.

(pH_o=11, $[B]_{initial}$ = 50 mg.L^{-1}, 0.7 g of sorbent, V = 100 mL, T_{room}, 1 atm)

Figure 6 also compares CA (the standard gel beads used in this work) with dried beads of calcium alginate. Isotherm plots of dried beads exhibit a similar trend as gel beads, indicating that the drying procedure has an influence on the equilibrium of boron adsorption.

Coefficients of the Langmuir and Freundlich equations are reported in Table 1. These results demonstrate that boron adsorption is modelled better by the Langmuir model, suggesting that adsorption occurs by superficial surface coverage with a monolayer on the adsorbent surface. Also, mean square residuals (reported in Table 1) were lower using the Langmuir equation, indicating a better fit with this model. The maximum sorption capacity obtained was 132 mg.g^{-1} for CA and 131 mg.g^{-1} for CAAl under these conditions.

To predict whether the adsorption process is favourable or unfavourable for Langmuir type isotherms, the dimensionless equilibrium parameter was determined using equation 12:

$$r_L = \frac{1}{1 + bC_0} \qquad (12)$$

where C_0 is the initial concentration and b is the Langmuir isotherm constant. Values of r_L <1 represent favourable adsorption and values greater than 1.0 represent unfavourable adsorption. Table 1 shows favourable adsorption at a boron concentration of 50 $mg.L^{-1}$ with CA and CAAl materials.

Table 1. Langmuir and Freundlich parameters

4.5 Kinetic studies

Kinetic studies were carried out to examine the effect of contact time on boron adsorption using CA and CAAl as adsorbents. Figure 7.a plots the kinetic profiles of boron adsorption, which are similar for the two materials. The kinetics demonstrate an initial rapid sorption followed by a slow-rate step when approaching the equilibrium. The removal of boron increases with time in the first 30 min, and the equilibrium curve then levels off. The results also confirm that adsorption capacity increases with increasing pH.

Figure 7.b presents the kinetic profiles of CA (the standard gel beads used in this work) and dried beads. Initially, the profiles are different: the first step in the kinetic profiles of CA is faster than that for dried beads. This can be attributed to the fact that the active sites in gel beads are more easily accessible to adsorbate molecules, resulting in a shorter time to reach equilibrium. The second step in the kinetic profiles is similar for dried and gel beads. In conclusion, the drying method does not affect the equilibrium, but it does affect the contact time of boron adsorption: 30 min is enough for gel beads and 200 min for dried beads to achieve equilibrium.

The theoretical q values obtained from the pseudo-first-order model and pseudo-second-order model are shown in Table 2. The best fit of the experimental data was obtained using the pseudo-second-order model, and the theoretical q_2 values agree perfectly with the experimental q_{exp} values. Östürk and Kavak, 2005 reported that the pseudo-second order model fit the chemisorption data.

Figure 7. Boron adsorption kinetics. 7.a Effect of pH. 7.b Effect of the drying process.

(pH_o=11, $[B]_{initial}$ = 50 mg.L^{-1}, 1.75 g of sorbent, V = 250 mL, T_{room}, 1 atm)

Table 2. Pseudo-first-order and pseudo-second-order kinetic parameters for boron removal

4.6 Effect of temperature

Figure 8 shows the effect of temperature on the adsorption of boron using CA and CAAl. The sorption uptake was found to decrease with increasing temperature, indicating that boron adsorption on the adsorbent was favoured at lower temperatures. These results verify the exothermic nature of the adsorption process.

Figure 8. Effect of temperature on boron adsorption.

(pH_o=11, $[B]_{initial}$ = 50 mg.L^{-1}, 0.7 g of sorbent, V = 100 mL)

The standard change of entropy ($\Delta S°$) and standard change of enthalpy ($\Delta H°$) values of the adsorption process were determined from the intercept and slope of the Van't Hoff equation (equation 9), plotting $\ln K_c$ vs 1/T. These thermodynamic parameters are presented in Table 3. Kavak, 2009 and Polowczyk et al., 2013 reported that the change in free energy for physisorption is generally between 0 and 20 kJ.mol^{-1}, but for chemisorption processes it ranges from 80 to 400 kJ.mol^{-1}. In this work, the enthalpy changes of CA and CAAl were -95.83 and -86.22 kJ.mol^{-1}, respectively, suggesting that boron adsorption follows a chemical mechanism. Adsorption involves strong attractive forces, and the negative values of enthalpy change confirm the exothermic nature of the adsorption process. The negative values of entropy change correspond to a decrease in the degrees of freedom of the adsorbed species. The positive values of $\Delta G°$ imply that the adsorption of boron on CA and CAAl is not

spontaneous; these results are comparable with the literature (Yurdakoç et al., 2005).

Table 3. Thermodynamic parameters of the adsorbents

4.7 Desorption

When considering the effectiveness of an adsorption process, the efficiency of desorption must be considered. Figure 9 shows the desorption of boron using distilled water (pH 7) as an eluent. In this study, the maximum boron recovery was 74 %. In this sense, it is possible to use water to regenerate the sorbents (CA and CAAl); this represents an advantage in comparison with other sorbents in water treatment processes which need expensive solvents to be regenerated. For example, Dowex-XUS 43594.00 and Diaion CRB 02 resins have been regenerated with 5% H_2SO_4 (Nabay et al., 2008), and Dowex 2x8 resins (Öztürk and Ennil-Köse, 2008) with 0.5 M HCl. Special effort is required to separate eluted boron from acid eluents.

Figure 9. Desorption of sorbents using distilled water.

(pH = 7, 0.7 g of sorbent, V = 100 mL)

5. Conclusions

This work investigated the effectiveness of the composite alginate-alumina (CAAl) as a new adsorbent for the removal of boron from aqueous solutions in comparison with alumina and calcium alginate beads (CA). The adsorption of boron onto adsorbents is heavily influenced by the pH and the initial boron concentration. This study shows how using CAAl improves the boron adsorbent performance compared with alumina. The presence of alginate increases the boron adsorption capacity compared with the total amount of adsorbent used (0.7 g), and enables adsorbent reuse, achieving desorption of more than 70 % of boron using distilled

water as the eluent. The comparison between CA and CAAl confirmed that the composite performed better than alginate gel beads at slightly acidic pH, which could be an advantage for some water treatment processes; nevertheless, the maximum adsorption capacity was obtained at pH 11 using CA, with 132 $mg.g^{-1}$ as the maximum uptake obtained in this study. The application of the equation models to the experimental results showed that the Langmuir equation fit better than the Freundlich equation.

Adsorption of boron onto CA and CAAl is strongly influenced by temperature; the adsorption is an exothermic process where an increase in temperature decreases adsorption. Thermogravimetric analyses revealed that composites are more stable than alginate beads at high temperatures, and a thermodynamic study showed enthalpy changes between -86.22 kJ/mol and -95.83 kJ/mol, confirming chemical adsorption. These results are in agreement with kinetic studies. Experimental results showed that boron removal can be described using the pseudo-second-order model, supporting the conclusion that adsorption takes place as a chemical process. Furthermore, the incorporation of alumina in the new composite alginate gel beads increases the strength of the beads, facilitating industrial application for column processes.

Acknowledgements

This work was supported by the Ministry of Science and Innovation of Spain (Project No. CTQ 2011-22412). The authors would like to thank Dr. Eric Guibal for his help and advice on this project.

References

Bouguerra, W., Mnif, A., Hamrouni, B., Dhahbi, M., 2008. Boron removal by adsorption onto activated alumina and by reverse osmosis. Desalination 223, 31-37.

Cengeloglu, Y., Arslan, G., Tor, A., Kocak, I., Dursun, N., 2008. Removal of boron

from water by using reverse osmosis. Sep. Purif. Technol. 64, 141–146.

Cengeloglu, Y., Tor, A., Arslan, G., Ersoz, M., Gezgin, S., 2007. Removal of boron from aqueous solution by using neutralized red mud. J. Hazard. Mater. 142, 412–417.

Del-Campo Marin, C., Gideon, O., 2007. Boron removal by the duckweed Lemna gibba: A potential method for the remediation of boron-polluted waters. Water Res. 41, 4579 – 4584.

Demey, H., Ruiz, M., Barron-Zambrano, J.A., Sastre, A.M., 2013. Boron removal from aqueous solutions using alginate gel beads in fixed bed systems. J. Chem. Technol. Biot., accepted manuscript JCTB-13-0429.R1.

Dosoretz, C., Geffen, N., Semiat, R., Eisen, M., Balazs, Y., Katz, I., 2006. Boron removal from water by complexation to polyol compounds. J. Membrane. Sci 286, 45-51.

Erdem, A. Yilmaz, A., Boncukcuoğlu, R., Muhtar-Kocakerim, M., 2007. A quantitative comparison between electrocoagulation and chemical coagulation for boron removal from boron-containing solution. J. Hazard. Mater. 149, 475–481.

Ho, Y., McKay, G., 1998. Sorption of dye from aqueous solution by peat. Chem. Eng. J. 70, 115–124.

Ho, Y., Mckay, G., 2000. The kinetics of sorption of divalent metal ions onto sphagnum moss peat. Water Res. 34, 735–742.

Itakura, T., Sasai, R., Itoh, H., 2005. Precipitation recovery of boron from wastewater by hydrothermal mineralization. Water Res. 39, 2543–2548.

Kabay, N., Sarp, S., Yuksel, M., Kitis, M., Koseoğlu, H., Arar, Ö., Bryjak, M., Semiat, R., 2008. Removal of boron from SWRO permeate by boron selective ion exchange containing N-Methylglucamine groups. Desalination 223, 49-56.

Kabay, N., Sarp, S., Yuksel, M., Kitis, M., Koseoglub, H., Arar, Ö., Bryjak, M., Semiat, R.,

2008. Removal of boron from SWRO permeates by boron selective ion exchange resins containing N-methylglucamine groups. Desalination 223, 49–56.

Karahan, S., Yurdakoc, M., Seki, Y., Yurdakoc, K., 2006. Removal of boron from aqueous solution by clays and modified clays. J. Colloid. Interf. Sci. 293, 36–42.

Kavak, D., 2009. Removal of boron from aqueous solutions by batch adsorption on calcined alunite using experimental design. J. Hazard. Mater. 163, 308-314.

Koparal, A.S., 2002. The removal of salinity from produced formation by conventional and electrochemical methods. Fresen. Environ. Bull. 12A, 1071–1077.

Lagergren, S., 1898. Zur theorie der sogenannten adsorption gelöster stoffe: Kungliga Svenska Vetenskapsakademiens, Handlingar 24, 1–39.

Liu, R., Ma, W., Jia, C., Wang, L., Li, H.Y., 2007. Effect of pH on biosorption of boron onto cotton cellulose. Desalination 207, 257-267.

Matsumoto, M., Matsui, T., Kondo, K., 1999. Adsorption mechanism of boric acid on chitosan resin modified by saccharides. J. Chem. Eng. of Japan. 32, 190-196.

McKay, G., Ho, Y., 1999. Pseudo-second order model for sorption processes. Process Biochem. 34, 451–465.

Morisada, S., Rin, T., Ogata, T., Kim, Y., Nakano, Y., 1997. Adsorption removal of boron in aqueous solutions by amine-modified tannin gel. Water Res. 45, 4028-4034.

Öztürk, N., Ennil-Köse, T., 2008. Boron removal from aqueous solutions by ion-exchange resin: Batch studies. Desalination 227, 233-240.

Öztürk, N., Kavak, D., 2005. Adsorption of boron from aqueous solutions using fly ash: Batch and column studies. J. Hazard. Mater. B127, 81–88.

Öztürk, N., Kavak,D., 2004. Boron removal from aqueous solutions by adsorption on waste sepiolite and activated waste sepiolite using full factorial design. Adsorption 10, 245–257.

Polowczyk , I., Ulatowska, J., Kozlecki, T., Bastrzyk, A., Sawinsky, W., 2013. Studies on removal of boron from aqueous solution by flash ash agglomerates. Desalination 310, 93-101.

Prats, D., Chillon-Arias, M.F., Rodriguez-Pastor, M., 2000. Analysis of the influence of pH and pressure on the elimination of boron in reverse osmosis. Desalination 128, 269-273.

Rodríguez-Pastor, M., Ferrándiz-Ruiz, A., Chillon, M.F., Prats-Rico, D., 2001. Influence of pH in the elimination of boron by means of reverse osmosis. Desalination 140, 145-152.

Ruiz, M., Roset, L., Demey, H., Castro, S., Sastre, A.M., Pérez, J.J., 2013. Equilibrium and dynamic studies for adsorption of boron on calcium alginate gel beads using principal component analysis (PCA) and partial least squares (PLS). Mat.-wiss. U. Werkstofftech. 44, 410-415.

Ruiz, M., Sastre, A.M., Guibal, E., 2005. Palladium sorption on glutaraldehyde-crosslinked chitosan. React. Funct. Polym.45, 155-173.

Ruiz, M., Tobalina, C., Demey-Cedeño, H., Barron-Zambrano, J., Sastre, A.M., 2013. Sorption of boron on calcium alginate gel beads. React. Funct. Polym. 73, 653-657.

Sabarudin, A., Oshita, K., Oshima, M., Motomizu, S., 2005. Synthesis of cross-linked chitosan possesing N-methyl-D-glucamine moiety (CCTS-NMDG) for adsortion/concentration of boron in water samples and its accurate measurement by ICP-MS and ICP-AES. Talanta 66, 136-144.

Seki, Y., Seyhan, S., Yurdakoc, M., 2006. Removal of boron from aqueous solutions by adsorption on Al_2O_3 based materials using full factorial design. J. Hazard. Mater. B138, 60–66.

Shanina, T.M., Gelman, N.E., Mikhailovskaya, V.S., 1967. Quantitative analysis of heterorganic compounds. Spectrophotometric microdetermination of boron. J.

Anal.Chem-USSR+ 22, 663-667.

Simonnot, M., Castel, C., Nicolai, M., Rosin, C., Sardin, M., Jauffret, H., 2004. Boron removal from drinking water with a boron selective resin: is the treatment really selective?. Water Res. 34, 109-116.

Water Health Organization, 2011. Guidelines for drinking-water quality, 4th ed. Geneva.

Yazicigil, Z., Oztekin, Y., 2006. Boron removal by electrodialysis with anion-exchange membranes. Desalination 190, 71–78.

Yurdakoç, M., Seki, Y., Karahan, S., Yurdakoç, K., 2005. Kinetic and thermodynamic studies of boron removal by Siral 5, Siral 40, and Siral 80. J. Colloid Interf. Sci 286, 440-446.

Figure

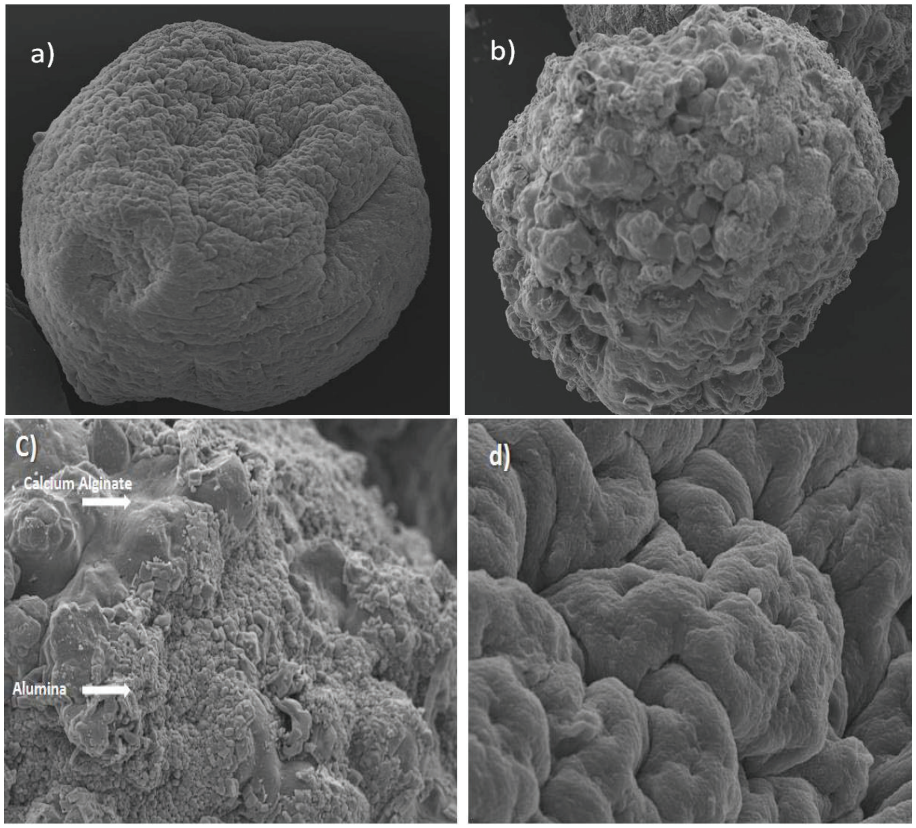

Figure 1. Adsorbent topography. 1.a CA surface at 90 X magnification, 20 kV. 1.b CAAl surface at 90 X magnification, 20 kV. 1.c CAAl surface at 1500 X magnification, 20 kV. 1.d CA surface, 1500 X magnification, 20 kV.

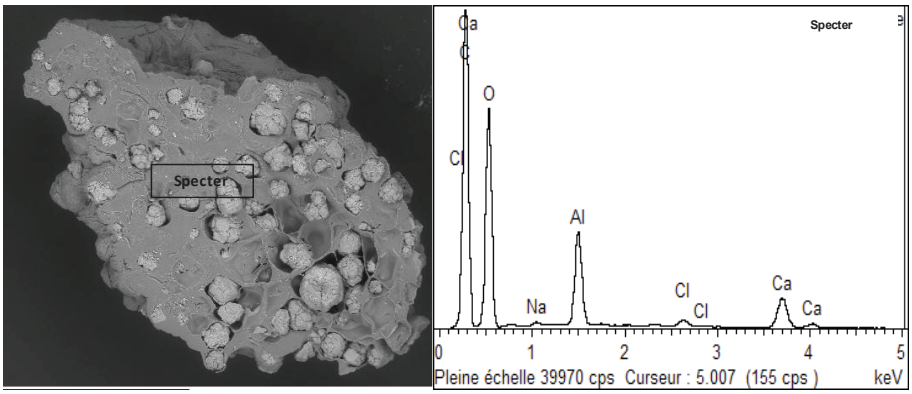

Figure 2. Cross-sectional area of CAAl materials.

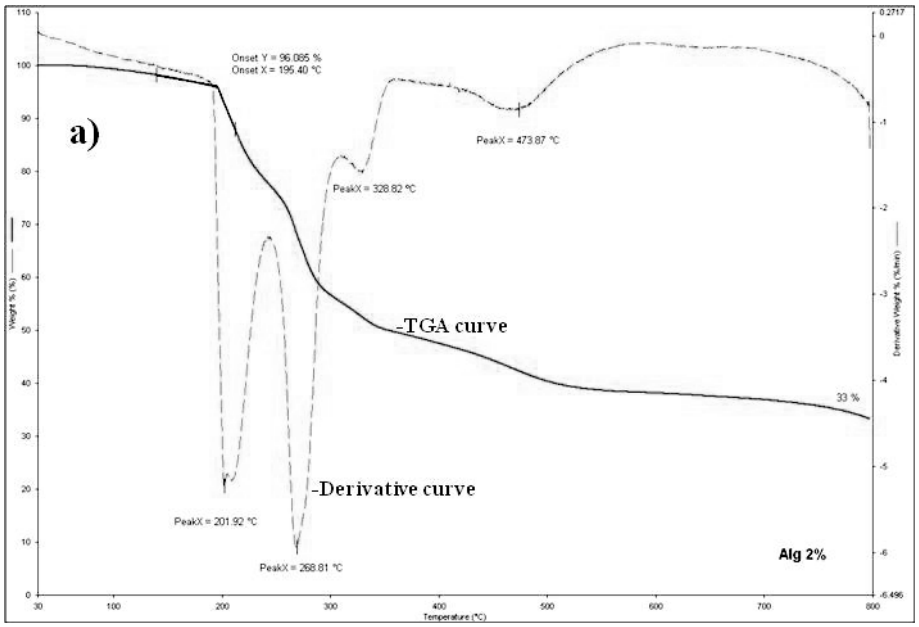

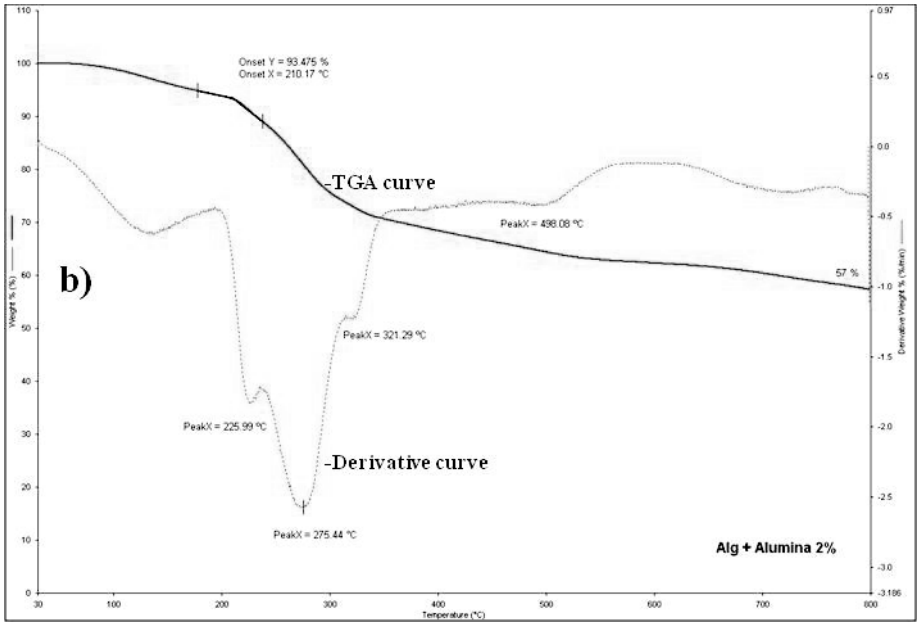

Figure 3. Thermogravimetric analyses. 3.a. TGA curve of CA. 3.b TGA curve of CAAl.

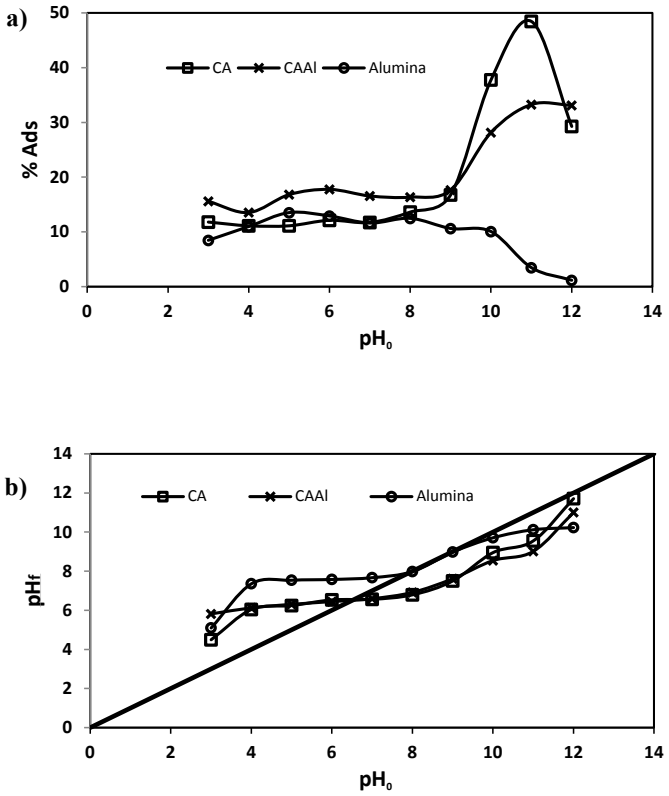

Figure 4. Influence of pH. 4.a Effect of boron removal using CA and CAAl.

4.b Variation in pH.

(pH_o=3-12, $[B]_{initial}$= 50 $mg.L^{-1}$, V = 100 ml, T_{room}, 1 atm)

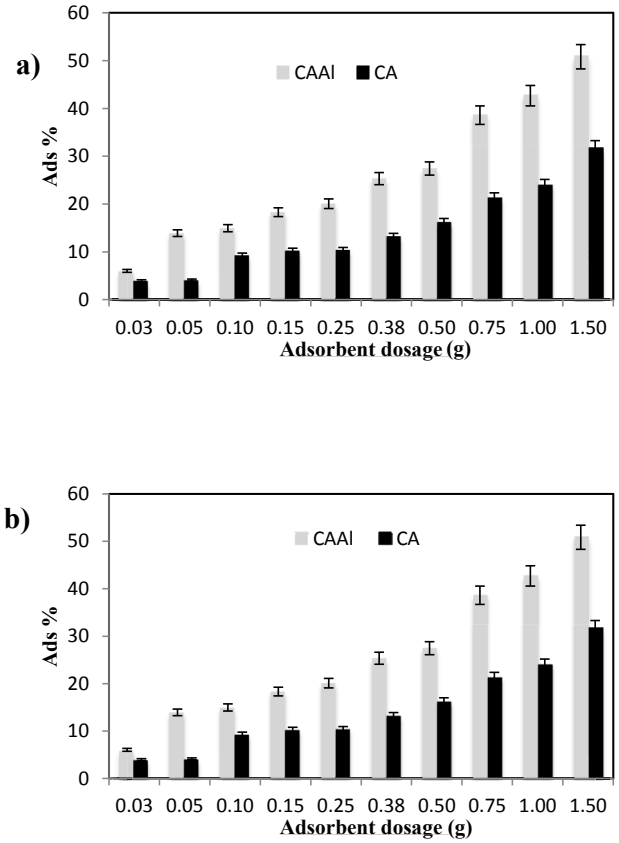

Figure 5. Effect of adsorbent dosage on boron removal. 5.a Effect at 5 mg.L^{-1} boron. 5.b Effect at 25 mg.L^{-1} boron.

(pH_o=7, $[B]_{initial}$= 5 mg.L^{-1}, V = 100 mL, T_{room}, 1 atm)

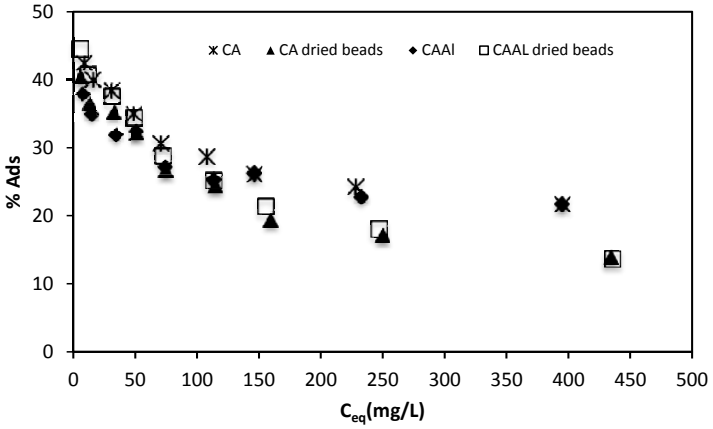

Figure 6. Boron adsorption isotherms.

(pH_o=11, $[B]_{initial}$ = 50 mg.L^{-1}, 0.7 g of sorbent, V = 100 mL, T_{room}, 1 atm)

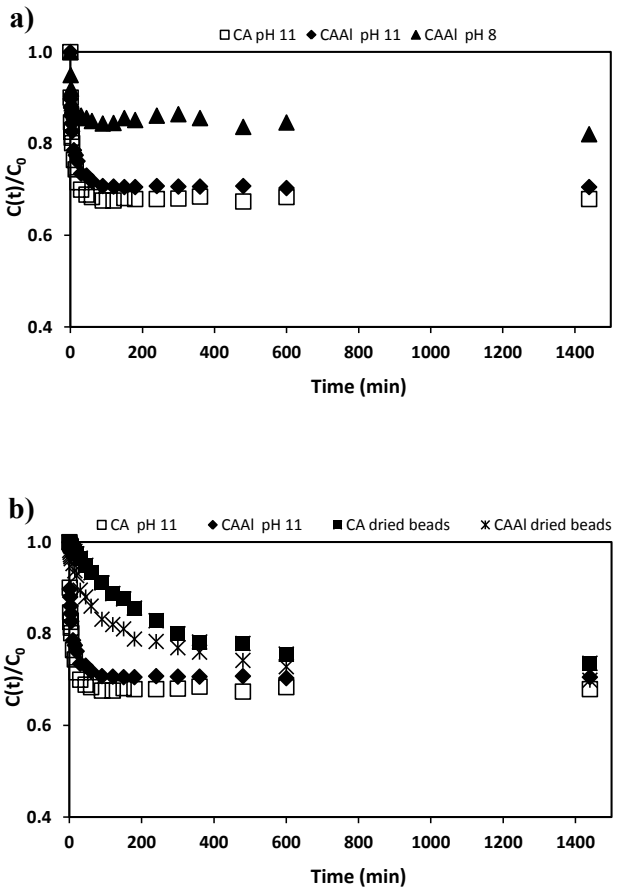

Figure 7. Boron adsorption kinetics. 7.a Effect of pH. 7.b Effect of the drying process.

(pH_o=11, $[B]_{initial}$ = 50 mg.L^{-1}, 1.75 g of sorbent, V = 250 mL, T_{room}, 1 atm)

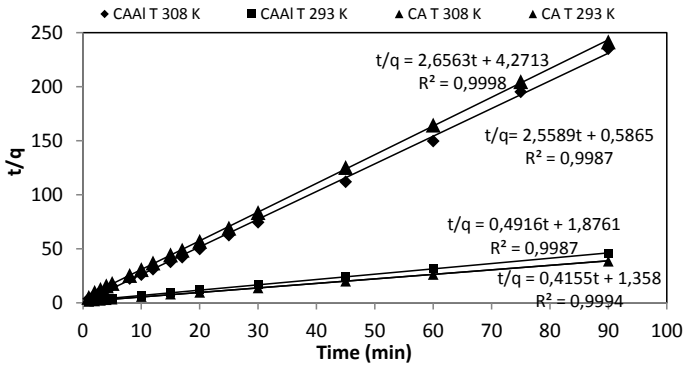

Figure 8. Effect of temperature on boron adsorption.

(pH_o=11, $[B]_{initial}$ = 50 mg.L^{-1}, 0.7 g of sorbent, V = 100 mL)

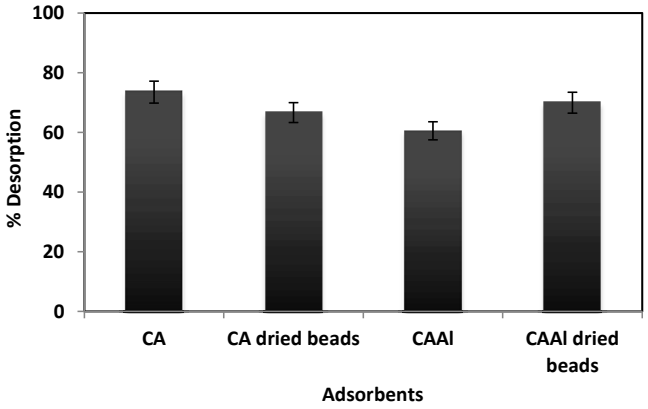

Figure 9. Desorption of sorbents using distilled water.

(pH = 7, 0.7 g of sorbent, V = 100 mL)

Table 1. Langmuir and Freundlich parameters

	Langmuir model				Freundlich model		
Adsorbent	q_m (mg g^{-1})	$b \cdot 10^4$ (L mg^{-1})	**MSR**	r_L	k_F ($mg^{1-1/n}$ g^{-1} $L^{1/n}$)	**n**	**MSR**
CA	132.05	3.98	1.82	0.98	0.15	1.29	3.63
CAAl	131.78	3.47	0.82	0.98	0.12	1.25	2.93
CA (dried beads)	90.46	4.06	1.62	0.98	0.18	1.42	1.86
CAAl (dried beads)	69.65	5.09	2.11	0.97	0.23	1.54	1.16

Table 2. Pseudo-first-order and pseudo-second-order kinetic parameters for boron removal

Adsorbent	Pseudo-first order model				pseudo-second order model		
	q_{exp} (mg g^{-1})	K_1 (min^{-1})	q_1 (mg g^{-1})	r^2	K_2 (min^{-1})	q_2 (mg g^{-1})	r^2
CA	2.4	0.23	2.25	0.942	0.15	2.34	0.989
CAAl	1.99	0.19	1.91	0.932	0.15	1.99	0.986
CA (dried beads)	1.83	$4.54 \cdot 10^{-3}$	1.82	0.998	$2.53 \cdot 10^{-3}$	2.09	0.992
CAAl (dried beads)	2.07	$1.15 \cdot 10^{-2}$	1.85	0.955	$7.29 \cdot 10^{-3}$	2.08	0.988
CAAl (pH 8)	1.37	0.36	1.06	0.876	0.51	1.09	0.906

Table 3. Thermodynamic parameters of the adsorbents

Adsorbent	Temperature (K)	K_c	$\Delta G^\circ \left(\frac{kJ}{mol}\right)$	$\Delta H^\circ \left(\frac{kJ}{mol}\right)$	$\Delta S^\circ \left(\frac{kJ}{mol}\right)$
CA	293	0.07	6.54	-95.82	-0.34
	308	0.01	11.78		
CAAl	293	0.06	6.84	-86.22	-0.31
	308	0.01	11.60		

ANNEX VIII

EFFECTS OF SODIUM SALTS ON BORON ADSORPTION ONTO ALGINATE GEL BEADS

EFFECT OF SODIUM SALTS ON BORON ADSORPTION ONTO ALGINATE GEL BEADS

H. Demey[1,2*], M. Ruiz[1], J.A. Barron-Zambrano[1], M.T. Coll, A. Fortuny, A. M. Sastre[2],

[1]Universitat Politècnica de Catalunya, Department of Chemical Engineering, EPSEVG, Av. Víctor Balaguer, s/n, 08800 Vilanova i la Geltrú, Spain,

[2]Universitat Politècnica de Catalunya, Department of Chemical Engineering, ETSEIB, Diagonal 647, 08028 Barcelona, Spain

*Ph: +34 938937778– Fax: +34 934017700– E-mail: hary.demey@upc.edu

Abstract

Different parameters affecting the bio-sorption of boron from aqueous solutions were studied in the present work; calcium alginate beads (CA) have been used as adsorbent in batch system. The effect of different sodium salts in solution and the effect of using three types of alginates (with different composition of guluronic and mannuronic acid) on boron recovery was investigated. Sodium salts reduce greatly the adsorption capacity. Adsorption isotherms and kinetics studies were performed; the Langmuir and Freundlich isotherms models were evaluated and the experimental data was very well fitted with the Langmuir model; maximun sorption capacity was found to be 12 mmol g^{-1} at pH 11. The results were compared with a commercial resin AMBERLITE-IRA 743. The pseudo-first order and pseudo-second order kinetic model were tested to fit the experimental data of kinetics studies; the results obeyed the pseudo-second order model. BET surface area, pore volume and pore size of the bio-sorbent were also determined: calcium alginate is a mesoporous material.

Keywords: Alginate, boron, salts, bio-sorption, beads

1. Introduction

Boron is an essential nutrient for plants growth, humans and animals; furthermore it is an element very important for economy of countries because it is widely used in industries; since it can be used in more than 300 applications grouped in four main end-uses: ceramics, detergents, fertilizer and glass. At present, the increase in worldwide production of boron-based products (for many applications) has disproportionately increased the pollution of surface and ground-waters. It is well known that all the water which is available in the planet only 1% is consumable, so it is necessary to take appropriate considerations to minimize the pollution and to search the solutions to recycle contaminated water and wastewaters.

The World Health Organization (WHO) has stated that short- and long- term oral exposures to boric acid or borax in laboratory animals have shown the male reproductive system to be a consistent target of toxicity: testicular lesions have been observed when boric acid or borax was provided in food (and drinking water) to dogs, mice and rats. The guide level for boron in drinking water was set to 2.4 $mg \cdot L^{-1}$ [1]. Although in plants, boron plays an important role in the structural stability and although it is an essential component of the cell walls; excessive levels of this element inhibits photosynthesis and root cell division, causes yellowish spots on the leaves, less fruit and also it can impede the deposition of lignin and chlorophyll [2,3].

In recent years, several techniques have been utilized for boron separation from aqueous solutions such as chemical coagulation [4], electro-coagulation [5], precipitation [6], electro-dialysis [7], ion-exchange with boron-specific resins [8,9], reverse osmosis [10-12], ultra-filtration [13], and adsorption: i) with recycle materials [14]; ii) with biomaterials [15]; iii) and with new composites [16]; e.g., Demey et al. [17] have recently developed an innovative chitosan/$Ni(OH)_2$-based sorbent for effectively remove boron from aqueous solutions.

The present work is focused in the utilization of biopolymers for boron adsorption, specifically polysaccharides such as alginates. Alginate is a copolymer comprised of β-D-mannuronic and α-L-

guluronic acid isolated from large brown algae (*Laminaria hyperborea, Laminaria digitata, Laminaria japonica*, etc) [18]. In presence of divalent ions, alginate gelation takes place as a result of the formation of a three-dimensional network, usually described by the ‘’egg-box’’ model [19]. Calcium alginate beads (CA) was used as adsorbent in this work.

In previous works [20, 21] it has been demonstrated the potentials abilities of alginates and its feasibility for boron removal, nevertheless before to design a large scale process it is very important to know the influence on boron recovery of the foreign ions (ionic strength), as well as the influence of the composition of monomeric blocks present in the adsorbent (mannuronic and guluronic blocks), which have not been studied before. The equilibrium adsorption data were evaluated using the Langmuir, and the Freundlich models. The uptake kinetics for boron removal has also been investigated, and the pseudo-first order and pseudo-second order models were evaluated to fit the experimental data.

2. Experimental

2.1 Materials

Boron solutions were prepared using boric acid ($B(OH)_3$) provided by Merck AG (Germany). The pH of each solution was adjusted to the required value using HCl and NaOH solutions before mixing it with the adsorbent. Sodium salts (NaCl, Na_2SO_4, Na_2CO_3, Na_2HPO_4) and calcium nitrate (used for sorbent preparation) were supplied by Panreac (France). Three different sodium alginates were used to manufacture the adsorbent beads: i) BCN (Panreac); ii) LF-240D (Acros); iii) LF-200S (Acros)

2.2 Preparation of sorbent

The sorbent was prepared following the procedure recommended by Demey et al. 2013 [20]. A solution of sodium alginate in water was prepared (2 w/w%) and vigorously shaken for a minimum of 5 h to ensure that it was completely homogenised. The speed was then lowered to allow air to dissipate and prevent the formation of air bubbles, which would make difficult the production of beads. The viscous

solution was then pumped and drop-wise through a thin nozzle (Ø 1.6 mm) into an aqueous solution of 0.05 M calcium nitrate solution under magnetic stirring to produce microspheres of calcium alginate. The calcium alginate gel beads were kept under stirring for 8 h at room temperature (25°C), and then were filtered and intensively washed with distilled water to remove the excess of calcium present on the surface of beads. Standard wet beads used in this work had an average diameter of 2.3 mm.

2.3 Characterization of sorbents

2.3.1 Composition of alginates

In order to determine the concentration of mannuronic and guluronnic acid (M and G blocks respectively) of sodium alginates, it was used NMR spectroscopy technique. The samples were prepared with 25 mg of the hydrolysed alginate solution, 7 mg of EDTA and 1 mL of D_2O; the NMR ^1H spectra were recorded at 400 MHz on a Bruker spectrometer at 90 ºC with an acquisition time of 5.11s, a delay of 4s and an accumulation of 512 spectra. Lorentzian deconvolution and integration of the lines were obtained using Origin 7.0 software.

2.3.2 BET surface and porosity

For determination of porosity and specific surface area of adsorbent, it was used a nitrogen-adsorption equipment (Micrometrics, Tristar 3000). The experiment were done by triplicate and the samples were washed with abundant distilled water previously and dried with a freeze dryer (Bioblock scientific, Christ) at 223K and 0.01 mbar. Then, the dried samples were degassed with N_2 at 100ºC for 6h prior to experiments in order to clean and to remove some traces of free calcium ions from the surface of the adsorbent (remained from beads production) [22]. Surface area, pore volume and pore diameter of adsorbent were determined by N_2 adsorption at 77 K using the BET method [23], and the pore size distribution was determined by using Barret-Joyner-Halenda (BJH) model [24].

106
2.4 Batch sorption experiments

107
The study of the pH-influence on the boron solution was performed by mixing a volume of 100 mL of a
108
boron solution (50 $mg \cdot L^{-1}$) with known amounts of adsorbent (0.2 g) in polyethylene flasks of 250 mL.
109
The concentration of protons was varied using 0.1M HCl and 0.1M NaOH solutions; the stirring speed
110
was set at 100 rpm at 20 °C, using an agitator Rotabit, J.P. Selecta (Spain). After 48 h of agitation, the
111
final pH was measured, and 5 mL of solution were filtered and analysed with an inductively coupled
112
plasma atomic emission spectrometer ICP-AES (HORIBA JOBIN YVON, France) at the wavelength of
113
249.7 nm for boron.
114
The pH-effect was also carried out to compare the performance of adsorbents beads (Ø 2.3 $\pm$ 0.1 mm)
115
manufactured from three different types of sodium alginate (Alginate BCN, alginate LF-240D, alginate
116
LF-200S). The sorption capacity was obtained using a mass balance equation, and it was expressed as
117
mg of boron per g of adsorbent.
118
Mono-component sorption isotherms were obtained by mixing a known volume of solution at different
119
boron concentrations at a pH 11 and a fixed mass of adsorbent (0.7 g) in 100 mL of boron solution. After
120
48 h of contact time, the pH of the solution was measured and the residual concentration of boron was
121
analysed, the results were compared with the results obtained with AMBERLITE-IRA 743 (provided by
122
Rohm and Hass).
123
The uptake kinetics experiment was performed by adding (under continuous stirring) a known amount of
124
adsorbent (i.e., 1.75 g) to 250 mL of boron solution (50 $mg \cdot L^{-1}$) at pH 11. Samples were withdrawn at
125
different times and filtered after 120 h of contact. The residual concentration was determined by ICP-
126
AES.
127
The influence of different salts was performed in order to study the effect of foreign ions on boron
128
uptake. The salts selected for this study were: NaCl, Na_2SO_4, Na_2CO_3, Na_2HPO_4. To perform this study
129
the salts were added at a concentration of 0.05 M to a boron solution (1 g L^{-1}), and adjusted to pH 5.
130
Then, 0.7 g of adsorbent was added to the solutions. After 48 h of contact time, the residual boron

concentration was analysed.

2.4.1 Fitting of sorption isotherms

Experimental sorption isotherms are commonly modeled by means of the mathemathical models of Langmuir [25] and Freundlich [26] which are represented by the following equations respectively:

$$q = \frac{q_{max} b C_e}{1 + b C_e} \quad (1)$$

$$q = k_F C_e^{\frac{1}{n}} \quad (2)$$

Where q is the amount of boron adsorbed per gram of sodium alginate gel beads at equilibrium (mg g^{-1}), qmax is the maximum adsorption capacity of the adsorbent (mg g^{-1}), Ceq is the boron concentration in solution at equilibrium (mg L^{-1}). The variable b in the Langmuir model is the affinity coefficient (L mg^{-1}), whereas k_F ($mg^{1-1/n}$ g^{-1} $L^{1/n}$) and n (dimensionless) are the Freundlich adsorption constants indicative of the relative capacity and adsorption intensity, respectively.

2.4.2 Fitting of sorption kinetics

Several kinetics models have been used to describe the experimental kinetic data of adsorption processes; the pseudo first and pseudo second order models are the most commonly used (PFORE and PSORE respectively). In this work, the Lagergreen [27] and Ho and Mckay [28] models, were used to describe the sorption kinetics of the boron uptake by the calcium alginate beads. The models are described as follows:

Pseudo-first order rate equation (PFORE) [27]:

$$\frac{dq_t}{d_t} = K_1(q_1 - q_t) \quad (3)$$

Integrating for the boundary conditions t = 0 to t = t and q_t =0 to q_t = q_t:

$$\log\left(q_{eq} - q_t\right) = \log(q_{eq}) - \frac{K_1}{2.303}t \quad (4)$$

Pseudo-second order rate equation (PSORE) [28]:

$$\frac{dq_t}{\left(q_{eq} - q_t\right)^2} = K_2 d_t \quad (5)$$

Integrating for the boundary conditions t = 0 to t = t and q_t =0 to q_t = q_t:

$$\frac{1}{q_t} = \frac{1}{K_2 q_{eq}^2} + \frac{1}{q_{eq}}t \quad (6)$$

where q_{eq} is the equilibrium sorption capacity (mg·g^{-1}), q_t is the sorption capacity (mg·g^{-1}) at any time *t* (min) and k_2 is the pseudo-second order rate constant (g·mg^{-1}·min^{-1}).The parameters q_{eq} and k_2 are pseudo-constants depending on the experimental conditions.

The intraparticle diffusion was obtained with equation 7 [29]:

$$q_t = K_p t^{1/2} + C \quad (7)$$

where C is the intercept, and K_p is the intraparticle diffusion rate constant.

3. Results and discussion

3.1 Characterization of sorbent

3.1.1 Composition of sorbent

From the results obtained by NMR spectroscopy; the alginates used in this work have a different molar composition of mannuronic and guluronnic acid. As it can see in table 1, the LF-200S alginate is the richest in G-blocks (70 %w/w), meanwhile the LF-240D alginate is the richest in M-blocks (67 %w/w); the BCN alginate has an intermediate composition (36 % w/w of G-blocks and 64 % w/w of M-blocks). The main features of commercial resin (AMBERLITE IRA-743) are summarised in table 2.

3.1.2 BET surface and porosimetry

The results obtained from nitrogen adsorption-desorption isotherms show that calcium alginate is a

mesoporous material in nature, according to IUPAC classification (2 nm < pore size < 50 nm); pore size of calcium alginate beads is 34 nm, the pore volume and the BET surface area are $4.8x10^{-3}$ cm^3 g^{-1} and 0.6 m^2 g^{-1} respectively.

The average BET surface area obtained from the raw material (sodium alginate powder) is not substantially different of calcium alginate's area: it is 0.9 m^2 g^{-1}; it is essentially a mesoporous material (pore size: 16 nm) and the pore volume obtained was $3.6\ x10^{-3}$ cm^3 g^{-1}. The difference between the size of pore in the raw material (16 nm) and calcium alginate (34 nm) suggest that freeze drying technique (used in the pre-treatment of the calcium alginate samples) may influence in the width of pores, similar conclusion was found by Haugh et al.[30].

3.2 Influence of pH

Figure 1 shows the strong influence of pH (in the interval 5-11) on boron adsorption capacity; good adsorption is obtained at pH>7, and the best results were found at pH 11. Similar trend was presented by Demey et al. [20], calcium alginate beads seems to be more efficient in presence of $B(OH)_4^-$, which begins to be the dominant specie from pH ≥ 9.2, according to equation 8

$$pK_a = 9.2 \qquad (8)$$

$$B(HO)_3 + H_2O \leftrightarrow B(OH)_4^- + H^+$$

At pH≤5, carboxylic groups in the alginate formed a weak base that neutralized the acid solution; this was verified for the variation in the initial and final pH of boron solutions in Figure 2 (a similar trend was also observed by Papageorgiou et al. [31] and Demey et al. [20]).

Among the three types of alginates used, a significant difference in the adsorption capacity was not observed, which is an advantage, since the boron species may react with the OH^-groups present in both G blocks and M blocks to form esters.

193 **Figure 1. Effect of pH on boron removal.**

194

195 **Figure 2. Variation of pH on boron removal.**

196

197 **3.3. Equilibrium studies**

198 The sorption isotherms of boron onto CA (prepared from three different alginates) are shown in Figure
199 3. The results confirm that sorption uptake is not seriously affected by the composition of alginates; the
200 experimental data were fitted to the theoretical isotherms models of Langmuir and Freundlich, table 3
201 shows the coefficients of both models; the results have been compared with the commercial
202 AMBERLITE-IRA 743 resin at the same operation conditions. It indicates that CA could be a good
203 alternative for boron removal since is a sorbent easy to prepare and the raw material comes from
204 renewable sources (*brown algae*).

205

206 **Figure 3. Boron sorption isotherms using three different alginates.**

207

208 **3.4. Influence of contact time**

209 Figure 4 shows the sorption kinetic of boron onto CA. It seems that at operation conditions used, the
210 type of alginate has little effect in the uptake of boron, the three obtained curves are very similar, there
211 are any differences in the time required to reach the equilibrium, nor in the initial slope of the curves.
212 Kinetics models of pseudo first and pseudo second order were used to fit the experimental data. Table 4
213 shows the obtained coefficients of each model; the experimental data fits better to the pseudo second
214 order model. The values of r^2 are higher than 0.95 for all the cases, the model also predict well the value
215 of q_e. The simplified equation for evaluating the contribution of the resistance to intraparticle diffusion
216 (equation 7) was tested (see Figure SM1 in Supplementary Materials Section). The linear plot did not
217 pass through the origin, verifying that intraparticle diffusion is not the unique step that controls the boron
218 uptake kinetics. The resistance to film diffusion may affect the control of uptake kinetics. Kp values

(Table 4) were obtained from the slope of the linear portions of the kinetics profiles. The obtained intraparticle diffusion coefficients for the three alginates are quite similar.

Figure 4. Kinetics profiles on boron removal.

3.4 Influence of salts

3.4.1 Influence on sorption capacity

Figure 5 shows the influence of several salts on boron adsorption capacity; it was found that sodium salts strongly affect the boron removal from aqueous solutions; it is due to ion-exchange process between Na^{+} and Ca^{+2} ions (from "egss-box" structure [19]) which conduct to the degradation of the gel structure. Similar conclusion was obtained by Bajpai and Sharma [32]: when calcium alginate beads were placed in a phosphate buffer saline (PBS) solution, the Na^{+} ions present in the external solution were exchanged with Ca^{+2} ions which are binding with COO^{-} groups mainly in the polymannuronate sequences. It indicates that the presence of sodium has a negative impact on boron uptake; it causes chain relaxation of the polymer and consequently the calcium present in the eggs-box structure is exchanged with the sodium of the aqueous medium; it eventually hinders the interaction between boron species and OH- groups of the sorbent [18]. Sodium salts induced a reduction on more than 50% of boron adsorption capacity.

Figure 5. Influence of different salts on sorption capacity.

3.4.2 Swelling of the beads

The mechanical properties and swelling of the alginate beads depend mainly of the divalent cations; it was observed the behavior of the beads immersed in bi-distilled water did not show any tendency to gain water. However, the behavior of the beads in bi-distilled water containing Na^{+} was completely different; they were observed to swell (Figure 6). This can be explained on the basis of ion-exchange

taking place between the Na^+ ions present in the solution and the Ca^{2+} ions presents inside the beads. It is supposed that when the majority of Ca^{2+} ions have been exchanged with Na^+ ions in the M blocks, the process then starts in the G blocks, resulting in the loss of the "egg-box" structure and allowing more water intake. Once equilibrium was reached, the highly hydrated "egg-box" structure begins to collapse and break down [32].

In short, the exchange of Na^+ ions (to bind to the carboxylate groups) is responsible for the degradation of the beads. Research carried out by Bajpai and Sharma [32] indicates that when using high concentrations of NaCl (0.25 and 0.5 M) the beads lose their structure and dissolve. The Na^+ ions present in the solution undergo ion exchange with Ca^{2+} ions (which are bounded to the COO^- groups of alginate). As a result, the electrostatic repulsion between the negatively charged COO^- groups increases, ultimately causing chain relaxation, and enhances the swelling of the gel.

Figure 6. Influence of different salts on the swelling of the beads.

The results shown in Figure 7 verifies that the amount of Ca^{2+} released from the beads into the solution increases in presence of Na+ ions.

Figure 7. Release of Ca^{2+} ions in the presence of different salts.

Conclusions

It was probed that calcium alginate is an effective mesoporous material for boron recovery; the sorption capacity of this promising sorbent is strongly influenced by the presence of sodium salts in solution: sorption uptake was reduced on more than 50%. Sodium salts particularly contribute to the swelling of the beads and promote the ion exchange between the sodium and calcium ions, resulting in a weakening of the ''eggs-box'' structure. The type of alginate (with different composition in M and G

blocks) has little effect on the boron sorption capacity; the kinetic experimental data was well fitted by using pseudo-second order model and equilibrium data was well adjusted by using the Langmuir model.

Acknowledgements

This work was supported by the Spanish Ministry of Economy and Competitiveness, MINECO (Project No. CTQ 2011-22412).

References

[1] World health organization, Guidelines for drinking-Water quality, fourth ed., Geneva, 2011.

[2] B. Wang, X. Guo, P. Bai, Removal technology of boron dissolved in aqueous solutions- A review, Colloids Surface A 444 (2014) 338-344.

[3] F. Xu, Advances in plant and animal boron nutrition, in: Proceedings of the 3rd International Symposium on All aspects of Plant and Animal Boron Nutrition, Springer, 2007.

[4] A. Erdem, A. Yilmaz, R. Boncukcuoğlu, M. Muhtar-Kocakerim, A quantitative comparison between electrocoagulation and chemical coagulation for boron removal from boron-containing solution, J. Hazard. Mater. 149 (2007) 475–481.

[5] A.S. Koparal, The removal of salinity from produced formation by conventional and electrochemical methods, Fresen. Environ. Bull. 12A (2002) 1071–1077.

[6] T. Itakura, R. Sasai, H. Itoh, Precipitation recovery of boron from wastewater by hydrothermal mineralization, Water Res. 39 (2005) 2543–2548.

[7] Z. Yazicigil, Y. Oztekin, Boron removal by electrodialysis with anion-exchange membranes, Desalination 190 (2006) 71–78.

[8] M. Simonnot, C. Castel, M. Nicolai, C. Rosin, M. Sardin, H. Jauffret, Boron removal from drinking water with a boron selective resin: is the treatment really selective?, Water Res. 34 (2004) 109-116.

[9] N. Kabay, S. Sarp, M. Yuksel, M. Kitis, H. Koseoglub, Ö. Arar, M. Bryjak, R. Semiat, Removal of

296 boron from SWRO permeate by boron selective ion exchange resins containing N-methylglucamine
297 groups, Desalination 223 (2008) 49–56.
298 [10] D. Prats, M.F. Chillon-Arias, M. Rodriguez-Pastor, Analysis of the influence of pH and pressure on
299 the elimination of boron in reverse osmosis, Desalination 128 (2000) 269-273.
300 [11] M. Rodríguez-Pastor, A. Ferrándiz-Ruiz, M.F. Chillon, D. Prast-Rico, Influence of pH in the
301 elimination of boron by means of reverse osmosis, Desalination 140 (2001) 145-152.
302 [12] Y. Cengeloglu, G. Arslan, A. Tor, I. Kocak, N. Dursun, Removal of boron from water by
303 using reverse osmosis, Sep. Purif. Technol. 64 (2008) 141–146.
304 [13] M. Palencia, M. Vera, B.L. Rivas, Modification of ultrafiltration membranes via interpenetrating
305 polymer networks for removal of boron from aqueous solution, J. Memb. Sci 466 (2014) 192-199.
306 [14] N. Öztürk, D. Kavak, Adsorption of boron from aqueous solutions using fly ash: Batch and column
307 studies, J. Hazard Mater 127 (2005) 81-88.
308 [15] R. Liu, W. Ma, C.Y. Jia, L. Wang, H.Y. Li, Effect of pH on biosorption of boron onto cotton cellulose,
309 Desalination, 207 (2007) 257-267.
310 [16] X. Li, R. Liu, S. Wu, J. Liu, S. Cai, D. Chen, Efficient removal of boron acid by N-methyl-D-
311 glucamine functionalized silica-polyallylamine composites and its adsorption mechanism, J. Colloid
312 Interf. Sci. 361 (2011) 232-237.
313 [17] H. Demey, T. Vincent, M. Ruiz, A.M. Sastre, E. Guibal, Development of a new chitosan/$Ni(OH)_2$-
314 based sorbent for boron removal, Chem. Eng. J. 244 (2014) 576-586.
315 [18] M. Ruiz, C. Tobalina, H. Demey-Cedeño, J.A. Barron-Zambrano, A.M. Sastre, Sorption of boron on
316 calcium alginate gel beads, React. Funct. Polym. 73 (2013) 635-657.
317 [19] G., Grant, E., Morris, D., Rees, P., Smith, D., Thom, Biological interactions between
318 polysaccharides and divalent cations: the egg-box model. FEBS Lett. 32(1) (1973) 195-198.
319 [20] H. Demey, M. Ruiz, J.A. Barron-Zambrano, A.M. Sastre, Boron removal from aqueous solutions
320 using alginate gel beads in fixed bed systems, J. Chem. Technol. Biot. 89 (2014) 934-940.

[21] M. Ruiz, L. Roset, H. Demey, S. Castro, A.M. Sastre J.J. Pérez, Equilibrium and dynamic studies for adsorption of boron on calcium alginate gel beads using principal component analysis (PCA) and partial least squares (PLS), Mat.-wiss. U. Werkstofftech. 44 (2013) 410-415.

[22] K.S.W. Singh, D.H. Everett , R.A.W. Haul, L. Moscou, R.A. Pierotti, J. Rouquerol, T. Siemieniewska, Reporting physisorption data for gas/solid systems with special reference to the determination of surface area and porosity, Pure Appl. Chem. 57 (1985) 603-619.

[23] S. Brunauer, P.H. Emmet, E. Teller, Adsorption of gases in multimolecular layers, J. Am. Chem. Soc. 60 (1938) 309-319.

[24] E.P. Barret, L.G. Joyner, P.P. Halenda, The determination of pore volume and area distributions in pourous substances. I. Computations from nitrogen isotherms, J. Am. Chem. Soc. 73 (1951) 373-380.

[25] I. Langmuir, The adsorption of gases on plane surfaces of glass, mica and platinum, J. Am. Chem. Soc. 40 (1918) 1361-1403.

[26] H.M.F. Freundlich, Über die adsorption in lösungen, Z. Phys. Chem. 57A (1906) 385-470.

[27] S. Lagergreen, Zur theorie der sogenannten adsorption gelöster stoffe: Kungliga Svenska Vetenskapsakademiens, Handlingar 24 (1898) 1-39.

[28] Y.S. Ho, G. McKay, Sorption of dye from aqueous solution by peat, Chem. Eng. J. 70 (1998) 115-124.

[29] C. Nemasivayam, R.T. Yamuna, Adsorption of direct red 12B by biogas residual slurry: equilibrium and rate processes, Environ. Pollut. 89 (1995) 1-7.

[30] M.G. Haugh, C.M. Murphy, F.J. O'Brien, Novel Freeze-drying methods to produce a range of Collagen-Glycosaminoglycan scaffolds with tailored mean pore sizes, Tissue Eng. Pt C-Meth 16 (2010) 887-894.

[31] S. Papageorgiou, F. Katsaros, E.P. Kouvelos, J.W. Nolan, H. Le Deit, N. K. Kanellopoulos, Heavy metal sorption by calcium alginate beads from Laminaria digitata. J. Hazard. Mater. B137 (2006) 1765–1772,

346 [32] S.K. Bajpai, S. Shubhra, Investigation of swelling/degradation behavior of alginate beads
347 crosslinked with Ca^{2+} and Ba^{2+} ions, React. Funct. Polymers 59 (2004) 129-140.

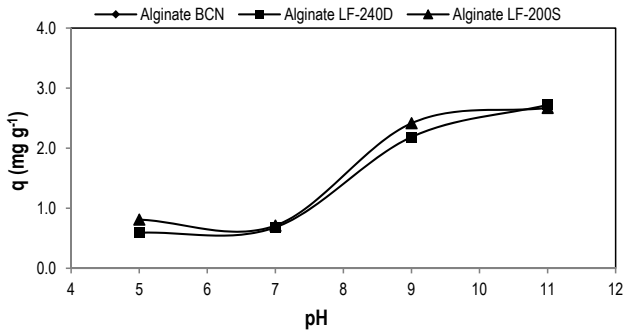

Figure 1. Effect of pH on boron removal.

(boron concentration, 50 mg L^{-1}; m= 0.2 g, V= 0.1 L).

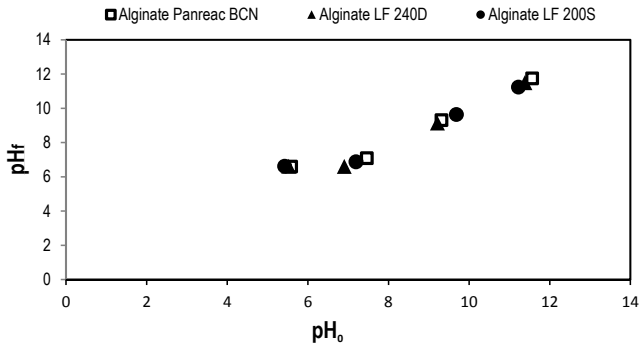

Figure 2. Variation of pH on boron removal.

(boron concentration, 50 mg L^{-1}; m= 0.2 g, V= 0.1 L).

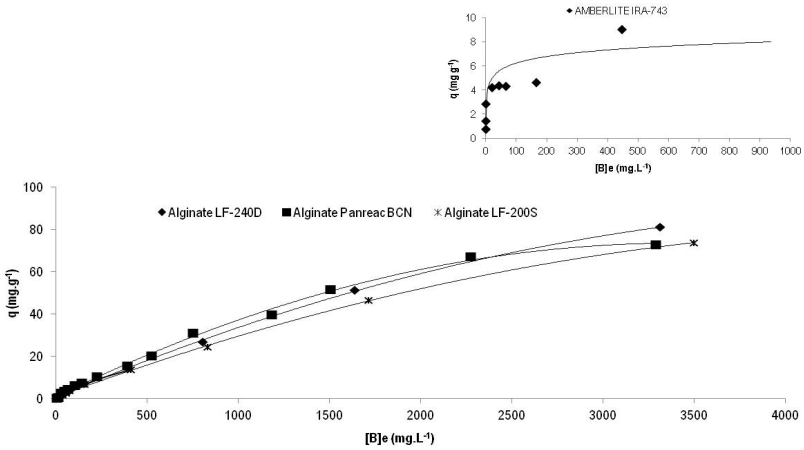

Figure 3. Boron sorption isotherms using three different alginates.

(m= 0.7 g, V= 0.1 L, pH 11).

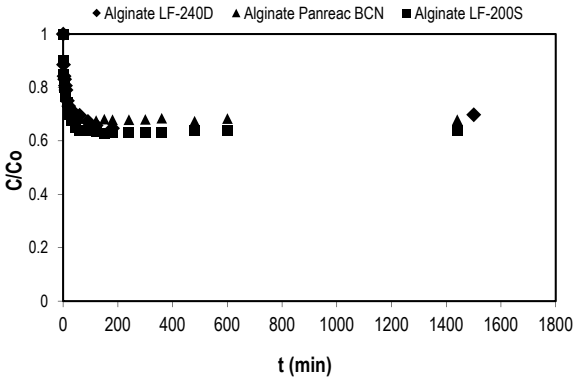

Figure 4. Kinetics profiles on boron removal.

(boron concentration, 50 mg L^{-1}; m= 1.75 g, V= 0.25 L).

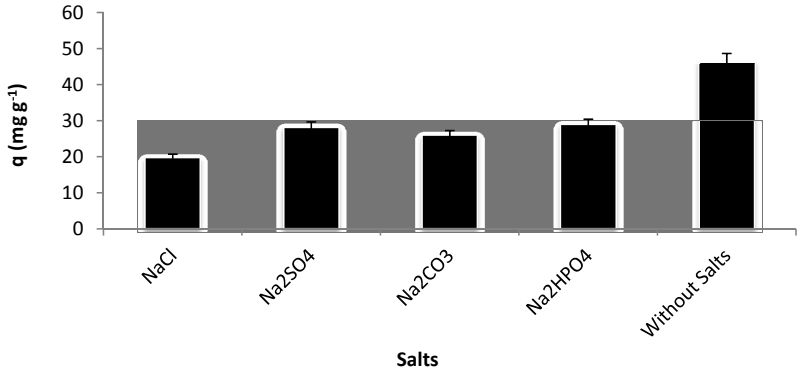

Figure 5. Influence of different salts on sorption capacity.
(Salt concentration, 0.05 M; boron concentration, 1 g L^{-1}; pH 5).

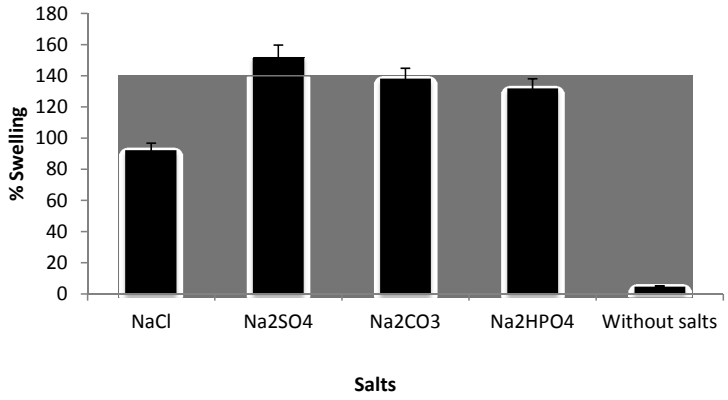

Figure 6. Influence of different salts on the swelling of the beads.

(Salt concentration, 0.05 M, pH 5).

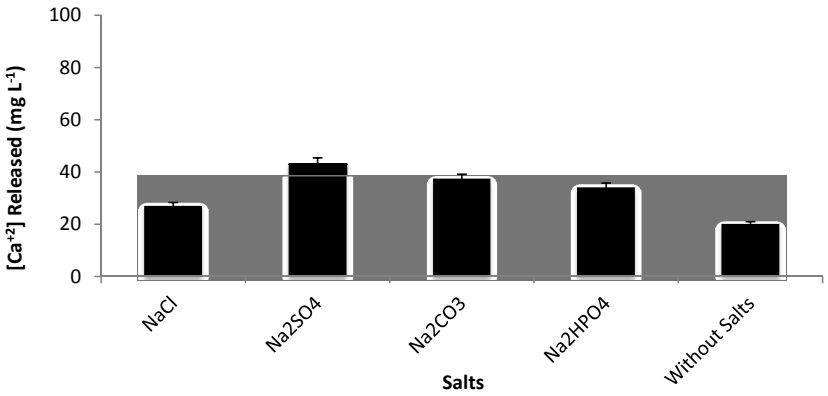

Figure 7. Release of Ca^{2+} ions in the presence of different salts.

(Salt concentration, 0.05 M, pH 5).

Table 1. Composition of Alginates

Alginates	Composition of G-blocks (% w/w))	Composition of M-blocks (% w/w)
Across LF-240D	33	67
Panreac BCN (Standard)	39	61
Across LF-200S	70	30

Table 2. Main features of AMBERLITE IRA-743

Properties	
Matrix	Macroporous polystyrene
Functional group	N-Methylglucamine
Ionic form	Free base (FB)
Total capacity	0.7 eq/L
Particle size	0.5-0.7 mm
Moisture holding capacity	48 to 54 % (FB form)

Table 3. Langmuir and Freundlich models parameters

	Langmuir model			Freundlich model		
Alginate	q_{max} (mg g^{-1})	**b** (Lmg^{-1})	r^2	k_F ($mg^{1-1/n}$ g^{-1} $L^{1/n}$)	**n**	r^2
LF-240D	91	5.81 E-04	0.999	0.11	1.21	0.998
Panreac BCN (Standard)	126	3.75 E-04	0.993	0.30	1.45	0.983
LF-200S	80	6.48E-03	0.996	0.12	1.25	0.990

Table 4. Pseudo-first-order and pseudo-second-order kinetic parameters for boron removal

	Pseudo-first order model				pseudo-second order model			
Alginate	q_{exp} (mg g^{-1})	K_1 (min^{-1})	q_1 (mg g^{-1})	r^2	K_2 (min^{-1})	q_2 (mg g^{-1})	r^2	Kp (mg g^{-1} $min^{-1/2}$)
LF-240D	2.4	0.13	2.24	0.891	0.08	2.38	0.957	0.21
Panreac BCN (Standard)	2.32	0.23	2.25	0.943	0.15	2.34	0.989	0.22
LF-200S	2.55	0.16	2.50	0.923	0.09	2.61	0.979	0.26

SUPPLEMENTARY MATERIALS

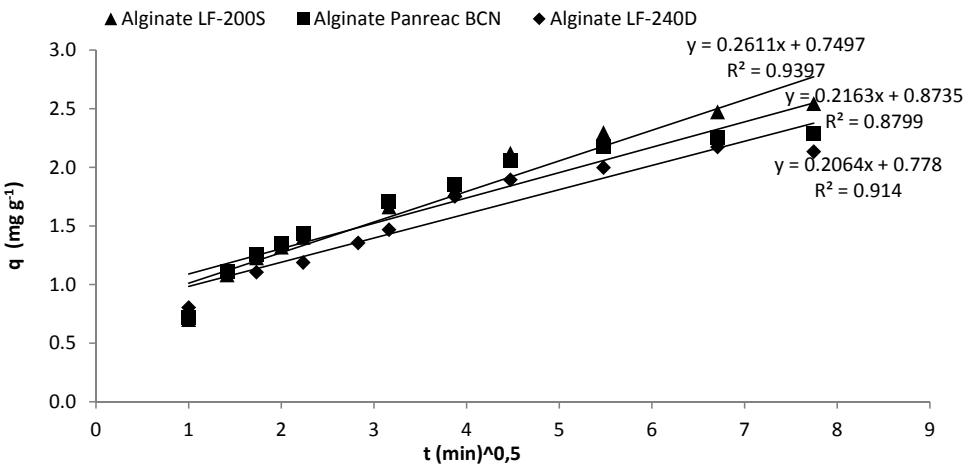

Figure SM1. Intraparticle diffusion plot for boron removal.